

**Characterisation of the structural properties and features of
M. tuberculosis complex proteins linked to tuberculosis
pathogenesis**

Sami Al-Harbi, MSci (King Abdulaziz, Jeddah)

Thesis submitted for the degree of Doctor of philosophy
Department of Biochemistry
University of Leicester

January 2011

Abstract: The genome of *Mycobacterium tuberculosis* encodes for 11 pairs of Esx family proteins such as EsxA/EsxB and EsxO/EsxP that are located in pairs within the genome. Despite the clear importance of the Esx family proteins in mycobacterial virulence and pathogenesis, the precise molecular functions and mechanisms of action for these proteins remain unknown. Initially expression vectors carrying EsxO and EsxP were constructed and used to express these proteins as inclusion products. The inclusion bodies of both proteins were successfully resolubilized and co-refolded. The final purification step by gel filtration chromatography shows that these proteins form a tight 1:1 heterodimeric complex. Analysis using circular dichroism (CD) spectroscopy of the purified refolded complex showed that it contained a high helical content (53%). The complex showed a significant resistance to heat-induced denaturation with co-operative denaturation observed that indicates a stable folded structure. In addition, significant chemical shift dispersion was seen in 1D¹H NMR of the EsxO/EsxP complex, which clearly indicates a folded structure.

Previous studies have shown that the EsxA/EsxB complex binds specifically to the surface of monocyte and macrophage cells. Fluorescence microscopy studies described here show specific binding of the EsxO/EsxP complex to the surface of monocyte and macrophage cells, suggesting that EsxA/EsxB and EsxO/EsxP complexes bind to specific target but distinct targets on the surface of host cells, which suggests possible roles in pathogen-host cell signalling. Further work, I investigated whether exposure to the EsxO/EsxP complex results in changes in host cell motility or gene expression. Analysis of macrophage motility over period of eight hours revealed that neither EsxA/EsxB nor EsxO/EsxP has any effect on the motility of macrophages. In addition, microarray analysis was used to identify any changes in the gene expression profile of monocyte cells when exposed to the EsxO/EsxP complex. Interestingly, after 30 minutes exposure to EsxO/EsxP complex only 6 genes showed significant change in expression, but three of these are involved in regulation of chromatin structure. After 2 hours exposure to EsxO/EsxP complex still only small numbers of genes showed significant changes, but no clustering to specific biological processes was apparent. The observation of specific cell surface binding of the EsxO/EsxP complex strongly suggests role in signaling, however the precise function of the complex remains to be elucidated.

Acknowledgements

Firstly I would like to thank the Saudi ministry of high education for the sponsorship and funding which made the completion of this project possible. I would like to acknowledge my supervisor, Professor Mark D. Carr, for the opportunity to work on this interesting project. I greatly appreciated his constant support and guidance provided to me throughout the period of this project.

I am also grateful to Professor John W. R. Schwabe and Dr. Christine Wells who served on my progress review panel, for providing me with useful feedbacks which have been valuable to my project. My thanks go to the members of our group for their support and cooperation throughout this project, especially to Dr. Kirsty L. Lightbody, Dr. Philip S. Renshaw and Dr. Alister. My gratitude extends to Dr. Kornelis R. Straatman (Kees) for his guidance in the using microscope. I greatly appreciated all your support and assistance.

Finally, a special thank to my parents for all their inspiration, my brothers for their supports and encouragement and my beloved wife and children for their patient, understanding and support throughout my studies.

Sami Al-harbi

January 2011

Table of Contents

Abstract -----	2
Acknowledgements-----	3
Table of Contents-----	4
Abbreviations -----	7
Chapter 1- Introduction-----	10
1.1 Tuberculosis: The current situation-----	10
1.2 Organism -----	13
1.3 Mycobacterium tuberculosis genome-----	17
1.4 Process of the disease-----	20
1.5 Recognition of <i>Mycobacterium tuberculosis</i> by immune cells-----	28
1.5.1Mycobacterium ESX-1 secreted virulence factors that interact with TLRs-----	36
1.6 Prevention and Control of Tuberculosis-----	38
1.6.1 TB vaccination-----	38
1.6.2 Treatment of Tuberculosis-----	40
1.7 Protein Secretion Systems in Mycobacterium-----	42
1.8 M. tuberculosis virulence factors-----	44
1.8.1 ESAT-6-CFP-10 protein family-----	45
1.9 Scope of the thesis-----	46
Chapter 2- Molecular features and properties of proteins encoded by <i>esxO</i> (Rv2346c) and <i>esxP</i> (Rv2347c) genes-----	48
2.1. Introduction-----	48
2.2 Methods and Materials-----	58
2.2.1 Agarose gel electrophoresis of DNA-----	58
2.2.2 SDS-PAGE-----	58
2.2.3 Ligation independent cloning (LIC-PCR)-----	59
2.2.3.1 PCR amplification of <i>esxC</i> (Rv3890c), <i>esxD</i> (Rv3891c), <i>esxO</i> (Rv2346c) and <i>esxP</i> (Rv2347c) genes-----	59
2.2.3.2 Ligation independent cloning (LIC-PCR) of the <i>esxO</i> , <i>esxP</i> , <i>esxC</i> and <i>esxD</i> coding regions-----	62
2.2.3.3 Transformation of DH5- α competent cells with recombinant plasmids-----	64
2.2.3.4 Sequencing of cloned DNA molecules-----	64
2.2.4 Protein expression trials-----	64

2.2.5 Purification of EsxO and EsxP proteins-----	65
2.2.6 Protein concentration-----	67
2.2.7 Far UV circular dichroism spectroscopy-----	67
2.2.8 Thermal denaturation studies-----	68
2.3 Results and Discussion-----	69
2.3.1 PCR amplification and ligation independent cloning of <i>esxC</i> , <i>esxD</i> , <i>esxO</i> and <i>esxP</i> genes-----	69
2.3.2 Protein expression trial for recombinant EsxO, EsxP, EsxC and EsxD with and without a hexa-histidine extension sequence.-----	71
2.3.3 Expression and purification of EsxO/EsxP complex-----	76
2.3.4 Structural characterization of EsxO/EsxP as a complex-----	83
2.3.4.1 Far UV circular-dichroism spectrum for the EsxO/EsxP complex-----	83
2.3.4.2 The effect of thermal variation on EsxO/EsxP as complex-----	85
2.3.4.3 1D ¹ H NMR analysis of the EsxO/EsxP complex-----	87
2.3.4.4 MALDI-TOF mass spectroscopy of the EsxO/EsxP complex-----	88
2.3.4.5 Prediction of structure of EsxO/EsxP complex-----	89
Chapter 3 Specific interaction of the EsxO/EsxP complex with host cells-----	95
3.1 Introduction-----	95
3.2. Method and Materials-----	99
3.2.1 Purification of the EsxO/EsxP complex-----	99
3.2.2 Fluorescent labelling of EsxO/EsxP complex-----	99
3.2.3 Cell culture-----	101
3.2.3.1 Monocytic cell line-----	101
3.2.3.2 Macrophage cell line-----	101
3.2.3.3 Fibroblast cell line-----	101
3.2.4. Fluorescence microscopy-----	102
3.2.5 Confocal fluorescence Microscopy-----	103
3.3 Results-----	104
3.3.1 Labelling of the EsxO/EsxP complex with Alexa Fluor 546-----	104
3.3.2 Fluorescence Microscopy-----	105
3.3.2.1 Binding of the EsxO/EsxP complex to the specific host cells-----	105
3.3.2.2 Specificity of EsxO/EsxP complex binding to a host cell-----	107
3.3.2.3 The location of the EsxO/EsxP complex in specific host cells-----	109

3.4 Discussion-----	111
Chapter 4 Assessment of potential Biological Roles of EsxO/EsxP complex-----	114
4.1 Introduction-----	114
4.2.1 Protein purification and removal of LPS-----	115
4.2.2 Cell Motility Assays-----	116
4.2.3 Microarray-----	117
4.3 Result-----	119
4.3.1 The purification of EsxO/EsxP complex and removal LPS-----	119
4.3.2 Assessment of the effects of Esx complexes on cell the motility-----	120
4.3.3 Microarray analysis of gene expression change of U937 cells treated with EsxO/EsxP complex at different time points-----	124
4.4 Discussion-----	135
5. Conclusions and Future Work-----	139
5.1 Conclusions-----	139
5.1.1 Interactions of secreted <i>M. tuberculosis</i> factors with host cells-----	139
5.1.2 Escape of <i>M. tuberculosis</i> from phagolysosome to the cytoplasm-----	140
5.1.3 <i>M. tuberculosis</i> induced cell death-----	140
5.1.4 ESX-mediated granuloma formation and early dissemination of <i>M.Tuberculosis</i> -----	141
5.1.5 <i>M. tuberculosis</i> -modulation of proinflammatory cytokine expression-----	142
5.2 Future Work-----	144
5.2.1 Identification of Host cell Receptors for the EsxO/EsxP complex-----	144
5.2.2 Cytokine assays-----	145
Appendix-1-----	147
Appendix-2-----	149
References-----	152

Abbreviations

Ag	Antigen
AIDS	Acquired immunodeficiency syndrome
Amp	Ampicillin
APC	Antigen-presenting cell
ATP	Adenosine-5'-triphosphate
BAC	Bacterial artificial chromosome
B-cell	Bursa-dependent lymphocyte
BCG	Bacille Calmette-Guérin
bp	Base pair
CD	Circular dichroism
CFP-10	Culture filtrate protein of 10 kD
Da	Dalton
DC	Dendritic cell
DOTS	Directly observed therapy short-course
DTT	L,4-Dithiothreitol
EDTA	Ethylene diaminetetraacetate
ESAT-6	Early secreted antigen target of 6 kDa
FPLC	Fast protein liquid chromatography
Gdn-HCl	Guanidine hydrochloride
HIV	Human immunodeficiency virus
INF γ	Interferon gamma
IL	Interleukin
IPTG	isopropyl β -D-thiogalactopyranoside
Kan	Kanamycin

kDa	Kilo Dalton
LB	Luria-Bertani
LDS	Lithium dodecyl sulphate
MDR	Multi-drug resistant
M	Marker
MW	Molecular weight
NH	Backbone amide group
Ni ²⁺ -NTA	Nickel-nitrilotriacetic acid
OD	Optical density
ORF	Open reading frame
PAGE	Polyacrylamide gel electrophoresis
PCR	Polymerase chain reaction
PE	Proline-Glutamic acid sequence
<i>Pfx</i>	<i>Pyrococcus sp. Platinum® Pfx</i>
<i>Pfu</i>	<i>Pyrococcus furiosus</i>
PPE	Proline-proline-glutamic acid sequence
RD	Region of difference
SDS	Sodium dodecyl sulphate
TB	Tuberculosis
T-cell	Thymus-dependent lymphocyte
TNF α	Tumour necrosis factor alpha
UV	Ultraviolet
v/v	Volume per volume
w/v	Weight per volume
WHO	World Health Organization
XDR	Extensively drug resistant

DNA bases

Adenine	A	Guanine	G
Cytosine	C	Thymine	T

Single and Three Letter Codes for Amino Acids

Alanine	A	Ala	Leucine	L	Leu
Arginine	R	Arg	Lysine	K	Lys
Asparagine	N	Asn	Methionine	M	Met
Aspartic acid	D	Asp	Phenylalanine	F	Phe
Cysteine	C	Cys	Proline	P	Pro
Glutamine	Q	Gln	Serine	S	Ser
Glutamic acid	E	Glu	Threonine	T	Thr
Glycine	G	Gly	Tryptophan	W	Trp
Histidine	H	His	Tyrosine	Y	Tyr
Isoleucine	I	Ile	Valine	V	Val

Chapter 1

Introduction

1.1 Tuberculosis: the current situation

Tuberculosis (TB) remains one of the most important health problems in the world. Annually, over two million people die from the disease. Recently, it has been reported that nearly one-third of world's population, which equates to about two billion people are infected with the TB bacillus. Also, it is suggested that new infections occur at a rate of one per second. According to the World Health Organisation (WHO) report, 5-10% of infected people become ill at some time during their lives, and people who have both HIV and TB infection are more than likely expected to develop TB (172, 188, 203, 220).

The WHO estimates that the majority of cases occur in the developing countries, particularly in Africa and south East Asia (220), primarily because of low socio-economic status, poor health systems at the government level, unsuitable care for sick patients, irregular and inefficient supply of anti-tuberculosis drugs which, might result in the emergence of multi-drug resistant (MDR) and extensively drug-resistant (XDR) tuberculosis, poverty, and the spread of HIV/AIDS in these countries (Figure 1.1). However, in developed or economically rich countries with advanced healthcare facilities, there are other risk factors, such as alcohol consumption, stressful lifestyles, and particularly the increasing percentage of immigration from developing countries, which has led to an increase in the number of reported TB cases. In the UK about 9,153

tuberculosis cases were reported in 2009; this equals a rate of 14.9 per 100,000 populations, an increase of 5.5% compared with the number of cases reported in 2008. The London region had the highest incidence with about 41% of the total cases. The greatest incidence of TB in the UK occurs in people between the ages of 15 and 44 years (202, 203, 220) (Figure 1.2).

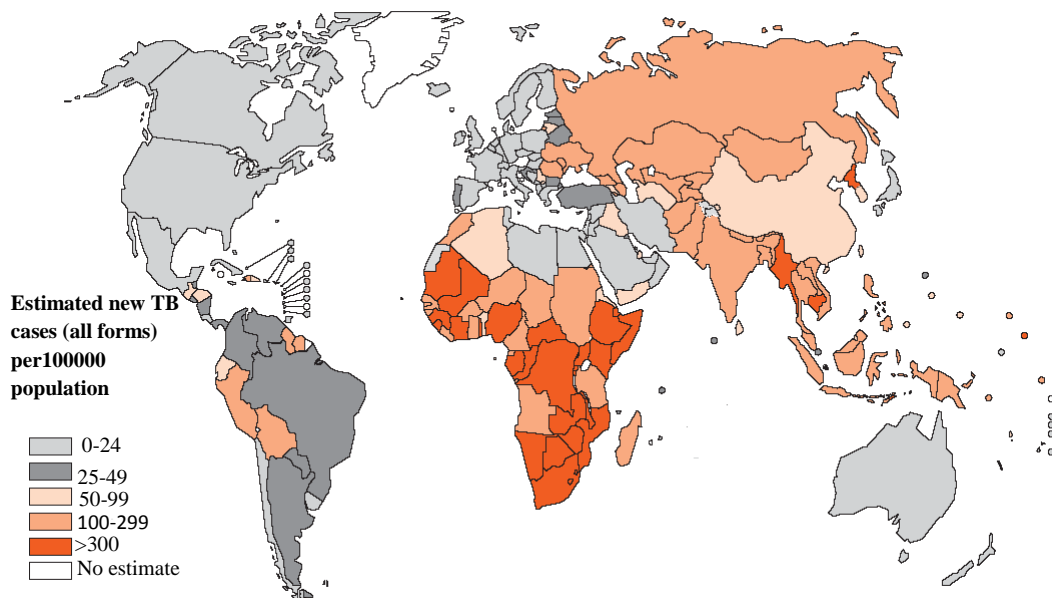


Figure 1.1 Estimated global TB incidence (2008). All forms of TB estimated per 100,000 populations. Reproduced from World Health Organization, Geneva, Switzerland (2009).

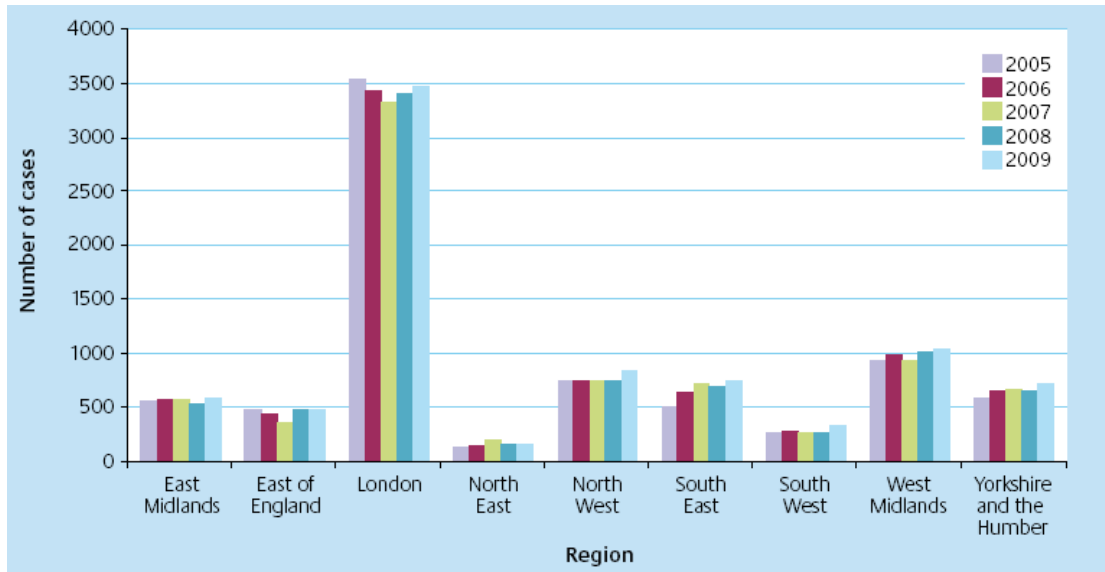


Figure 1.2 The number of Tuberculosis cases for England, Wales and Northern Ireland (2005-2009) reported by region/country. Reproduced from Health Protection Agency, (2010).

1.2 Organism

TB is caused by bacteria which are called *Mycobacterium tuberculosis*, first discovered by Robert Koch in 1882. These bacteria are non-motile, acid-fast and aerobic. The bacteria belong to the genus *Mycobacterium*. The *Mycobacterium* is member of the phylum *Actinobacteria*, which have GC rich (61-71%) sequence content in their DNA and their cell wall contains a very high proportion of lipids. Most species of *Mycobacterium* replicate without restraint in the natural ecosystem and seldom cause disease in higher vertebrates including humans, however a few are pathogenic. Their method of pathogenesis is very puzzling because they use macrophages (which are the front-line defence mechanism in the immune system) as a safe haven for their reproduction and growth (31, 186, 202).

Host-dependent mycobacteria include *M. avium* subspecies *paratuberculosis*, *M. leprae*, and the members of the *M. tuberculosis* complex. The *Mycobacterium tuberculosis* complex contains *M. tuberculosis*, the causative agent in the majority of human tuberculosis cases, *M. africanum*, cause of TB in Africa, *M. canetti* (TB infection by this strain is rare), *M. microti*, causative agent of tuberculosis in voles, *M. bovis*, which causes TB infection in a wide range of mammalian species including humans and cattle, and *M. bovis* BCG (Bacillus Calmette-Guérin), which is lab attenuated *M. bovis* and the only known vaccine against TB. The members of the complex have high levels of genetic similarity, resulting in a level of DNA sequences identity greater than 99%, however the *M. tuberculosis* complex members show differences in their biochemistry and mechanism of pathogenesis (31, 186).

Under the microscope tuberculosis bacilli appear as straight or slightly curved rods. However, this microscopic morphology was shown to be dependent on growth condition and age of the culture and therefore a change was seen from short coccobacilli to long rods. This change in morphology is rarely seen in *M. tuberculosis*, in contrast to other actinomycetes and some fast-growing mycobacteria (202).

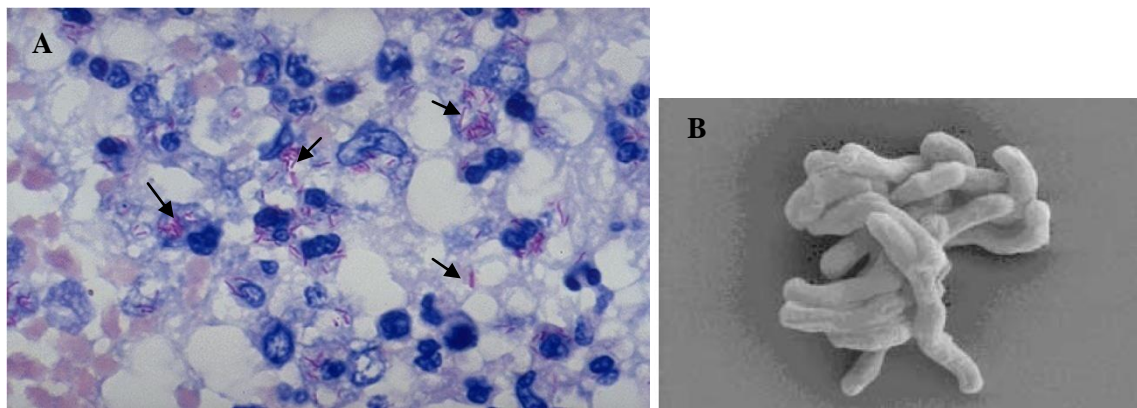


Figure 1.2.1 (A) Acid-fast Ziehl-Neelsen staining of *Mycobacteria* in infected lung tissue (as shown with arrows); (B) Electron microscopic structure of *M. tuberculosis* (92, 202).

As noted previously, the main distinguishing feature of mycobacteria is the cell envelope. Mycobacteria do not have an extra outer cell membrane when compared with Gram-negative bacteria. The cell wall of mycobacterium looks structurally similar to Gram-positive bacteria. However, the mycobacterium contains largely lipids in its cell wall, whereas the cell wall of Gram-positive bacteria is mainly made up of polysaccharides and proteins. Therefore, mycobacterium is not classified into the Gram-positive class of bacteria. Due to this high lipid content, mycobacteria cannot be observed by gram staining (2, 202). Hence, Ziehl-Neelsen staining, or acid-fast staining, is used to see these bacteria under a light microscope (Figure 1.2.1). The current

biochemical investigations of the mycobacterial cell envelope, have revealed that the mycobacteria have a thick cell envelope that contains an inner plasma membrane, a unique cell wall which includes two polymer layers (peptidoglycan and arabinogalactan surrounded by a very hydrophobic lipid [mycolate]), and a capsule. This cell wall causes problems for the secretion of bacterial products, and also creates a barrier against killing mechanisms mediated by the mammalian immune system. The cell wall mainly consists of three different types of compounds (peptidoglycan, mycolic acid, and arabinogalactan) which are covalently attached. The covalent attachment of mycolic acids forms the hydrophobic layer (called a mycomembrane), and thus this layer is characterised by its hydrophobicity and low fluidity. As shown in figure 1.2.2, the outer layer of the membrane is composed of different lipids, including Cord factor, dimycolyltrehalose, and phenolic glycolipids, which interact with mycolic acids. The composition of the capsule consists primarily of polysaccharides (arabinomannan and glucan) and forms the outer part of the mycobacterial envelope (2, 186, 202).

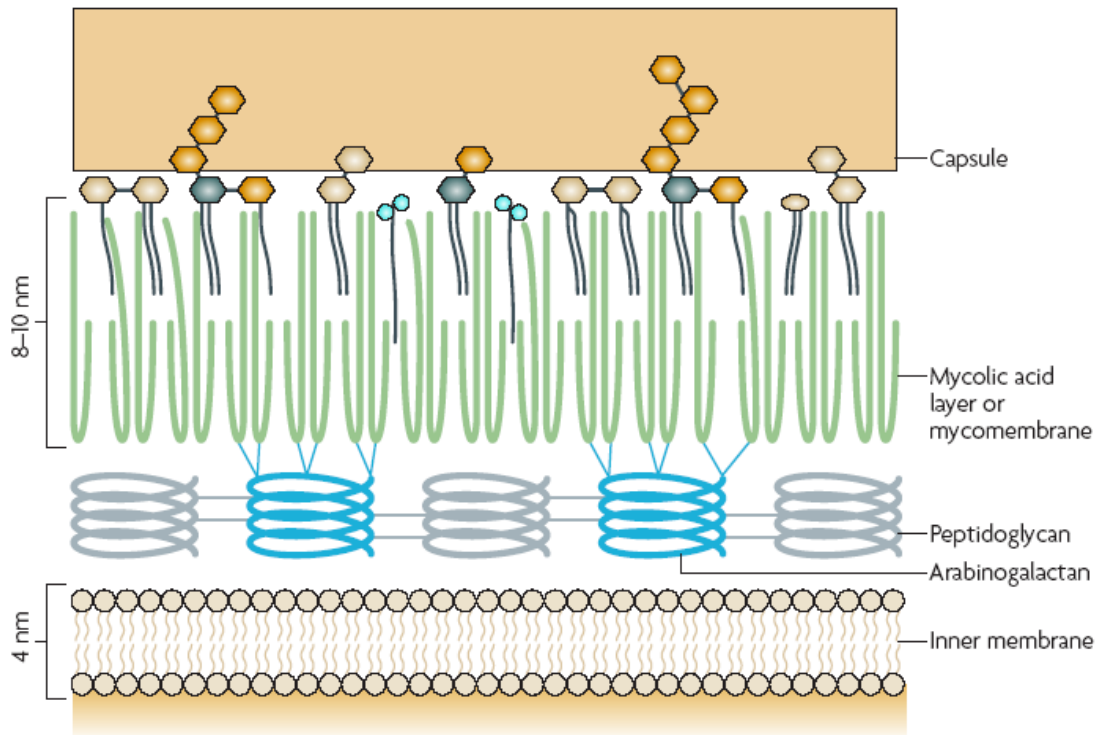


Figure 1.2.2 Structure of the cell envelope of *M. tuberculosis*. The cell envelope includes an inner plasma membrane, a unique cell wall which includes three polymer layers ((I) peptidoglycan (grey), (II) arabinogalactan (blue), and (III) mycolic acids (greens)). The covalent linkage of mycolic acid provides an extremely hydrophobic layer known as the mycomembrane, and the outer part of this layer contains various free lipids including Cord factor, dimycolyltrehalose, phenolic glycolipids, phosphatidylinositol mannosides, and sulpholipids, which are intercalated with mycolic acids. Most of these lipids are specific for mycobacteria. The capsule is mainly made up of polysaccharides (glucan and arabinomannan). Reproduced from Abdallah *et al.*, 2007.

The growth of *M. tuberculosis* is slow, as it divides in 12-24 hours under favourable laboratory conditions. It can also survive for weeks in a dry state; therefore, it takes a long time for antibiotic treatment to kill all of these bacteria. This unusual resistance to ‘growth’ as well as to ‘death’ is likely due to the unique lipid content of the cell wall, and it also might be a key virulence factor. The slow growth rate is probably associated

with the impermeability of the *M. tuberculosis* cell wall and the restricted nutrient uptake by *M. tuberculosis* (186, 202).

1.3 *M. tuberculosis* Genome

M. tuberculosis H37Rv has been extensively used as model of the virulent strain of *M. tuberculosis*. The sequence of the H37Rv genome was published by Cole *et al.* in 1998. The H37Rv strain has a singular circular chromosome that consists of approximately 4.4 Mb, and it is G/C rich, about 65%. The *M. tuberculosis* proteome comprises approximately 4,000 proteins, and 52% of those proteins have been attributed a predicted function (34). The *M. tuberculosis* genome has unusual characteristics compared with other bacteria. The unusual feature of the genome sequence of *M. tuberculosis* is that there are a large number of genes, which are responsible for fatty acid metabolism. Many of these genes are required for the production of different types of lipids, which include basic fatty acids to the complex mycolic acids, which form the protective cell wall (39). Because of these lipids, the permeability of the *M. tuberculosis* cell envelope is very low. The barrier formed by these lipids suggests that this may be one of the intrinsic mechanisms of resistance to some antibiotics (107). Another unusual characteristic of *M. tuberculosis* is that PE and PPE proteins constitute 4% of the *M. tuberculosis* genes. This equals 170 proteins encoded by two large multi-gene families of unknown function, which may be involved in antigenic variation. The PE and PPE protein families are recognised by their N-terminal proline-glutamic acid and proline/proline-glutamic acid motifs respectively. PE and PPE genes are surface exposed and have differential expression, which suggests the ability to change the pattern of antigens released during progression of the infection (28, 68, 143, 213).

Another protein family involved in virulence and pathogenicity is the CFP-10/ESAT-6 family. The function and mechanism of action of the CFP-10/ESAT-6 proteins are not yet known. Comparative genomic studies have been used to determine genetic differences between members of the *M. tuberculosis* complex which, help in the understanding of virulence and attenuation, as well as in identifying vaccine candidates. Comparative analysis between *M. tuberculosis* and *M. bovis* BCG genomes identified 14 regions deleted from attenuated BCG strains. Only one region known as RD1 (region of difference) was present in all virulent laboratory and clinical isolates and absent from all BCG daughter strains (18, 126). Furthermore, a functional study of RD1 has demonstrated that the proteins encoded by this region have a critical role in pathogenesis and virulence, because when this region is deleted from *M. tuberculosis*, it leads to decreased virulence. In contrast, the re-introduction of RD1 into *M. bovis* BCG significantly increases virulence of the recombinant strain, but this increase is not at the same level of virulence as *M. tuberculosis* (131, 154, 155).

A recent study has proposed that a ‘systemic nomenclature’ for all components of the secretion system should be used in the literature. At present a small number of genes within different ESX loci of mycobacterium have been named, but the original genome annotation numbers are still in use for most genes. These original gene numbers are not the same among different species or strains of the same species. Therefore, comparative studies become difficult and confusing. This nomenclature is focused on the ESX-1 system of *M. tuberculosis* and all ESX systems in various mycobacteria. The proposed rules for this nomenclature system include: i) only genes that are homologous in at least four of the ESX systems will be given a general name, whereas locus-specific genes

will not get general names, as they have a more particular name related to their specific function, ii) three letter acronyms will be given for conserved components (for example, *ecc* is used for ‘*esx* conserved component’), and iii) the *esxA* and *esxB* genes (which encode the ESAT-6 and CFP-10 proteins, respectively) and other *esx* genes will not be renamed because these names are informative and well accepted in the literature (Table 1.3.1). Similarly, the *pe* and *ppe* genes are not renamed because different mycobacterial species have a large number of genes that are members of these gene families and, therefore, it would further confuse the system to rename some of these genes (23).

Table 1.3.1: *Esx* genes of *M. tuberculosis* H37Rv. The names in the brackets are the previously used names of these genes (23).

Gene Family	ESX-1	ESX-2	ESX-3	ESX-4	ESX-5	No Similarity To Cluster
ESAT-6	<i>esxA</i> (<i>esat6</i> , <i>rv3875</i>)	<i>esxC</i> (<i>rv3890c</i>)	<i>esxH</i> (<i>cfp7</i> , <i>tb10.4</i> , <i>rv0288</i>)	<i>esxT</i> (<i>rv3444c</i>)	<i>esxN</i> (<i>mtb9.9A</i> , <i>Rv1793</i>)	
CFP-10	<i>esxB</i> (<i>lhp</i> , <i>cfp10</i> , <i>rv3874</i>)	<i>esxD</i> (<i>rv3891c</i>)	<i>esxG</i> (<i>tb9.8</i> , <i>rv0287</i>)	<i>esxU</i> (<i>rv3445c</i>)	<i>esxM</i> (<i>tb11.0</i> , <i>rv1792</i>)	
ESAT-6 homologues elsewhere in the genome			<i>esxR</i> (<i>tb10.3</i> , <i>rv3019c</i>), <i>esxQ</i> (<i>tb9</i> , <i>rv3017c</i>)		<i>esxI</i> (<i>mtb9.9D</i> , <i>rv1037</i>), <i>esxL</i> (<i>mtb9.9C</i> , <i>rv1198</i>), <i>esxO</i> (<i>mtb9.9E</i> , <i>rv2346c</i>), <i>esxV</i> (<i>mtb9.9D</i> , <i>rv3619c</i>)	<i>esxE</i> (<i>rv3904c</i>)
CFP-10 homologues elsewhere in the genome			<i>esxS</i> (<i>rv3020</i>)		<i>esxJ</i> (<i>tb11.0</i> , <i>Rv1038c</i>), <i>esxK</i> (<i>tb11.0</i> , <i>Rv1197</i>) , <i>esxP</i> (<i>rv2347c</i>), <i>esxW</i> (<i>rv3620c</i>)	<i>esxF</i> (<i>rv3905c</i>)

1.4 Process of the disease

The first stage of the TB infection is usually initiated in the respiratory system. A low dose of bacilli is required to initiate infection, but only 5-10% of infected people develop to clinical disease (186). Usually, the host gets these bacilli through inhalation of infected aerosol or nuclei from the atmosphere (172). It is known that nuclei, each containing one bacterium, remain alive in the atmosphere for several hours. Most of the inhaled *M. tuberculosis* remain in the upper respiratory tract and are removed from the trachea by the mucociliary escalator. A few of them reach the alveoli of the lungs and are phagocytosed by the alveolar macrophages. At this stage of infection, there are three possibilities : (I) Immediately, the immune system kills the bacteria, (II) the disease progresses to primary tuberculosis, in which the host immunity fails to mount an effective innate immune response against these bacteria. Most commonly this occurs in patients with suppressed or defective immunity and neonates. (III) *M. tuberculosis* enters into the cells of immune system and the patient undergoes a latent tuberculosis infection (61).

Macrophages can recognise various molecules (lipoproteins, lipids and glycolipids), that are extensively synthesized by mycobacteria. These molecules stimulate different receptors on the surface of the macrophage cell membrane and therefore induce specific cell signalling pathways that regulate initial inflammatory response. For example, when mycobacterial lipoproteins stimulate Toll-like receptors (TLR)-2, which play a key role in the innate immune system, specific cell-signalling pathways are triggered leading to a pro-inflammatory response. This response can either kill the bacilli or promote apoptosis of infected macrophages (172). Other receptors, such as TLR-1 and TLR6,

have critical roles in the response to bacterial lipoproteins, leading to a proinflammatory response. On the other hand, mannose-capped lipoarabinomannan leads to an anti-inflammatory response through the Dendritic Cell-Specific Intercellular adhesion molecule-3-Grabbing Non-integrin (DC-SIGN) receptors, which are present on the surface of dendritic cells, thereby decreasing anti-mycobacterium activity and stimulating release of IL-10. Therefore, a balance between these innate immune signalling (pro-inflammatory and anti-inflammatory) regulates the strength of the initial inflammatory response (172, 188).

It is a common suggestion that following phagocytosis of bacilli by alveolar macrophages, the activated host innate immune cells are triggered to attack the lung epithelium (63, 204). In vitro analysis has shown that human and murine macrophages release strong pro-inflammatory cytokines (IL-1, IL-6, IL-12 and TNF- α), as their TLR were found to be activated when antigens on the surface of bacilli come into contact with the receptor (188).

Tumour necrosis factor (TNF- α) along with these inflammatory chemokines produced by infected macrophages lead to chemoattraction of several inflammatory mediators, immune cells and antigen presenting cells (such as neutrophils, macrophages, dendritic cells, natural killer cell, CD4⁺ and CD8⁺ cells), which secrete their own cytokines and chemokines that increase cellular motility and remodel the sites of infection in lung tissue (172, 188). The inflammatory response is controlled and followed by cellular immune activity that causes the generation of INF- γ . Actually, at this stage of infection the newly recruited cells are used as building blocks of tubercles.

In later stages, granulomas then become more mature and vascularised. Then extensive fibrotic and extracellular matrix are developed along with collagens, that create a barrier between granulocytes, macrophage and giant cells. Finally, the granulomas become necrotic and lose their vascular appearance (172) (Figure 1.4.1).

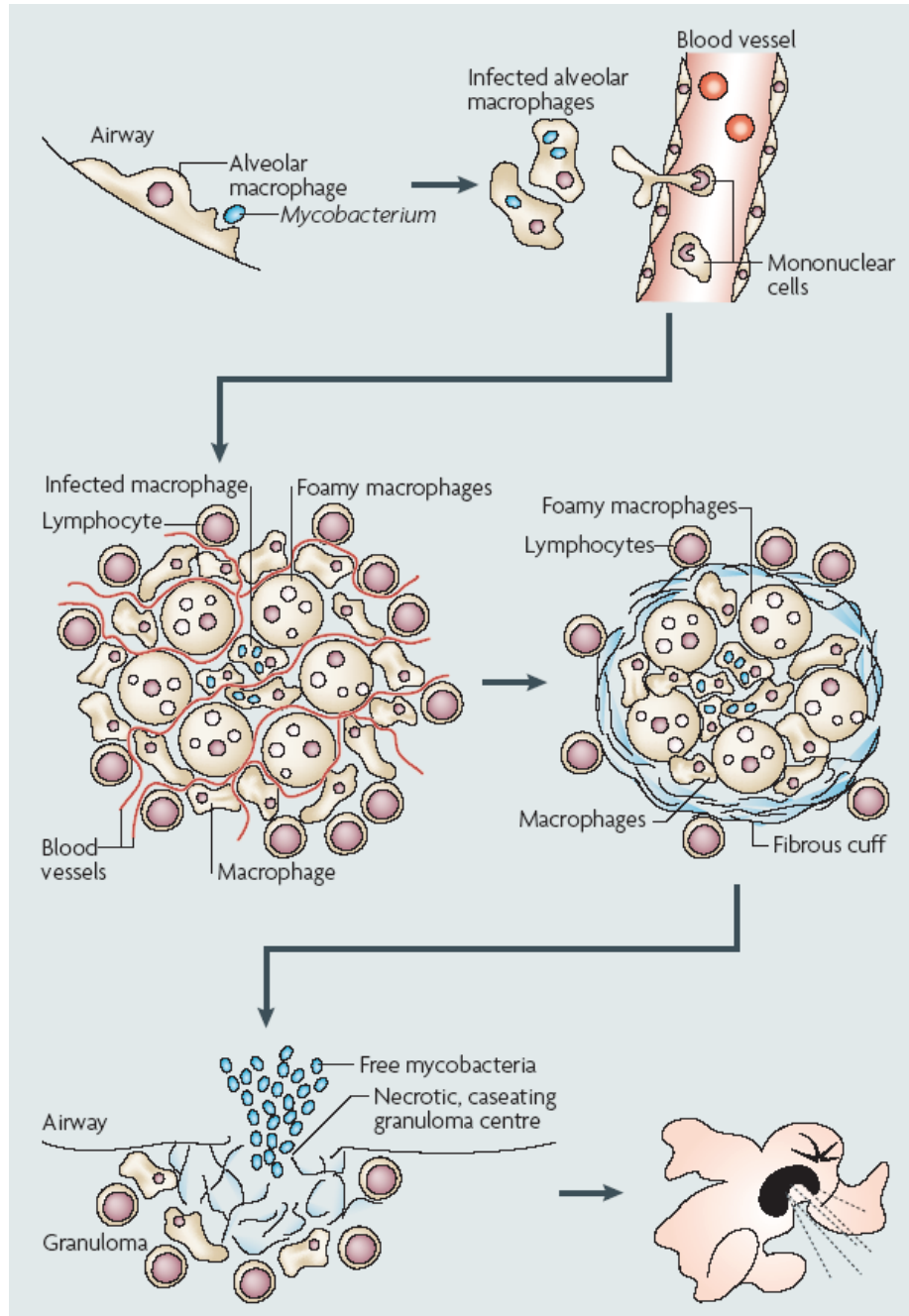


Figure 1.4.1 Events leading to the development of tuberculosis infection. The host usually takes up *M. tuberculosis* via inhalation into alveolar macrophages and dendritic cells. This is followed by the migration of the infected cells that enter the lymph nodes and stimulates naïve T-cell populations, including CD4⁺ and CD8⁺ T-cells. The response of T-cells to the antigens causes the granuloma formation that contains *M. tuberculosis* infection. The bacilli can be contained within the granuloma for several years; this can turn into caseated granulomas in immunocompromised individuals leading to active transmission of the bacilli to new hosts. Reproduced from Russell *et al.*, 2007.

Generally, it is believed that the central part of the granuloma has an important role in host pathogen interaction, but the follicle-like structures outside of the tuberculomas are primary sites of host-pathogen interaction. The secretion of cytokines as well as the differentiation of lymphocytes usually take place in those structures that are often associated with harbouring B-lymphocytes, antigen presenting cells (APCs) and T-lymphocytes (CD4⁺ and CD8⁺ T-cells) (109, 129). This role of follicle-like structures is further supported by histological studies of human tuberculomas and has shown that a considerable proportion of the bacteria or bacterial products are associated with macrophages found both around the central necrotic regions and the outer fibrotic margin where lymphocytes proliferate (172). Interestingly, the mycobacteria in peripheral macrophages were positive for isocitrate lyase expression (59, 60). The expression of the enzyme is known to be up-regulated in macrophages by *M. tuberculosis* when treated with activating cytokines (134, 172). This observation suggests that dynamic interaction exists between macrophages and T-cells (172).

Previous studies have indicated that the cell wall of the bacterium confined in *M. tuberculosis* containing vacuoles is degraded and its components, containing lipoarabinomannan and arabinomannan are then accumulated in multilamellar vesicles. These vesicles are released as exosomes (which contain bacterial lipids and proteins). Then these bacterial lipids and proteins are internalised by neighbouring (bystander) immune cells. The antigenic lipids and proteins are finally presented by the MHC-II and CD1 molecules (present on the surface of APCs) to stimulate T-cells. This results in proliferative response seen at periphery of tuberculomas (172, 188). Moreover, current investigations that have explored a lipid-bead granuloma model in order to

histologically assess the bioactivity of the mycobacterial cell wall lipids in relation to tuberculoma formation, immune cell recruitment and cytokine production. In this model, individual BCG-derived cell wall lipids are fractionated and then lipid-coated particles are incorporated into extracellular matrix gel, which is then injected into mice peritoneum. These analysis have shown that mycobacterial cell wall fractions containing trehalose mono-and di-mycolates (TMD) were found to be the most bioactive component in mycobacterial cell wall fractions, because of its intense recruitment of immune cells and granuloma development (165, 172, 188). Furthermore, a study has shown that any modification of TMD by addition of a cyclopropane results in a significantly increased inflammatory response. This suggests that the pathological features of the lipid account for some degree of the damage that allows or promotes the survival of bacilli and the formation of granulomas (172).

The main function of granulomas appears to be the control of infection and prevention of the spread of bacteria as explained above. In this classical model, it is believed that granulomas were formed only after initiation of adaptive immunity. In a study of tuberculosis using animal models, a rapid bacterial growth was observed in the first two weeks of the infection, and then a stationary phase (plateaus) occurred simultaneously with the development of adaptive immunity. Therefore, based on the classical model of granuloma formation, adaptive immunity is a critical pre-requisite for the formation of the granuloma thus playing an important role in limiting bacterial dissemination to other areas of tissues (139, 193). Recent studies by Davis and Ramakrishnan have suggested that granulomas have a role in promoting expansion of infection. This suggestion casts a significant doubt on the classic model of granuloma formation. Hence, they have

refuted the model because they found that: i) First, epitheloid granulomas formed within days after initial infection, long before adaptive immunity was developed ii) Second, the rapid expansion of the bacteria occurred simultaneously as granuloma formation with the former taking precedence iii) Finally, in *M. marinum* removal of the ESX-1/RD1 secretion system locus (Δ RD1 Mm) resulted in attenuated infection with poor granuloma formation. Hence, these observations suggested that granuloma formation has an important function in expanding the infection. Therefore this locus might be essential in the induction of macrophage recruitment to the infection sites within granulomas (45) (Figure 1.4.2).

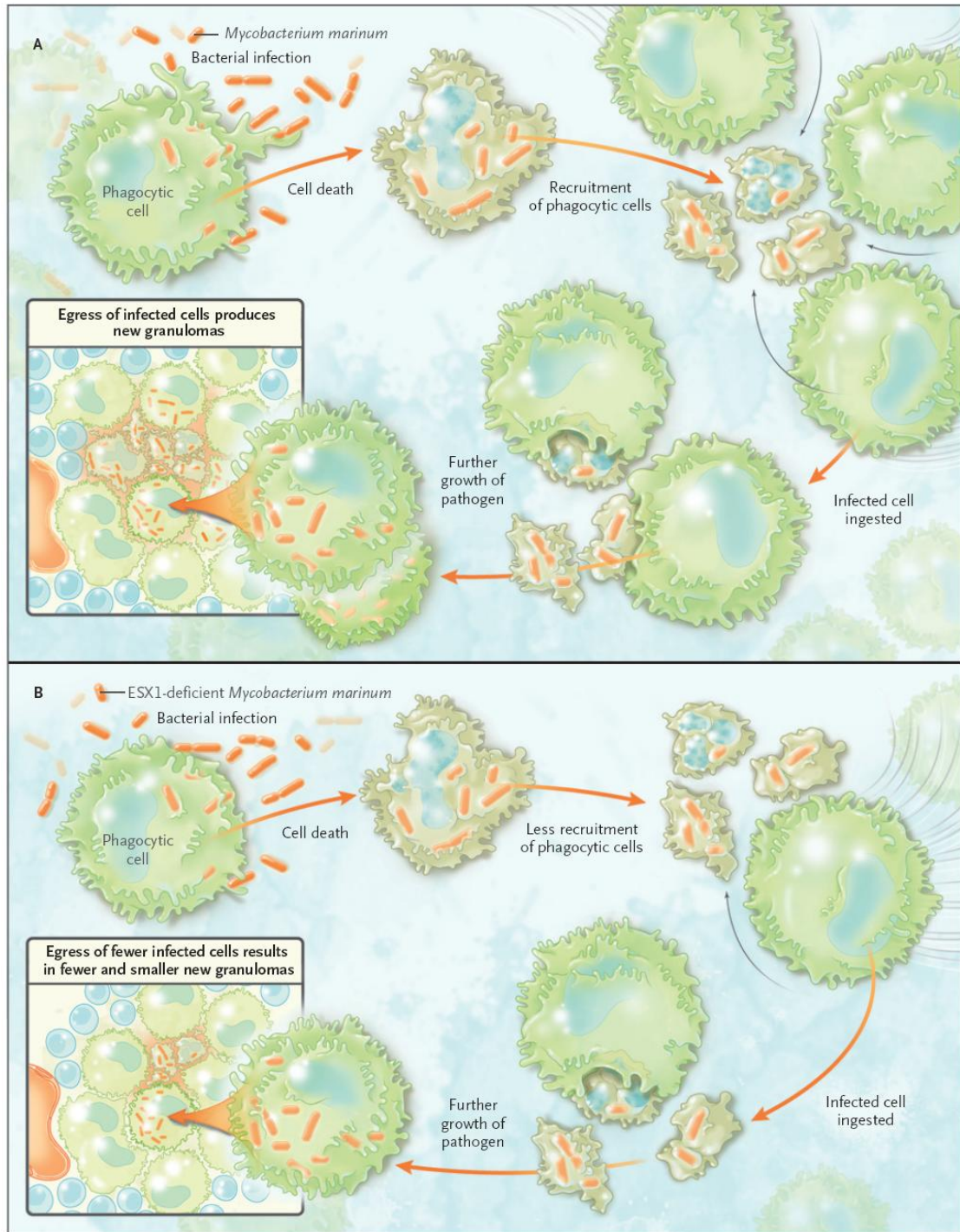


Figure 1.4.2 The survival of *M. marinum* within the phagocytic cell of zebra fish caused cell death. (Panel A) The uninfected cells were recruited by the infected ones. Some of these cells have taken up dead infected cells that provided a safe harbour for the survival of pathogen and allow egress of infected cells to form granulomas. (Panel B) Infection with bacteria that lacked the significant virulence region ESX1 led to less recruitment of uninfected cells, hence fewer bacteria, smaller lesions, and fewer new granulomas. Reproduced from Rubin *et al.*, 2009.

1.5 Recognition of *Mycobacterium tuberculosis* by Immune Cells

The innate immune system is a vital defence mechanism against the invasion of *M. tuberculosis*. This is initiated through the recognition of *M. tuberculosis* or its products by the cells of the innate immune system. Consequently, this recognition of microbial patterns by an infected host is a very significant determining factor for an efficient innate and adaptive response (6, 174). Detection of bacterial pathogens is mediated by cell surface receptors that including Toll-like receptors (TLRs), nucleotide-binding oligomerisation domain-(NOD-) like receptors (NLRs), and C-type lectins. Other possible receptors include complement receptors, scavenger receptors, surfactant protein A receptors (Sp-A), and cholesterol receptors (6).

Toll-like receptors comprise a family of protein receptors that have the ability to detect a variety of microbial molecules, commonly referred to as pathogen-associated molecular patterns (PAMPs). The recognition of PAMPs by TLRs leads to the activation of innate immunity and subsequently improves adaptive immunity. TLRs are mainly expressed on the surface of the cell membrane or on the endocytic vesicles that include immune cells, such as macrophages and dendritic cells (DCs). The interaction of *M. tuberculosis* with TLRs stimulates an intracellular signalling pathway which coincides with the secretion of pro-inflammatory mediators. However, the bacterium has developed strategies that can trigger signals able to counter or modulate the innate immune response, which might favour the pathogen (6, 81, 174). The initial event of interaction of the *M. tuberculosis* with the host cells and TLR signalling (mainly TLR2 and TLR4) is the main route of the innate immune reaction during infection (81, 109, 174, 228).

Innate immune responses post mycobacterial infection are initiated by recognition of mycobacterial components by pattern recognition receptors (PRRs), with mycobacterial components activating several TLRs (Figure 1.5.1) (174). The immunostimulatory activity of mycobacterial DNA has been attributed to the existence of palindromic sequences including, the 5'-CG-3' motif, now called the CpG motif, which recently have been reported to activate TLR9 (90, 146).

When *M. tuberculosis* ligand(s) interact with TLRs, it ultimately leads to the activation of nuclear transcription factor (NF)- κ B and expression of pro-inflammatory cytokines, such as tumour necrosis factor (TNF)- α , interleukin (IL)-1, IL-12, chemokines, and nitric oxide, by myeloid differentiation primary response protein 88(MyD88)-dependent or MyD88-independent pathways (87,109, 110, 156).

The intracellular adaptor protein MyD88 is used by most of TLRs (with the exception of TLR3) to link receptor recognition with activation of IL-1R-associated kinase and TNFR-associated factor, translocation of NF- κ B and gene transcription (87, 109). Comparison of the susceptibility of wild-type and knockout mice to *M. tuberculosis* infection has revealed that MyD88 might be essential for the activation of innate immunity against the invasion of *M. tuberculosis* (64). It also has been reported that TLR4 can induce intracellular signals through the alternative pathway, which is mediated by an adaptor molecule, Toll/IL-1R (TIR), domain-containing adapter inducing interferon (IFN)- β (TRIF). Recently, this MyD88-independent, TRIF-dependent, TLR4-signalling cascade was revealed to be involved in LPS-induced

autophagy (222). However, various studies of TLR2-deficient mice have revealed variable susceptibility to *M. tuberculosis* infection (53, 189). It has been demonstrated that TLR4-deficient mice were not highly susceptible to *M. tuberculosis* infection (85, 160), whereas mice lacking both TLR9 and TLR2 showed high susceptibility to *M. tuberculosis* infection (12). These observations suggest that multiple TLRs are likely to be involved in mycobacterial recognition. On the other hand, it has been recently reported that triple knockout mice lacking TLR2/TLR4/TLR9 showed a milder phenotype in comparison to MyD88-deficient mice (87). Due to these findings, it could be suggested that further research is needed to explore whether TLRs, or molecules other than TLRs activating MyD88, mediate innate immune responses to mycobacterial infection.

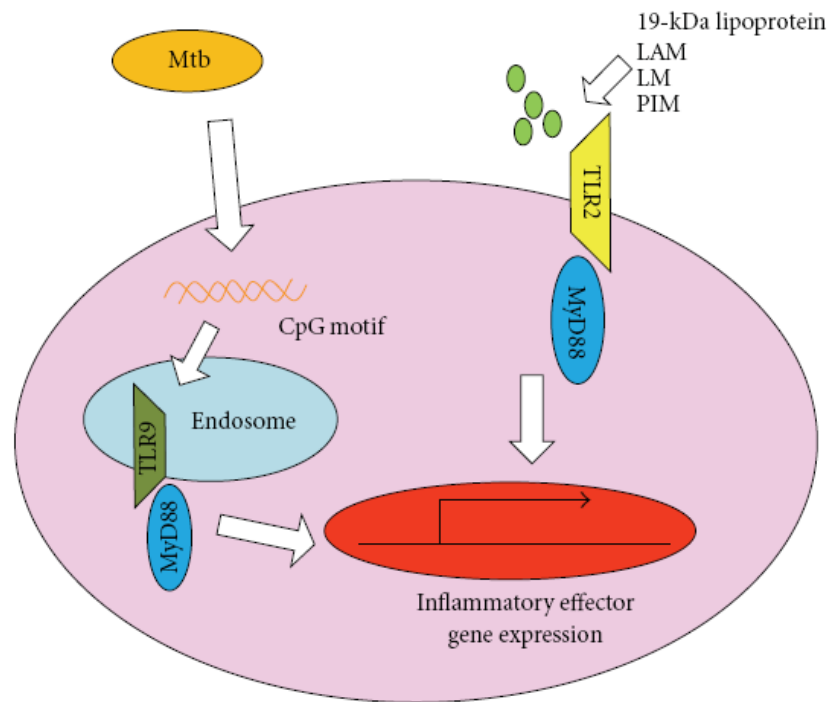


Figure 1.5.1 Toll-like receptors' recognition of mycobacteria. TLR2 recognises various components derived from mycobacteria. TLR9 identifies the DNA of mycobacteria including the CpG motif inside the endosomal compartments. TLR-dependent recognition of mycobacteria stimulates activation of signalling pathways through the adaptor molecule MyD88, resulting in the induction of gene expression. Reproduced from Saiga *et al.*, 2011.

The *M. tuberculosis* cell envelope is made up of a cell wall that is enclosed by a thick waxy mixture of lipids and polysaccharides, as well as a high content of mycolic acids. The most significant cell surface ligands of *M. tuberculosis* that interact with TLR and other receptors include the 19 and 27 kDa lipoproteins, 38 kDa glycolipoprotein, lipomannan (LM), and mannose-capped lipoarabinomannan (ManLAM) (110, 140). It has been reported that the 19kDa lipoprotein of *M. tuberculosis* can activate TLR2, thereby modulating the innate immune response and antigen-presenting cell function (8,

29, 72, 140). Studies have demonstrated that prolonged TLR2 signalling by *M. tuberculosis* lipoproteins could inhibit major histocompatibility complex (MHC)-II expression and processing of antigens by macrophages (66, 72, 140). Therefore, a subset of infected macrophages with a reduced ability for antigen presentation might not be able to present *M. tuberculosis* antigens to CD4⁺ T cells, thus leading to deficient stimulation of effector T-cells and resulting in evasion of immune surveillance by creating niches that ensure the survival and persistence of *M. tuberculosis* (109, 140, 168).

Recently, several publications have suggested that PRRs such as NOD-like receptors (NLRs), and C-type lectin receptors other than TLR might be responsible for activating innate immune responses (109, 194, 149, 227). Among these PRRs, NOD-like receptors and C-type lectin receptors have been implicated in the innate recognition of mycobacteria (Figure 1.5.2).

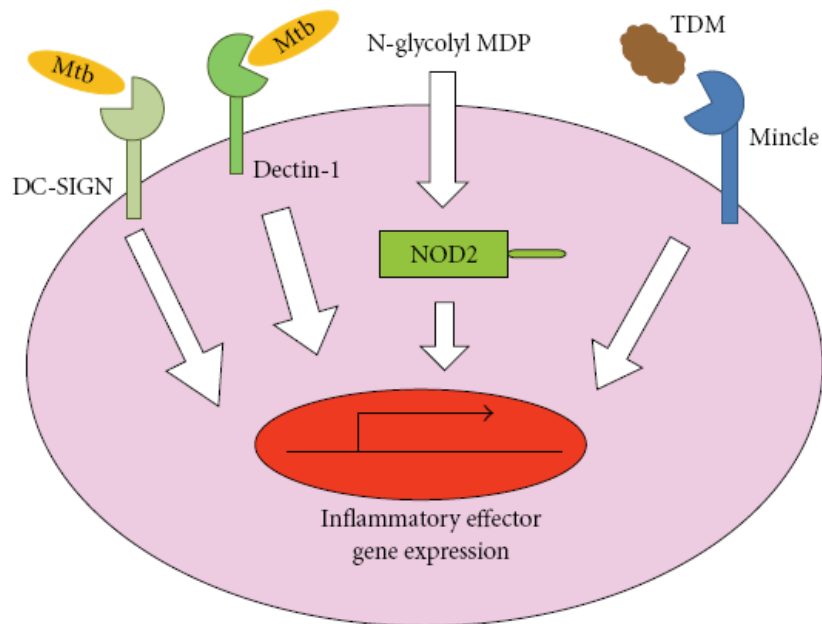


Figure 1.5.2 Mycobacterial recognition by pattern recognition receptors. Several pattern recognition receptors (for example NOD-like receptors and C-type lectin receptors) mediate the TLR-independent recognition of mycobacteria. NOD2, which belongs to the family of NOD-like receptors, recognises mycobacterial N-glycolyl MDP inside the cytoplasm. DC-SIGN and Dectin-1 are members of the class of C-type lectin receptors that are involved in mycobacterial recognition. Also, Mincle has been shown to identify TDM (a mycobacterial cell wall glycolipid). Reproduced from Saiga *et al.*, 2011.

Nucleotide-binding oligomerisation domain 2 (NOD2) is categorised under the family of NLRs, which are responsible for recognition of the bacterial peptidoglycan muramyl dipeptide (MDP) in the cytoplasmic compartment. The ligand for NOD2, MDP, is mostly N-acetylated in many bacteria. Mycobacteria, convert their MDP to an N-glycolylated form through the action of N-acetyl muramic acid hydroxylase (NamH) (42). Investigations using NOD2- knockout mice and *M. smegmatis* namH mutants have suggested that NOD2 recognises N-glycolyl MDP. The study also revealed that N-acetyl MDP is less potent compared to N-glycolyl MDP. This evidence suggests that NOD2 plays a significant role in the recognition of mycobacteria (149, 229). In addition, a study carried out on macrophages derived from NOD knockout mice demonstrated ineffective cytokine secretion post *M. tuberculosis* infection (51). Furthermore, it has been shown recently that *M. tuberculosis* can induce cytosolic NOD2 pathways, causing damage to the phagosomal membrane (149).

Other NLR family members, such as NLRP1, NLRP3, and IPAF can stimulate assembly of the inflammasome that results in caspase-1-dependent secretion of IL-1 β and IL-18 (178). However, the contribution of IL-1 β and IL-18 to mycobacterial infection was earlier demonstrated in studies using knockout mice (190, 226). A recent study demonstrated that mycobacteria inhibit the inflammasome-dependent caspase-1 activation that results in ineffective IL-1 β secretion (132). Therefore, it might be suggested that *M. tuberculosis* has developed a mechanism which evades inflammasome-mediated innate immune responses.

The C-type lectin receptors include the dendritic cell-specific intercellular adhesion molecule-grabbing non-integrin (DC-SIGN), Dectin-1, and Mincle (81,109, 227). DC-SIGN has been reported to identify mycobacteria and thus modulate the function of dendritic cells (76, 195). Dectin-1 recognition of mycobacteria resulted in stimulation of the expression of genes such as TNF- α , IL-6, and IL-12 (170, 224). A recent study revealed that macrophage inducible C-type lectin (Mincle) recognises trehalose-6,6'-dimycolate (TDM), which is the most explored mycobacterial cell wall glycolipid as far as the immunostimulatory component of *M. tuberculosis* is concerned (179, 96). The interaction between Mincle and TDM leads to modulation of macrophage activation.

TLRs and C-type lectin receptors are mainly produced on the plasma membrane or the endosomal/phagosomal membrane, while NOD-like receptors are expressed within the cytoplasm. In fact, distinct patterns of TLR- and NLR-mediated gene expression profiles have been reported in intracellular bacterial infection (114). Therefore, several PRRs recognise mycobacteria in distinct locations inside the host cells (macrophages) to synergistically induce effective host defence responses.

1.5.1 Mycobacterium ESX-1 secreted virulence factors that interact with TLRs

CFP-10 and ESAT-6 are secreted proteins expressed by the RD1 region, which contains part of the ESX-1 secretion system in *M. tuberculosis* that has been reported to play a significant role in the pathogenesis of tuberculosis during primary pulmonary infection (79, 91). The two proteins also have been identified as virulence factors in macrophages, lung epithelial cells, and dendritic cells (79, 206). A number of studies have investigated potential functions of the individual proteins. ESAT-6 has been shown to damp down expression of pro-inflammatory mediators such as the IL-12 p40 chain (IL-12p40), tumour necrosis factor (TNF), and nitric oxide¹³ through attenuation of the innate immune response (150). Data has shown that ESAT-6 is reduced TLR signalling by blocking the assembly of the cytosolic MyD88-dependent signalling scaffold (150). ESAT-6, interacting with TLR2, results in the activation of signalling dependent on phosphatidylinositol-3-OH kinase (PI(3)K)-Akt kinase, but not MyD88-IRAK-IKK (an inhibitor of NF- κ B (I κ B) kinase). The binding of ESAT-6 to TLR2 blocked ligand-mediated recruitment of IRAK4 to MyD88, thus preventing activation of NF- κ B (150). A recent study has identified TLRs (especially TLR2), which are present on the extracytosolic side of the plasma cell membrane and directly interact with a single peptide (from ESAT-6). This leads to inhibition of TLR signalling molecule assembly, which is essential for innate immune responses (150). ESAT-6 also induced the release of NO, as well as the expression of B7.1, MHC-II, and ICAM-1 surface molecules, but only when the macrophages were activated with IFN- γ (181).

Recently ESAT-6 has been reported to induce expression of matrix metalloproteinase-9 (MMP9) in epithelial cells surrounding infected macrophages. MMP9 increased recruitment of macrophages, promoting maturation of nascent granuloma cells and encouraging bacterial growth (211). However, T-cell interferon gamma secretion, IL-17, and TNF- α were inhibited by ESAT-6, which was not affected by the inclusion of CFP10 as part of the ESAT-6/CFP10 heterodimer (176, 214).

A series of reported studies have shown that CFP-10 and ESAT-6 occur in 1:1 ratio to form a stable heterodimeric complex (117, 163). The CFP-10/ESAT-6 complex is known to stimulate an immune response in the host organism (5, 135). The genes encoding both proteins are arranged as an operon that is co-transcribed and co-translated (21). Detailed biophysical investigations have compared ESAT-6, CFP-10, and the complex, and have shown that the complex is more thermodynamically and biochemically stable than the individual proteins (136, 162, 163). Earlier studies also have shown that a recombinant BCG strain that produced ESAT-6 alone could not provide more enhanced protection than the BCG strain (15), suggesting that the CFP-10/ESAT-6 complex might confer an enhanced protection *in vivo* compared to each of the proteins individually (CFP-10 or ESAT-6). Therefore, all the evidence points towards the suggestion that the native proteins function as a complex rather than individually. Moreover, fluorescence microscopy investigations have identified that the flexible C-terminal of the CFP-10 arm is responsible for specific binding to macrophages and monocytes. It has been suggested that a possible receptor-mediated signalling role may be attributed to the complex (162).

1.6 Prevention and Control of Tuberculosis

1.6.1 TB vaccination

Bacillus Calmette-Guérin (BCG) is the current vaccine to protect against tuberculosis. The BCG vaccine was derived from *M. bovis* at the Institute Pasteur in Lille, France, and the first use of BCG in humans was reported in 1921. Bacille Calmette-Guérin (BCG) is a live vaccine derived from attenuated strain of *M. bovis*, which is very closely linked to *M. tuberculosis* (138, 202). However, there are multiple genomic differences between them, including a region of difference (RD1) that is deleted from all types of the BCG strain but is present in all virulent species. The RD1 region includes the genes encoding ESAT-6 and CFP-10, which have been shown to play an important role in virulence during infection. Several studies have indicated that the deletion of RD1 from *M. tuberculosis* leads to a decrease in virulence (138, 144, 154, 163).

It is estimated that as of today the BCG vaccine has been given to over three billion people, making this vaccine the most used in the world. However, the current vaccine, *M. bovis* (BCG), provides inconsistent efficacy, varying between 0 and 80%. The precise causes of this variability have not yet been clarified (27, 48, 62). However, several hypotheses have been suggested to explain the limitation of BCG efficacy, for example, the use of different BCG strains, the age of individuals at vaccination, and the influence of prior infection with environmental mycobacteria. Another drawback of BCG vaccination is that it alters the skin hypersensitivity test and makes it unreliable. This skin test is used to determine the delayed type hypersensitivity (DTH) response by using purified protein derivative (PPD). The PPD contains TB antigens that are present in both pathogenic mycobacteria and non-pathogenic mycobacteria; hence this test

cannot distinguish between TB infection and BCG-vaccinated individuals or exposure to environmental mycobacteria (9, 208).

As mentioned above, the BCG vaccine has shown variable efficacy. If the BCG vaccine is to be successfully implemented in future vaccination programmes, it is necessary to improve its effectiveness. Therefore, several efforts to enhance the efficacy of the BCG vaccine have been made by using different strategies, including the complementation of the BCG vaccine with the expression of antigens that either are not expressed or have a very low level of expression in the BCG strain (48, 154). Previous studies have demonstrated that recombinant BCG(rBCG30) vaccine secreting the Ag85B protein (rBCG30) is more potent than the conventional BCG vaccine (88). Furthermore, other vaccine studies have shown that reintroduction of RD1 to BCG increases the amount of Ag-specific CD8⁺ T-cells, and also raises protection against tuberculosis in guinea pigs and mice (88, 144). Another strategy to improve the efficacy of the BCG vaccine is to use a combination of BCG, subunit vaccines, and DNA vaccines to increase the strength of BCG-induced immunity. This protective immunity was found to be due to activation of CD⁺4 and CD⁺8 T-cells, which produce INF- γ (159).

1.6.2 Treatment of Tuberculosis

Tuberculosis (TB) is an infectious disease and antibiotics are used to treat the patients. This practice has been going on for many years. These drugs are not used singly, because the regimens that use only single drugs result in the rapid development of resistance to a single drug and result in treatment failure (17). Therefore, the WHO has recommended DOTS, which stands for ‘Directly Observed Therapy, Short-course’, for its global TB eradication programme. Since its start in 1995, DOTS has been employed to treat millions of TB patients throughout the world. Since the introduction of DOTS, improvements in treatment outcomes for many patients have been observed (82, 221). In 2004, the WHO reported that 84% of newly diagnosed patients registered with DOTS were successfully treated. The standardised treatment in DOTS includes a six-month regimen comprising isoniazid (INH), rifampicin (RMP), and pyrazinamide (PZA) given for two months, followed by INH and RMP for four months. Ethambutol (EMB) is usually included in the initial regimen as well, because there is little possibility of drug resistance (17, 43, 173, 221).

It has been proposed that slow acting anti-tubercular agents coupled with a poor health care system might have led to a lack of treatment completion, relapse, and especially generation of resistant mycobacterial strains. Certainly, these risk factors could result in genetic mutation mostly detected in the targets or activator drugs, which might lead to a loss of susceptibility to anti-tubercular agents. The first-line anti-tubercular drugs including INH, RMP, and EMB, and second-line drugs such as ethionamide and capreomycin, with their respective mechanisms of action, are shown in Tables 1.6.2.1. and 1.6.2.2, respectively. These tables also, show some common mutations for current

first- and second-line anti-tubercular drugs, and refer to their respective mechanisms of action (173).

Drug-resistant strains of *M. tuberculosis* can be generally categorised into three groups: (I) strains that are resistant to one of the first-line anti-tuberculosis agents (Table 1.5.2.1) and have become common, (II) multidrug-resistant (MDR-TB) strains that are resistant to many antibiotics that are used to treat tuberculosis, particularly the first-line drugs INH and rifampicin and (III) extensively drug-resistant (XDR) bacilli, which show the greatest level of drug resistance (173).

Table 1.6.2.1: Mechanism of action of resistance of current first-line anti-tuberculosis agents (173).

Antibiotic	Mechanism and target	Mutations associated with resistance
Isoniazid	Inhibits mycolic acid synthesis; main target is <i>InhA</i> and secondary targets are <i>KasA</i> and <i>DfrA</i>	<i>KatG</i> (required for drug activation); <i>InhA</i> (promoter mutation)
Rifampicin	Inhibits transcription RNAPolymerase β subunits	<i>rpoB</i>
Ethambutol	Inhibits arabinogalactan synthesis;possibly EmbB	<i>embB</i>
Pyrazinamide	Unknown possibly inhibits FAS-or changes membrane energetic	<i>pncA</i> (required for drug activation)

Table 1.6.2.2: Mechanism of action, resistance of current second-line anti-tuberculosis agents (173).

Antibiotic	Mechanism and target	Mutations associated with resistance
Ethionamide	Inhibits mycolic acid synthesis; InhA	<i>ehtA</i> (required for drug activation and inhA promoter mutations)
Capreomycin	Inhibits protein synthesis; methylated nucleotides in both ribosomal subunits	<i>tlyA</i> and <i>rrs</i>
p-aminosalicylic acid	Inhibits folate metabolism; possibly dihydropteroate synthase	<i>tlyA</i>
Kanamycin	Inhibits protein synthesis	<i>Rrs</i>

1.7 Protein Secretion Systems in Mycobacterium

The ability of many bacteria to produce a pathogenic response depends on the secretion of virulence factors or toxins. These factors are: i) secreted in the extracellular environment of the host, ii) or inserted into host cells, iii) or displayed on the bacterial cell surface (2). Like other bacteria, mycobacteria use the General Secretion Pathways (GSP or Sec Secretion system) to secrete unfolded proteins with an N-terminal signal sequence across its plasma membrane. The composition of the GSP is SecA (ATPase), SecF, SecD, SecY, SecE and SecG membrane proteins. The function of SecA is that it recognises the signal sequence present at the N-terminal of the secreted proteins.

Interestingly, like Gram-positive bacteria, the mycobacterial GSP does not contain SecB (a molecular chaperone), which brings the unfolded form of the protein substrates from the ribosome to SecA. The mechanism used by mycobacterium to transport proteins across the thick cell wall and mycolate layer is unclear (49, 180). In contrast to the Sec-pathway, the mycobacteria also use a Sec-independent secretion pathway to export the folded proteins across the lipid bilayer of the plasma membrane using an energy-dependent pathway. This pathway is known as the Twin Arginine Transporter (Tat) and is used to export or translocate those proteins that have a specific N-terminal signal sequence. This signal sequence is somewhat similar to the structure of the Sec signal sequence, but also contains a specific motif containing two (twin) arginines followed by two uncharged amino acids close to the N-terminus (49, 153). Previous experimental studies have demonstrated that the mycobacterial Tat system is similar in structure and function to that of Gram-positive and Gram-negative bacteria (153).

Some secreted proteins lack conventional signal sequences and mycobacteria have a novel secretion pathway called the ESX (or Snm) secretion system (2, 153). This system has been shown to be responsible for secretion of Esx-like proteins, including ESAT-6 and CFP-10, which lack conventional signal sequences at their N-terminals. Snm systems are complicated pathways and use many proteins encoded by different loci in the genome of *M. tuberculosis*. *M. tuberculosis* has five gene clusters (ESX-1 to ESX-5) for ESX secretion systems. The most extensively studied ESX secretion system is the ESX-1 secretion pathway (23, 49, 117). Genetic analyses have shown that many of the proteins of the ESX-1 pathway are encoded at the genomic locus known as Region of Difference-1 (RD-1) (2, 49, 65, 124, 157). Using *M. bovis* BCG and *M. microti* strains

complemented with an extended RD1 region, Rv3868, Rv3870, Rv3871, Rv3872, and Rv3877 were found to be essential for secretion of the ESAT-6-CFP-10 complex. In addition to the RD1 region, another locus coding for Rv3616c-Rv3612c is required for the secretion pathway (65, 124, 157).

1.8 *M. tuberculosis* Virulence Factors

During recent years, a lot of knowledge has been obtained about *M. tuberculosis*, however, the causes of virulence and pathogenesis are still not clearly understood. Recently, several methods of investigation, such as proteomic analysis, genetic analysis, and comparative genomic approaches have allowed researchers to identify many important genes and their products believed to be involved in the pathogenesis of this bacterium. One of the protein families secreted by *M. tuberculosis* is the ESAT-6/CFP-10 protein family which are considered as virulence factors. For instance, ESAT-6 and CFP-10 proteins which are a member of this family appear to be involved in the pathogenesis of *M. tuberculosis* because the deletion of RD1 (that contains ESAT-6 and CFP-10 proteins) from virulent *M. tuberculosis* led to a significant reduction in the virulence of this pathogen (65, 155). However, the reintroduction of this region into the *M. bovis* BCG strain (non-pathogenic) results in a significant increase in virulence of the recombinant BCG strains (155).

1.8.1 ESAT-6/CFP-10 Protein Family

The ESAT-6 (EsxA) and CFP-10 (EsxB) proteins are members of a large family called the ESAT-6/CFP-10 protein family (ESX). Genomic analysis has shown that the *M. tuberculosis* genome has 22 genes encoding for ESAT-6/CFP-10 related proteins, which are found at 11 loci (117, 118, 142, 163). The family are typically arranged as tandem pairs within the genome, suggesting that they are co-transcribed, as demonstrated for ESAT-6 and CFP-10, which form a tight 1:1 complex. The presence of other *esx-like* genes in tandem in the *M. tuberculosis* genome suggests that their protein products could also form complexes (117, 118). Proteins in this family contain approximately 100 residues and most family members are preceded by PE/PPE proteins and are characterized by their conserved central tryptophan-variable-glycine (WXG) motif (2, 117, 118, 142, 163). The WXG motif is present in the loop that connects the two main helices of ESAT-6 and CFP-10 (discussed in chapter 2). In addition, the ESAT-6/CFP-10 protein family includes a number of immune-dominant antigens such as ESAT-6/CFP-10, Rv0287/Rv0288 and members of the subfamilies are called the M.tb9.9 family, consisting of five genes (*esxI*, *esxL*, *esxN*, *esxO* and *esxV*) and second subfamily, the QILSS family, includes five neighbouring genes (*esxJ*, *esxK*, *esxM*, *esxP* and *esxW*), which are strongly recognised by T-cells from infected individuals or in animal models of tuberculosis (166, 169, 182, 183). Although members of the ESAT-6/CFP-10 family lack a signal sequence, they are shown to be present in short-term culture filtrates of *M. tuberculosis*.

1.9 Scope of the Thesis

The aims of the work described in this thesis include:

I) The determination of the molecular features of the proteins encoded by *esxO* and *esxP*, which are members of Esx family and might be very important virulence factors involved in TB pathogenesis. The primary aim of this chapter was to determine molecular features of the proteins, to describe and characterise the stability of complex formation between the EsxO and EsxP. Furthermore, the structure of EsxO/EsxP complex will be predicted based on multiple sequence alignments across Esx family members and the knowledge of structures of EsxA/EsxB and EsxG/EsxH complexes.

II) Investigation of the binding of EsxO/EsxP complex to the surface of host cells. Fluorescence microscopy assays were used to determine the binding of Alexa Fluor labelled EsxO/EsxP complex to the surface of host cells, including monocyte, macrophage and fibroblast cell lines. The demonstration of specific binding between the complex and the surface of host cell lines was carried out by exposure of the host cells to both labelled and unlabelled complex. A confocal microscope was used to determine the location of the complex, whether on the surface of host cells or within host cells. In addition, the interaction between EsxO/EsxP complex and host cells was compared with the interaction between EsxA/EsxB complex and host cells, which was demonstrated in a previous study.

III) Examination of the two potential roles of the EsxO/EsxP complex as previous findings in chapter three suggested earlier. Firstly, I examined whether the EsxO/EsxP

complex has any function that influences the motility of macrophages when J774 cells were exposed to the complex. Lastly, microarray analysis was used to identify any changes in the gene profile expression when the treated and untreated cells were compared.

Chapter 2

Molecular features and structural properties of proteins encoded by *esxO* (Rv2346c) and *esxP* (Rv2347c) genes.

2.1 Introduction

Comparative genomic studies identified five RD1-like regions (region of difference) (regions 1-5), which are present in the genome of *M. tuberculosis* (3, 7). These five loci contain two members of the ESX family; most of these family members are preceded by a PE PPE pair, as well as being flanked by genes encoding putative ABC transporters, ATP binding proteins, and other potential membrane proteins. Moreover, in some of the regions there are some unique genes, which might encode specific molecules or secreted substrates (2, 73, 117, 142).

There is a striking homology among regions 1, 2 and 5, as shown in figure 2.1. Regions 2 and 5 have another complex of ESX-like genes as a tandem pair, preceded by *pe-ppe* genes, which is similar to the RD1 region that has *esxA* (ESAT-6), *esxB* (CFP-10) genes (73, 117, 142). The EsxA/EsxB (ESAT-6/CFP-10) complex and Esx-like proteins lack conventional signal sequences, suggesting that genes are situated surrounding the Esx family genes, that may have an important role in the secretion system (2, 117). It has been demonstrated that ESAT-6, CFP-10 and Esx protein family members secreted, EsxG, EsxH by region 3 and EsxN, EsxM by region 5, as well as the Esx family which has high similarity to region 3 (EsxS/EsxR) and region 5 clusters (EsxI/EsxJ, EsxK/EsxL, EsxO/EsxP and EsxV/EsxW), have been detected in the culture supernatant

of *M. tuberculosis* (2, 117, 128). However, there is no experimental evidence that Esx family homology of regions 2 and 4 are secreted in the culture supernatant (2).

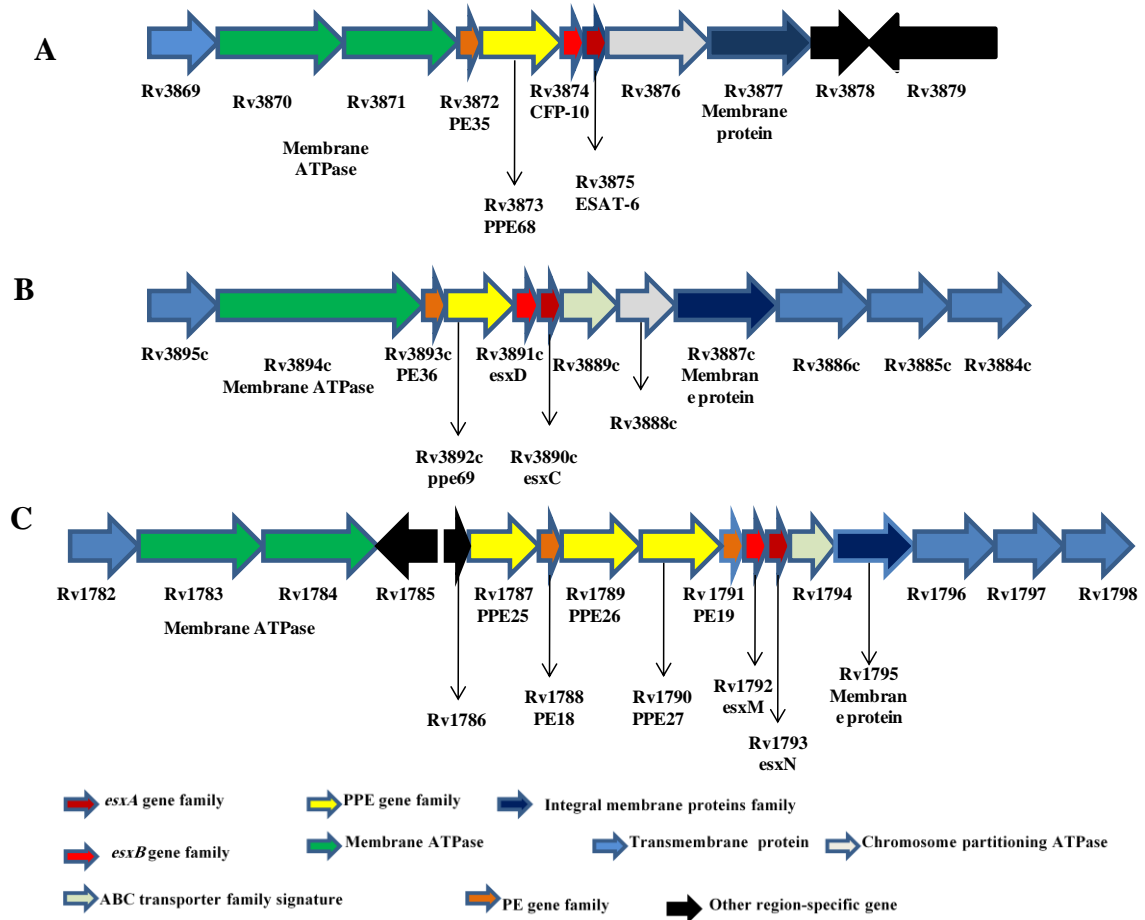


Figure 2.1 Schematic representation of *M. tuberculosis* *esxA/esxB* (ESAT-6/CFP-10) gene clusters 1 (RD1) (A), region 2 (B), and region 5 (C). The figure shows that the ESX-like genes are present in all regions, indicated by red and dark red colours. The supposed membrane associated proteins are shown by the dark blue colour. The putative membrane ATPase is highlighted by the green colour. Region 5 is likely to be responsible for exporting several closely related pairs Esx family complexes include the EsxO/EsxP complex (2, 73).

The distinct similarity between these regions (ESX-1-ESX-5) is the presence of ESX family members. For instance *esxA* (ESAT-6) and *esxB* (CFP-10) (Rv3874 and Rv3875 genes respectively) are found in the RD1, which contains nine genes from Rv3971 to Rv3979. This region has an important role in the virulence of *M. tuberculosis*. Hence, deletion of RD1 from *M. tuberculosis* led to a significant reduction in the virulence of the pathogen but when the region was re-introduced into the *M. bovis* BCG strain, this resulted in enhanced virulence of the recombinant strain. Therefore, it is clearly indicated by this evidence that EsxA (ESAT-6) and EsxB (CFP-10) are implicated in *M. tuberculosis* pathogenesis (65, 117, 154, 155). Furthermore, both EsxB (CFP-10) and EsxA (ESAT-6) are potent T-cell antigens in a range of TB infected hosts, including guinea pigs, cattle and humans (32, 186, 208). Although there is extensive research interest in the EsxA/EsxB (CFP-10 ESAT-6) complex, the function and mechanism of the action of this protein complex remains unknown. However, studies have suggested that EsxB (CFP-10) and EsxA (ESAT-6) mediate the aggregation of host macrophages that help in the intracellular spread of the mycobacterium (58, 212).

Previous studies have shown that EsxB (CFP-10) and EsxA (ESAT-6) proteins depend on each other for secretion, stability and dimer formation. The high resolution solution structure of the EsxA/EsxB complex has revealed that the complex contains two helix-turn-helix hairpin structures formed from the individual proteins, which are held together by extensive hydrophobic interactions and lie anti-parallel to each other to form a four-helix bundle, as shown in figure 2.2 (117, 128, 147, 164). The carboxy-terminal of EsxB (CFP-10) does not contribute to the formation of the dimer. The

flexible arm in the C-terminal of EsxB (CPF-10) is believed to be responsible for binding to a surface receptor on macrophages (162).

In addition, another member of Esx family, EsxG/EsxH, has been shown to form a tight complex consisting of a four helix bundle (93). Therefore, it could be speculated that the formation of a tight complex will be a common feature across the whole family.

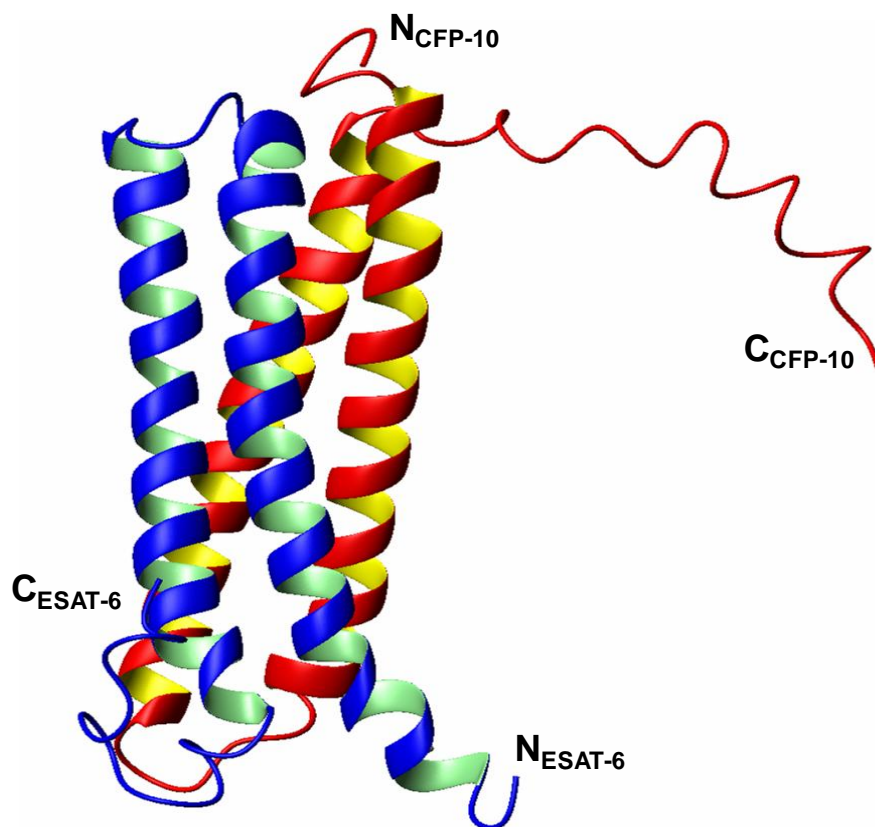


Figure 2.2 The solution structure of the EsxA/EsxB complex, illustrating two helix-turn-helix hairpin structures formed from individual protein EsxA (ESAT-6) (blue) and EsxB (CFP-10) (red). The proteins lie anti-parallel to each other to form a stable four-helix bundle. It is clearly shown that the C-terminal of EsxB (CFP-10) is unstructured and does not participate in the complex formation). Reproduced from Renshaw *et al.*, 2005.

Several members of the Esx family have been demonstrated to be potent T-cell antigens, suggesting that this family might have a critical role in pathogenesis (7, 50, 130). Moreover, the Esx family is conserved in *M. leprae*, which indicates their importance in the pathogenesis of mycobacteria. It is because the *Mycobacterium leprae* genome has undergone extensive reductive evolution that they retained the minimum number of functional genes that produce proteins responsible for a pathogenic mycobacterium (39).

The phylogenetic tree depicted in figure 2.3 clearly illustrates that EsxA (ESAT-6) and EsxB (CFP-10) are conserved individually in *M. leprae* (ML0049 and ML0050), whereas the single pair of *M. leprae* proteins (ML1055/1181 and ML1056/1180) seems to substitute for five pairs of *M. tuberculosis* proteins in groups A/A' (EsxI/EsxJ (Rv1037c/Rv1038c), EsxK/EsxL (Rv1197/Rv1198), EsxM/EsxN Rv1792/Rv1793, (EsxO/EsxP) Rv2346c/Rv2347c and (EsxV/EsxW) Rv3619c/Rv3620c). This might indicate some function redundancy, and may possibly provide greater functional flexibility within *M. tuberculosis* (118, 163).

Some members of the Esx-like protein family are more closely related than others. For instance, the high sequence relatedness between members within groups A and A' is approximately >90%. The high degree of sequence homology can be used to divide the Esx family into further individual gene protein subfamilies. One of these subfamilies is called the M.tb9.9 family, consisting of five genes (*esxI*, *esxL*, *esxN*, *esxO* and *esxV*). The second subfamily, the QILSS family, includes five neighbouring genes (*esxJ*, *esxK*, *esxM*, *esxP* and *esxW*), whose C-terminal pentapeptide is QILSS (117, 182). However,

groups C/C' (EsxA/EsxB) and D/D' (EsxC/EsxD) seem to be more distantly related, indicating the unlikely formation of a non-genome partner complex (163).

The groups A/A' share a high level of homology at the amino acid level (>90%), suggesting gene duplication within *M. tuberculosis*. Different studies have shown that several members of groups A and A' have been detected in the culture supernatant of *M. tuberculosis* (7, 130, 225). However, EsxN/EsxM is the only pair of these groups present in a large cluster gene called region 5, which has genes coding components of the secretion system and is situated surrounding EsxN/EsxM. Therefore, it is likely that the region is responsible for exporting closely related pairs EsxO/EsxP, EsxI/EsxJ, EsxK/EsxL and EsxV/EsxW out of the cytoplasm of the bacterium.

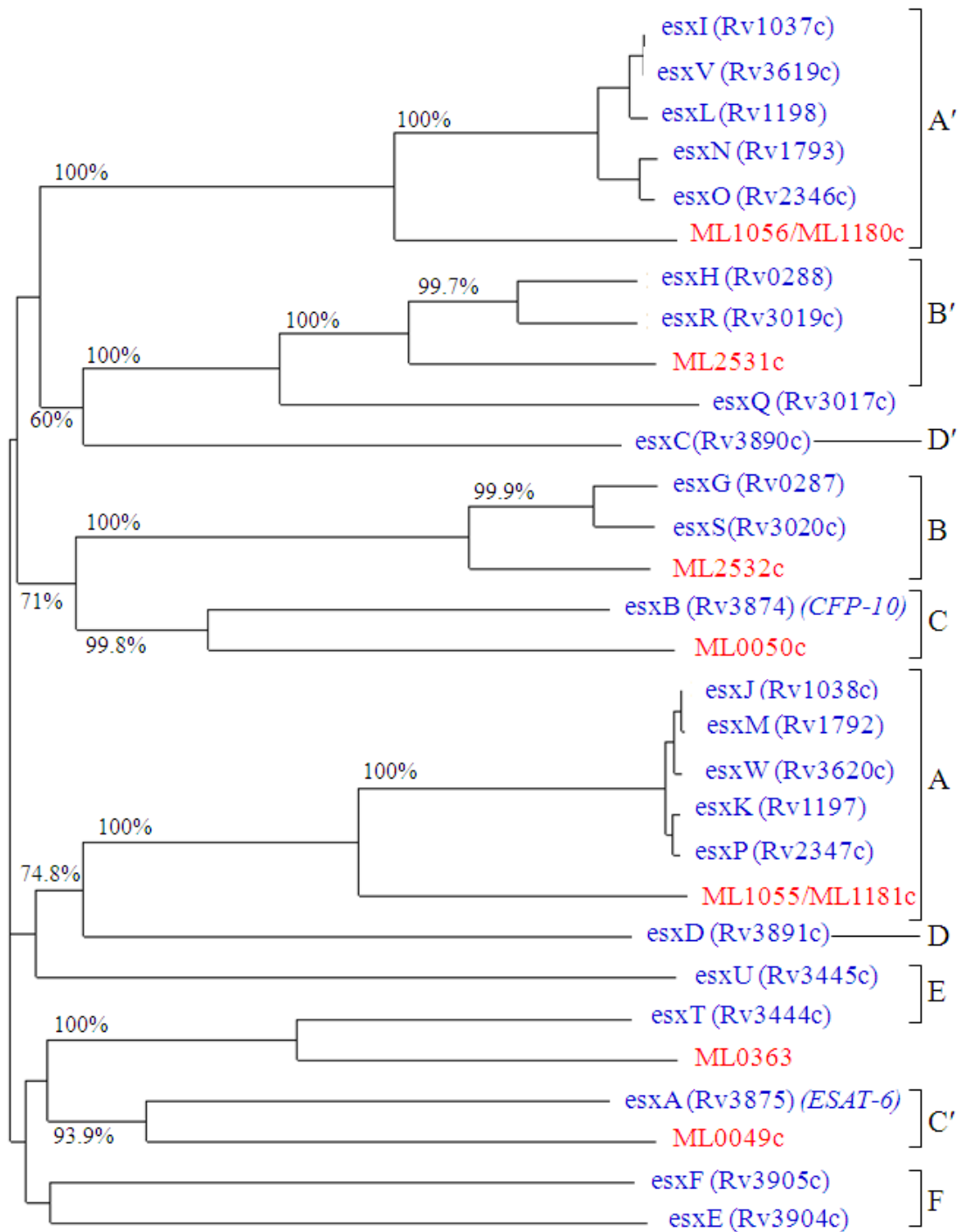


Figure 2.3 Phylogenetic tree for the Esx protein family *M. tuberculosis* (prefixed by Rv, blue) and their *M. leprae* homologues (prefixed by ML, red). There are 23 members of the Esx family. Twenty-two genes of this family are arranged as tandem pairs in 11 loci in the *M. tuberculosis* genome. Major pairings are indicated by square brackets and labelled (A pairs with A' etc.). Reproduced from Renshaw *et al.*, 2002.

Previous studies have indicated that EsxN and EsxM were encoded by the region 5 cluster. In addition, it has been shown that ESX family members such as EsxO and EsxP, which have a high similarity to EsxN and EsxM were present in the culture supernatant (7, 35, 183). Therefore, it is highly likely that EsxO and EsxP proteins secreted by the secretion system are present in region 5. Furthermore, an intact region 5 has fundamental function for secretion of ESX family membrane EsxN and EsxM by *M. tuberculosis*, which leads to region 5 being a functional secretion system, similar to region 1 (2, 4). Interestingly, it has been suggested that region 5 might have an effect on the cell-cell migration and might be required to transport PE and PPE proteins (3, 4).

The EsxO and EsxP are secreted proteins of *M. tuberculosis*, which are members of the Esx family (35, 128, 183). These genes are arranged in an operon-like structure on the *M. tuberculosis* genome, suggesting that they are transcribed as one messenger, as illustrated for ESAT-6 and CFP-10 genes (117, 123). EsxO and EsxP act as antigens that are strongly recognized by T-cells (1, 7, 182). There is no direct experimental evidence for the contribution of EsxO and EsxP to the virulence and pathogenesis of *M. tuberculosis*. However, some findings suggest a role for the Esx-like proteins in *M. tuberculosis* pathogenesis:

(I) Comparison between the level of synthesis of EsxO and EsxP secreted proteins in culture supernatant between two strains, the virulent H37Rv and attenuated H37Ra identified that EsxO and EsxP were absent from the culture supernatant of H37Ra when compared to the virulent H37Rv. This was due to a large number of mutations in genes

of *M. tuberculosis* H37Ra, contrasted with the corresponding *esxO* and *esxP* of *M. tuberculosis* H37Rv (111, 225).

(II) Bioinformatic analysis has shown that mycobacterial core genes include 219 genes conserved within *M. tuberculosis* H37Rv, *M. leprae* and other mycobacterial strains. *esxO* and *esxP* are found in this core, which indicates their importance to pathogenic mycobacteria (129).

(III) *M. leprae* closely resembles *M. tuberculosis*. However, the massive gene deletion observed in *M. leprae*, merely retains the minimum genes function required for pathogenic mycobacteria. This suggests that these genes functions are very significant for *M. leprae* pathogenesis and they also may be significant for other mycobacteria. *esxO* and *esxP* genes have homology, with identical genes pairs within *M. leprae* (ML1055/1056 and ML1180/ML118 respectively), that suggest their involvement in the pathogenesis of *M. tuberculosis* (39, 73, 117).

(IV) Moreover, genes encoding EsxO and EsxP were deleted from BCG strains; therefore, these proteins can be used as markers to differentiate between BCG vaccination and *M. tuberculosis* infections, which was demonstrated for ESAT-6 and CFP-10 in RD1, which is absent from BCG strains. Interestingly, although there is a high genome sequence homology between *M. tuberculosis* and *M. bovis*, the latter lacks a number of genes such as *esxO* and *esxP* genes. These genomic changes between the bacilli might be related to changes in their pathogenic properties (111, 164).

(V) It has been suggested that region 5 appears to influence cell to cell spread and escape from the macrophage. As previously mentioned, it is believed that EsxO and

EsxP use region 5 as a secretion system to transport out of the bacteria. Therefore, it may be suggested that these proteins are involved in pathogenesis if that region has a role in cell to cell spread and macrophage escape (2, 3).

(VI) The main feature of *M. tuberculosis* is that these organisms survive within macrophages and dampen maturation of the phagosome. Therefore, it is believed that many proteins secreted by *M. tuberculosis* play an important biological role by interacting with macrophages and that they inhibit killing mechanisms inside macrophages, suggesting that secreted proteins, such as Esx family proteins, play a crucial role in the virulence of *M. tuberculosis* (128).

2.2 Methods and Materials

2.2.1 Agarose gel electrophoresis of DNA

The preparation of PCR products and plasmid DNA were analysed by agarose electrophoresis using 1% w/v agarose gel in Tris-acetate-EDTA (TAE), pH 8. The DNA was prepared for analysis by mixing 1 μ l aliquots of PCR reaction sample with 4 μ l deionised H₂O and 1 μ l 6x Blue/orange loading dye (Promega). DNA gels were stained with ethidium bromide (EtBr) and visualised under UV light. The marker was used to identify the size of the DNA, 100 bp DNA ladder (Promega). The sample DNA and markers were applied on the gel and electrophoresis was carried out for 45 minutes at 100 V.

2.2.2 SDS-PAGE

SDS-PAGE was used to analyse and monitor the progress of protein purification. Usually 20 μ l protein samples were combined with 10 μ l DTT (50 mM) and 10 μ l 4x Nu-PAGE^(R) LDS sample buffer (Invitrogen). Samples were heated for 10 minutes at 70°C prior to loading on 4-12% acrylamide gradient, NuPAGE^(R) Bis-Tris Gels (Invitrogen) and run in MES SDS running buffer (Invitrogen), at a constant of 200 V for 35 minutes. Molecular weight markers (Ultra-low) were used for protein size reference. The gels were stained for 1 hour with Coomassie Brilliant Blue stain (2.59 g/L in 45% v/v methanol and 10% v/v acetic acid) and then de-stained, initially in fast Destain solution I (40% v/v methanol and 10% v/v acetic acid) for 30 minutes and then in Destain Solution II (10% v/v methanol and 5% v/v acetic acid) over night.

2.2.3 Ligation independent cloning (LIC-PCR)

In order to express EsxO and EsxP proteins with removable His₆-tag, the corresponding coding regions were cloned into the pLEICS-01 and pLEICS-05 expression vectors using Ligation independent cloning (LIC-PCR) method (also known as ligase-free cloning) to increase the speed and efficiency of the cloning of PCR products. In addition, with LIC-PCR, there is no need to ligate PCR products to a vector, and it does not depend on restriction sites. In this method, a complementary sequence is designed into the vector and PCR primers are used to amplify the target DNA. Controlled digestion of the PCR product and the vector with a 3'—5' exonuclease such as (Exonuclease III) was then used to create complementary bases for the 3' terminal sequence. When the insert and the vector are mixed, the PCR products are annealed to the constructed vector. The recombinant DNA vector is then used to insert into *E.coli* and the ligase of bacterial cells seals the single-stranded nicks and generates a covalently closed circular molecule of plasmid (11, 141).

2.2.3.1 PCR amplification of *esxC* (Rv3890c), *esxD* (Rv3891c), *esxO* (Rv2346c) and *esxP* (Rv2347c) genes

The *esxC*, *esxD*, *esxO* and *esxP* genes were amplified by PCR from the Bacterial Artificial Chromosome (Bac13, Bac134) DNA templates using Pfx DNA polymerase (Invitrogen). There were two types of primer used to amplify these genes, PCR prime designed with an N-terminal Tag and PCR primer designed without a Tag.

Table 2.2.3.1.1: PCR primer design for an N-terminal His₆- Tag of these genes

Primer name	The sequences of primer (5'—3')
<i>esxC</i> Forward	TACTTCCAATCC <u>ATGTCAGATCAAATCACGTATAAC</u>
<i>esxC</i> Reverse	TATCCACCTTTACTG <u>TCATTAGAACAAGCCCGCGAT</u>
<i>esxD</i> Forward	TACTTCCAATCC <u>ATGGTGGCAGACACAATTCAGGTA</u>
<i>esxD</i> Reverse	TATCCACCTTTACTG <u>TCAGGATCCGTGGCTAGC</u>
<i>esxO</i> Forward	TACTTCCAATCC <u>ATGACCATCAACTATCAGTTC</u>
<i>esxO</i> Reverse	TATCCACCTTTACTG <u>TCAGGCAGCTGGAGCCGAC</u>
<i>esxP</i> Forward	TACTTCCAATCC <u>ATGGCAACACGTTTTATGACG</u> <u>GATCGCG</u>
<i>esxP</i> Reverse	TATCCACCTTTACTG <u>TCAGCTGCTGAGGATCTG CTGGGA</u>

Table 2.2.3.1.2: Design without Tag of these genes

PCR primer	The sequences of primer (5'— 3')
<i>esxC</i> Forward	AGGAGATATTACAT <u>ATGTCAGATCAAATCACGTAT</u>
<i>esxC</i> Reverse	GAAGTAACAAGGTTCTCT <u>TCATTAGAACAAGCCCGC GAT</u>
<i>esxD</i> Forward	AGGAGATATACATAT <u>TGGTGGCAGACACAATTCAGGT</u>
<i>esxD</i> Reverse	GAAGTACAGGTTCTCT <u>TCAGGATCCGTGGCTAGCG</u>
<i>esxO</i> Forward	AGGAGATATACATAT <u>TGACCATCAACTATCAGTTC</u>
<i>esxO</i> Reverse	GAAGTACAGGTTCTCT <u>TCAGGCCCAGCTGGAGCCGAC</u>
<i>esxP</i> Forward	AGGAGATATACATAT <u>TGGCAACACGTTTTATGACGGA</u> <u>TCCGCACGCGAT</u>
<i>esxP</i> Reverse	GAAGTACAGGTTCTCT <u>TCAGCTGAGGATCTGCTG GGA</u>

Each reverse primer contained a stop codon, immediately after the last amino acid codon. PCR amplification was carried out in 50 µl reaction volume using a TECHNE thermal cycling system (TECHGCNE), 5 minutes initial denaturation at 94°C followed by 30 cycles of 1.0 minute at 94°C, 1.0 minute at 50°C for annealing, and 2.0 minutes at 68°C for extension. The final extension cycle was 5.0 minutes at 68°C. PCR products were identified by electrophoresis using 1% (w/v) agarose gel (section 2.2.1), and purified using the QIAquick PCR purification kit.

2.2.3.2 Ligation independent cloning (LIC-PCR) of the *esxO*, *esxP*, *esxC* and *esxD* coding regions

The pLEICS-01 and pLEICS-05 expression vectors (Figure 2.2.1, panels A and B; received from our collaborators at the University of Leicester) were digested by the restriction enzyme *Bse*RI to remove the inserted lethal *SacB* gene (the *Bacillus subtilis sacB* gene encodes levansucrase that induces lethality upon exposure to 5% (w/v) sucrose in the growth medium) (152). The freeze-dried 3'-5' exonuclease (supplied by In-fusion™ PCR Cloning Kit, Clontech) was then dissolved completely in 5 µl dH₂O. 2 µl of this enzyme, the linearised vector, and the purified PCR products were mixed together. This mixture was incubated at 37°C for 30 minutes in a water bath and then left to ligate at room temperature for 5 minutes.

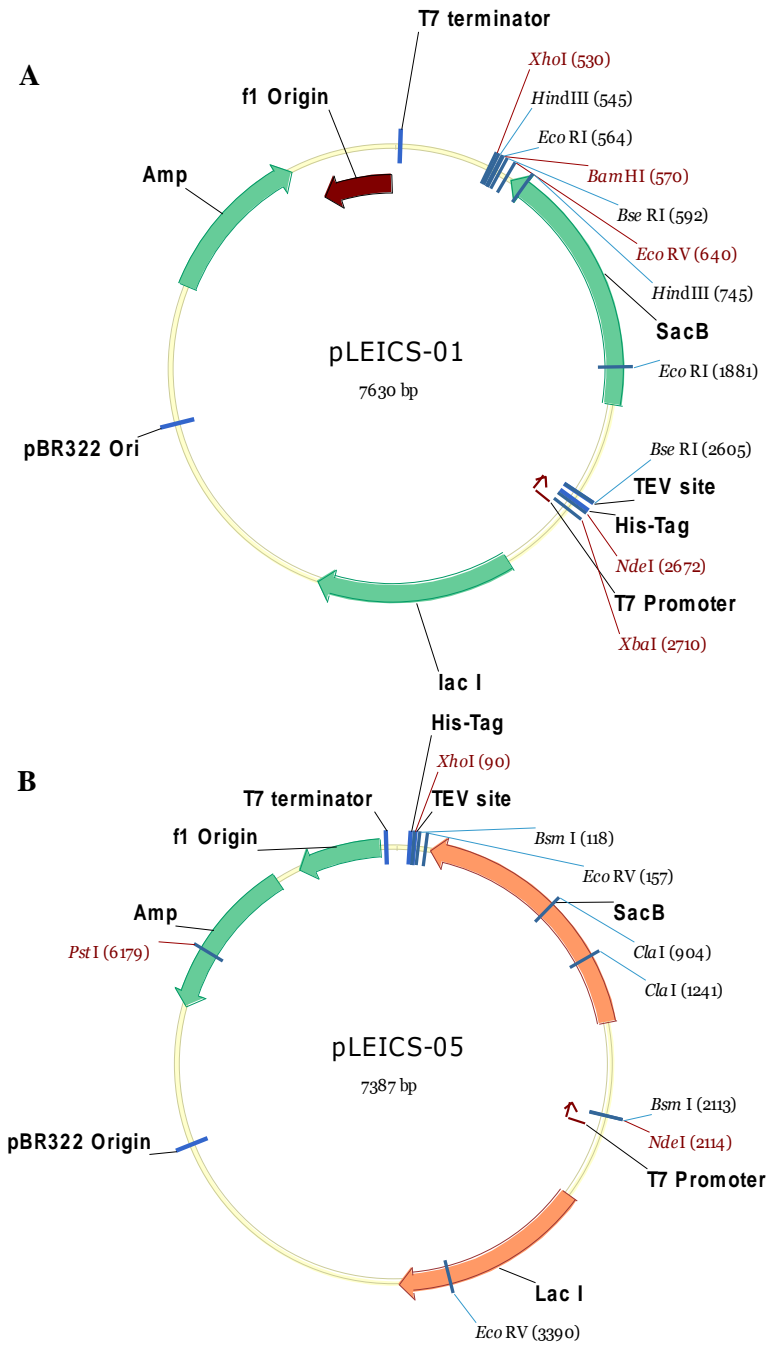


Figure 2.2.1 Maps of pLEICS vectors. Panels A and B show maps of pLEICS-01 and pLEICS-05 expression vectors, which are used to produce the proteins with N-terminal His₆-tag with pLEICS-01 and without His₆-tag with pLEICS-05 (because we added a stop codon before His-tag in the C-terminal). The vectors carry TEV protease cleavage site to remove the tags from the expressed proteins. Both vectors contain a bacterial origin of replication, which is indicated by (f1 origin). The vectors also contain the ampicillin resistance gene, indicated by (Amp) and the lethal *sacB* gene, indicated by (SacB), for the selection of transformed bacteria. As highlighted in the panels, both vectors contain two *BseRI* restriction sites, which allow for the removal of the lethal *sacB* gene.

2.2.3.3 Transformation of DH5- α competent cells with recombinant plasmids

Transformation was carried out by taking 50 μ l of *E.coli* DH5- α competent cells with constructs (Section 2.2.3.2). The transformants were incubated at 37°C for 30 minutes prior to plating out on LB agar plates supplemented with 5% (w/v) sucrose and 100 μ g/ml ampicillin. 5 % (w/v) sucrose and 100 μ g/ml ampicillin were used as markers for the selection of transformants (Section 2.2.3.2).

2.2.3.4 Sequencing of cloned DNA molecules

Five colonies were transferred separately into five tubes containing 10 ml LB broth and 100 μ g/ml ampicillin. These cultures were then incubated at 37°C in a shaker at a speed of 200 rpm overnight. The centrifuged cells were separated and used for extraction of plasmids using Miniprep (Promega). After isolation of the plasmids, the DNA from the plasmids was used for DNA sequencing, which was performed at the Protein Nucleic Acid Chemistry Laboratory (PNACL), at the University of Leicester.

2.2.4 Protein expression trials

Time-course expression trials were carried out using *E.coli* BL21star (DE3) strains transformed with the respective constructs. 50 ml of LB starter cultures containing 100 μ g/ml ampicillin were inoculated with one colony of each selected transformant and grown overnight at 37°C, and 200 rpm in a shaker. The cells were then centrifuged for 10 minutes at 5000 rpm. The pellets were resuspended in 1 ml fresh LB (without antibiotic) and subcultured into 50 ml LB broth containing 100 μ g/ml ampicillin, to a final OD_{600nm} of about 0.1. The cultures were grown at 37°C until

mid-log phase (OD_{600nm} 0.6-0.7), and 1 ml of each culture was removed and stored at -20°C for analysis of protein by SDS-PAGE. The cells were induced by addition of isopropyl β-D-thiogalactopyranoside (IPTG) 0.5 mM for transformants transfected with pLEICS-01 and pLEICS-05 constructs respectively, and 1 ml of cells were harvested every hour post-induction for 4 hours. Normalised pre- and post-induction samples were analysed by SDS-PAGE.

For the purpose of evaluation of the solubility of the expressed proteins, the induced cultures were subjected to centrifugation at 5000 rpm for 15 minutes then re-suspended and lysed by 15 ml lysis buffer. The samples were then incubated at room temperature for 30 minutes and then sonicated. 20 µl of the whole cell lysates were removed for SDS-PAGE analysis and the remaining samples were centrifuged at 12500 rpm for 20 minutes using a Beckman Coulter Avanti J-130I centrifuge. 20 µl of soluble fractions were finally removed for SDS-PAGE analysis.

2.2.5 Purification of EsxO and EsxP proteins

The full-length coding regions for *esxO* (*Rv2346c*) and *esxP* (*Rv2347c*) were cloned into pLEICS-01 and pLEICS-05 expression vectors as described previously (Section 2.2.3). The pLEICS-01 generated the construct encoding an N-terminal His₆-tag and TEV protease cleavage site (ENLYFQSM), followed by the *esxP* coding sequence. Expression was performed in *E.coli* BL21 (DE3) cells at 37°C, which were induced for 4 hours by the addition of isopropyl β-D-thiogalactopyranoside (IPTG) (1 mM) at an optical density of 0.6 at 600 nm (the mid-log phase of bacterial growth). With these experimental conditions, both EsxO and EsxP were found to be insoluble and

were initially isolated as inclusion bodies. EsxO and EsxP were co-refolded by solubilising the inclusion body pellets in a 25 mM NaH₂PO₄, 6 M guanidine HCl buffer (pH 8) at a protein concentration of 0.5 mg/ml, followed by dialysis against the same buffer without the denaturant at 4°C.

The protein concentration was estimated based on Coomassie blue staining of different concentration of lysozyme (0.1 mg/ml, 0.2 mg/ml and 0.3 mg/ml) on PAG (polyacrylamide gel). Based on this estimation, concentration of His₆-tagged EsxP and EsxO were approximately 0.2 mg/ml and 0.3 mg/ml respectively. EsxO and His₆-tagged EsxP were resolubilized individually in 30 ml of 6 M guanidine HCl buffer, after which the proteins were mixed together in final volume of 60 ml with a concentration of 0.5 mg/ml. The His₆-tagged EsxP and EsxO were mixed with molar ratio of 1:1.5 to make sure the tagged protein was saturated with protein without His₆-tag.

The soluble protein complex obtained was purified by nickel affinity chromatography (Ni²⁺-NTA affinity column). The volume of Ni²⁺-NTA affinity column was 6 ml and the gradient of imidazole concentration was from 0 to 500 mM. The EsxO and EsxP complex was eluted from the column in the 20 mM Tris-HCl buffer containing 172.5 mM imidazole. FPLC fractions containing the fusion proteins were pooled, and then treated with TEV protease. The His₆-tag was then removed by cleavage with the His₆-tagged TEV protease and the two products (the tag and the EsxO and EsxP complex) were separated by a second Ni²⁺-NTA affinity chromatography step. The protein was finally subjected to a polishing purification step by gel filtration chromatography on a Superdex 75 16/60 pre-packed column (Amersham Biosciences). The purified protein contained in 100 mM sodium chloride, 25 mM

sodium phosphate and 0.02% NaN_3 , at pH 6.5 was found to be greater than 95% pure by SDS-PAGE (Invitrogen 4-12% Bis-Tris NuPAGE gel system).

2.2.6 Protein concentration

The protein sample was concentrated by lyophilisation. In this technique the protein samples were frozen by liquid nitrogen, and the frozen samples were placed in a lyophiliser (ThermoSavant). The frozen water in the protein sample was then sublimated directly by a vacuum pump from solid to gas. The lyophilised samples were then resolubilised using an appropriate amount of distilled water to obtain the concentrated sample.

2.2.7 Far UV circular dichroism spectroscopy

The secondary structure of the purified proteins was determined by analysing for UV CD spectra acquired on a Jasco J-715 spectropolarimeter. All CD spectra were obtained from protein samples dissolved in a 100 mM NaCl and 25 mM NaH_2PO_4 buffer at pH 6.5 with a protein concentration of about 15-25 μM . Normally, spectra were recorded from 180 to 250 nm, with a scan speed of 20 nm per minute, response time 1 second, with each spectrum representing an average of 10 accumulations. During acquisition, the sample was maintained at a regulated temperature (25°C) in a 0.1 cm path length cell. Spectra were corrected for the buffer and converted to molar CD per residue before analysis by CD Pro package software (75, 99).

2.2.8 Thermal denaturation studies

The CD spectrum was used to study the effect of increasing temperature on the structural integrity of the purified proteins, which was studied by following the change in the CD spectra over a range of temperature from 5 to 100°C, increasing in 5°C increments. All CD spectra were obtained from protein samples dissolved in a 100 mM NaCl and 25 mM NaH₂PO₄ buffer at pH 6.5 with a protein concentration of about 15-25 µM for a path length of 0.1 cm and allowed to equilibrate at each temperature before data collection.

2.3 Results and Discussion

2.3.1 PCR amplification and ligation independent cloning of *esxC*, *esxD*, *esxO* and *esxP* genes

PCR amplification of *esxC* (288bp), *esxD* (324bp), *esxO* (285bp) and *esxP* (297bp) open reading frames were confirmed by agarose gel electrophoresis , as depicted in figure 2.3.1, which clearly shows the amplification of the genes of expected size.

The genes were purified and then cloned into pLEICS-01 and pLEICS-05 expression vectors by using ligation independent cloning (LIC-PCR), as described in section 2.2.3. All recombinant plasmids were transformed into DH5- α competent cells. Plasmids were then isolated by miniprep. The integrity of the expression vector was confirmed by DNA sequencing at the PNAC, at the University of Leicester.

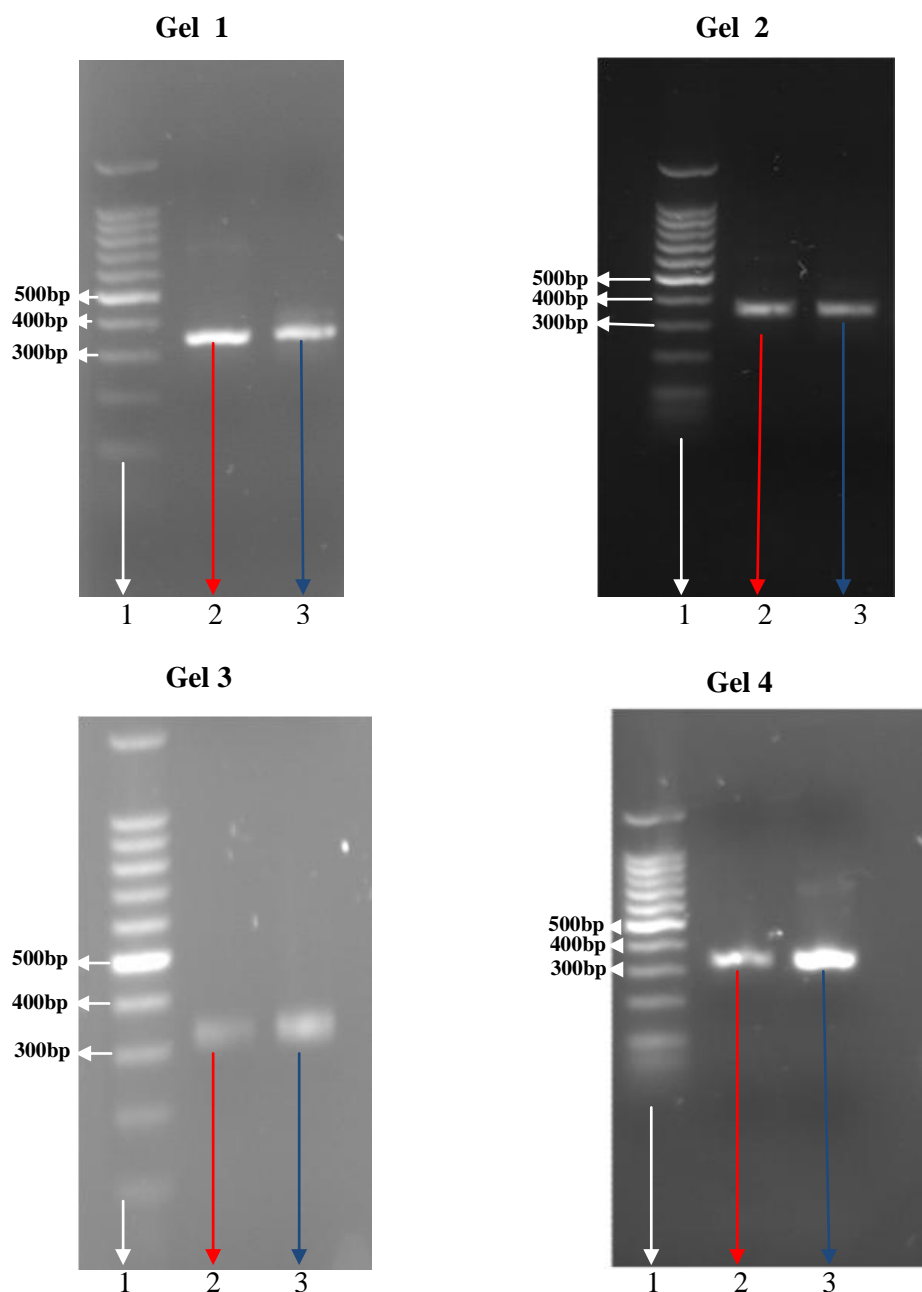


Figure 2.3.1 PCR amplification of *esxC*, *esxD*, *esxO* and *esxP* genes. Gel 1, 2, 3 and 4 are 1% w/v agarose gels viewed under UV light with ethidium bromide stain. In all gels lane 1 contains a 100bp DNA ladder. Gel 1; Lanes 2 and 3 correspond to PCR products of *esxC* with pLEICS-01 and pLEICS-05 vectors extension respectively. Gel 2; Lanes 2 and 3 correspond to PCR products of *esxD* with pLEICS-01 and pLEICS-05 vectors extension. Gel 3; Lanes 2 and 3 correspond to PCR products of *esxO* with pLEICS-01 and pLEICS-05 vector extension respectively. Gel 4; Lanes 2 and 3 correspond to PCR products of *esxP* with pLEICS-01 and pLEICS-05 vectors extension respectively.

2.3.2 Protein expression trial for recombinant EsxO, EsxP, EsxC and EsxD with and without a hexa-histidine extension sequence.

The evaluation of protein expression was performed using time course expressions. The results of expression trials for EsxO and His₆-tagged EsxO, EsxP and His₆-tagged EsxP, EsxC, His₆-tagged EsxC, EsxD and His₆-tagged EsxD were analysed by SDS-PAGE and are shown in figures 2.3.2, 2.3.3, 2.3.4 and 2.3.5. All the gels show the results of protein expression following a four hours time course and the solubility of the protein products using post-induction whole cell lysates and supernatant samples.

The evaluation of whether expressed proteins were produced as soluble or insoluble (inclusion bodies) products was determined by the difference in band intensities between the supernatant fraction, and the whole cell lysate post-induction fractions. The proteins were induced by using 0.45 mM IPTG at 37°C. For example, in figure 2.3.2, the expressed protein is clearly predominant in the soluble fraction after cell lysis.

The EsxO and EsxP proteins were expressed in significant amounts in the BL21 star system, with His₆-tag or without-His₆-tag systems (Figures 2.3.2 and 2.3.3), whereas the EsxC and EsxD proteins were expressed in host cells only when expressed without a His₆-tag (Figures 2.3.4 and 2.3.5). A series of experiments were conducted under different conditions, such as different concentrations of IPTG and different temperatures, but the expression of target proteins with His₆-tag was not achieved.

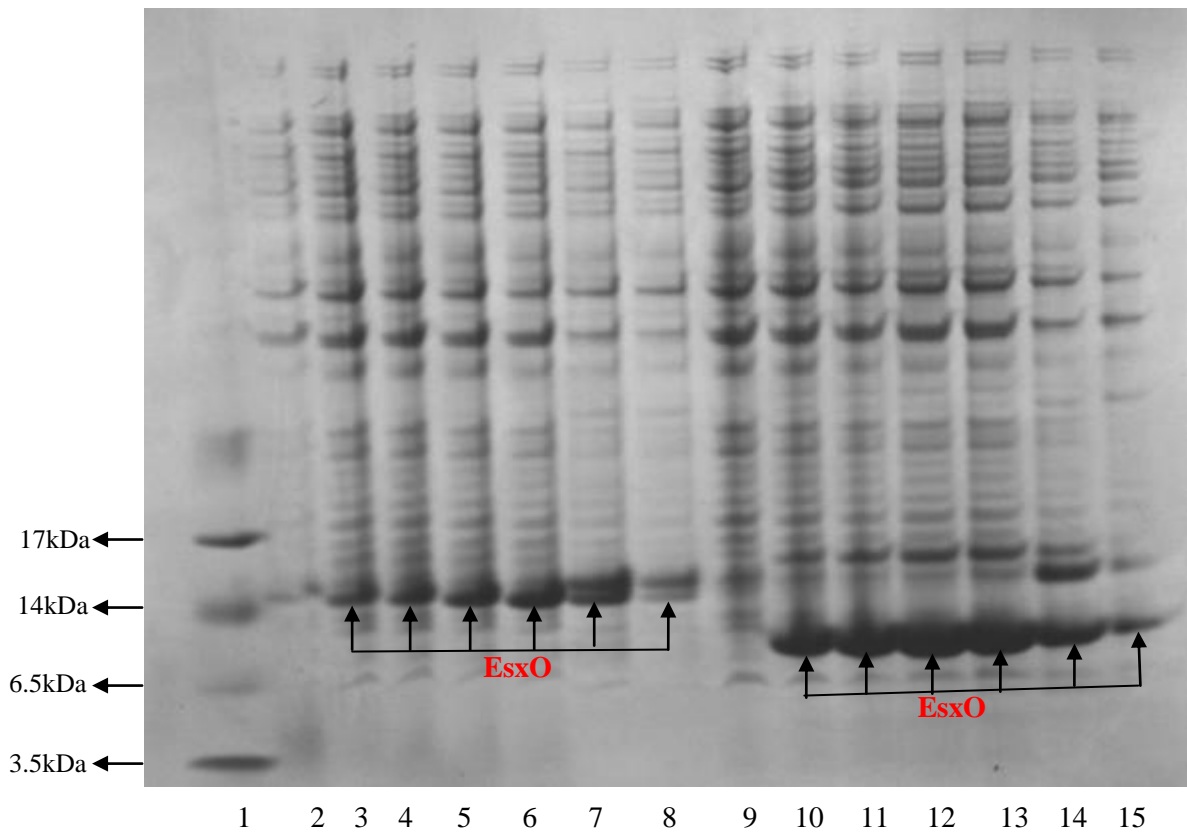


Figure 2.3.2 SDS-PAGE gel of EsxO expression trial. The gel shows a time course expression of the His₆-tagged EsxO and EsxO in *E.coli BL21star*(DE3) host strains. The solubility of the protein can also be judged from the gel. Lane 1 is a low molecular weight marker. Lane 2 is pre-induction. Lanes 3-6 are post-induction cell lysate of His₆-tagged EsxO fractions taken at 1, 2, 3 and 4 hours respectively. Lane 7 is whole cell lysate and lane 8 is supernatant of EsxO. Lane 9 is pre-induction. Lanes 10-13 are post-induction cell lysate of EsxO fractions taken at 1, 2, 3 and 4 hours respectively. Lane 14 is whole cell lysate and lane 15 is supernatant.

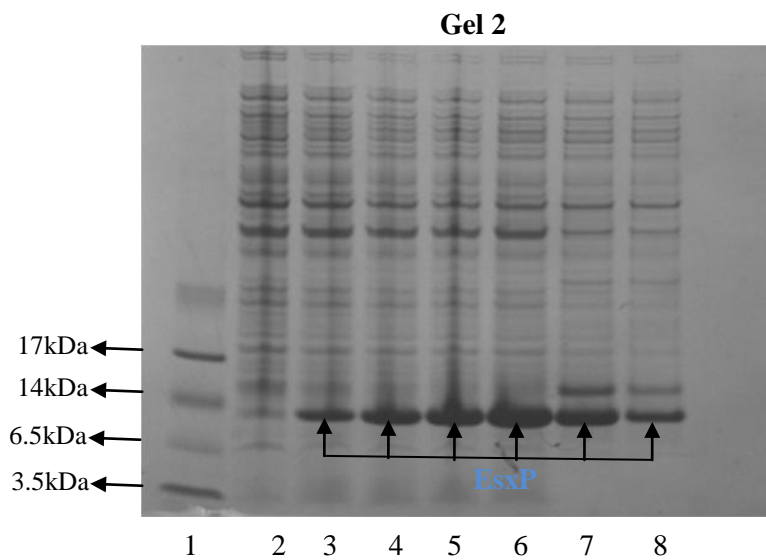
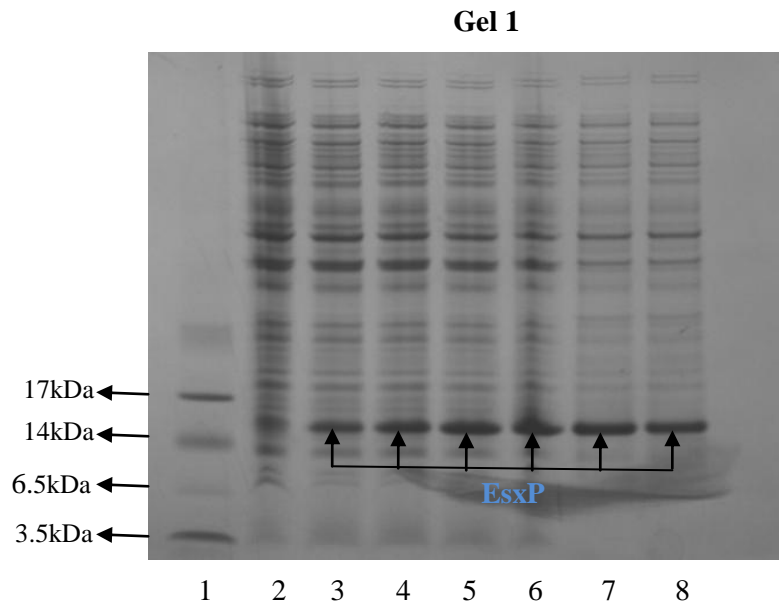
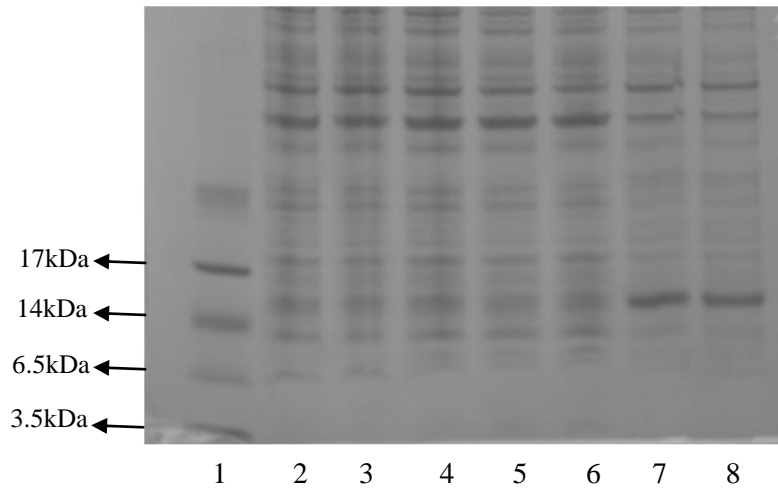


Figure 2.3.3 SDS-PAGE gels of EsxP expression trails. Gel 1 shows expression of the His₆-tagged EsxP in *E.coli BL21star* (DE3) host strains. Lane 1 is the low molecular weight marker. Lane 2 is pre-induction. Lanes 3-6 are post- induction cell lysate fractions taken at 1, 2, 3 and 4 hours respectively. Lane 7 is whole cell lysate and lane 8 is supernatant. Gel 2 is a time course expression of the EsxP in *E.coli BL21star* (DE3) host strains. Lane 1 is the low molecular weight marker. Lane 2 is pre-induction. Lanes 3-6 are post-induction cell lysate fractions taken at 1, 2, 3 and 4 hours respectively. Lane 7 is whole cell lysate and lane 8 is supernatant.

Gel 1



Gel 2

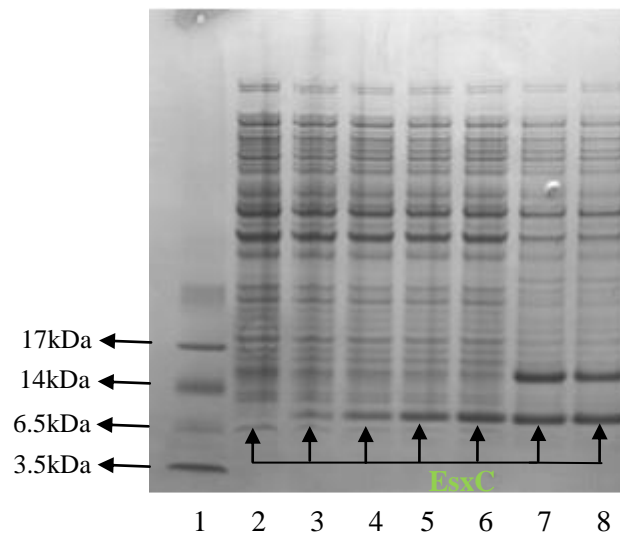


Figure 2.3.4 SDS-PAGE gels of EsxC expression trails. Gel 1 shows expression the His₆-tagged EsxC in *E.coli BL21star* (DE3) host strains. There is no evidence of EsxC expression. The Gel 2 is a time course expression of EsxC without a His₆-tag in *BL21star* cells. Lane 1 is the low molecular weight marker. Lane 2 is pre-induction. Lanes 3-6 are post-induction cell lysate fractions taken at 1, 2, 3 and 4 hours respectively. Lane 7 is whole cell lysate and lane 8 is supernatant.

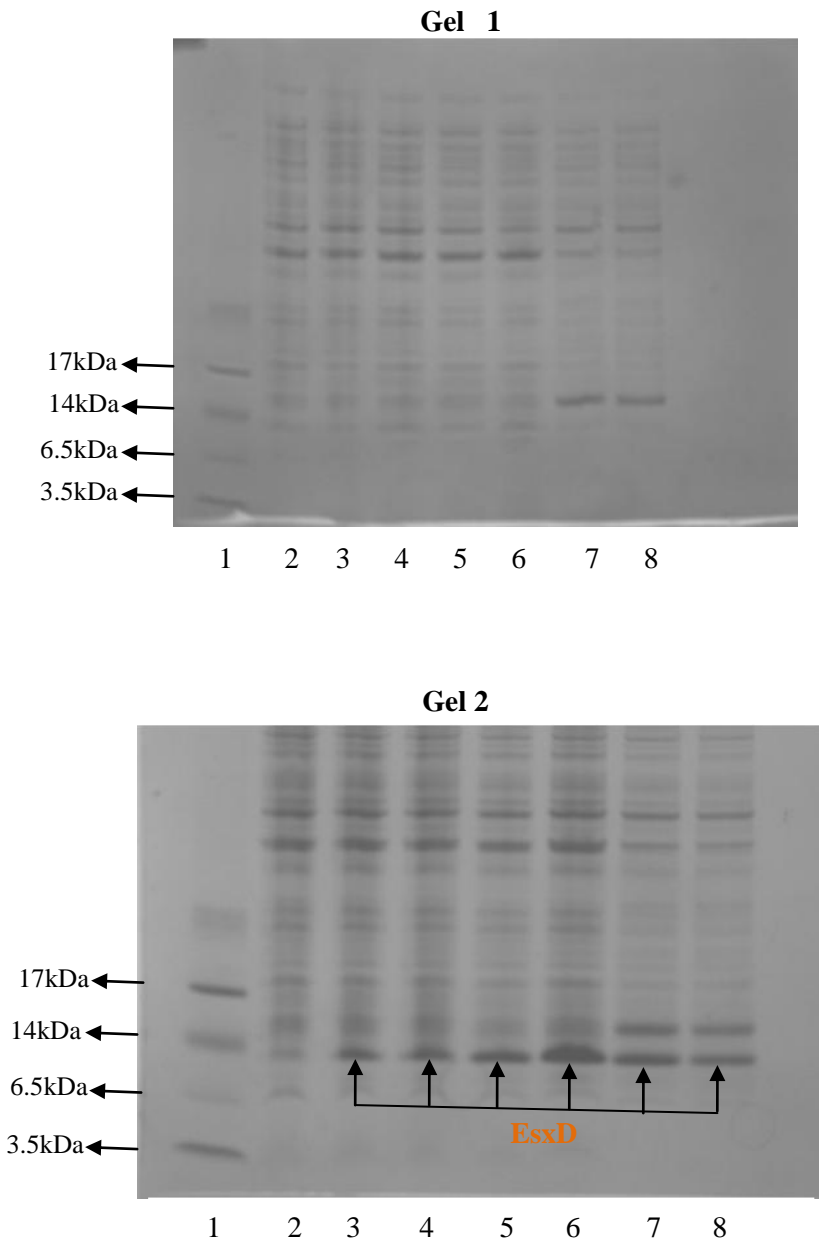


Figure 2.3.5 SDS-PAGE gels of EsxD expression trails. Gel 1 shows expression of the His₆-tagged EsxD in *E.coli BL21star* (DE3) host strains. There is no evidence of EsxD expression. The Gel 2 is a time course expression of EsxD without a His₆-tag in *BL21star* cells (DE3). Lane 1 is the low molecular weight marker. Lane 2 is pre-induction. Lanes 3-6 are post-induction cell lysate fractions taken at 1, 2, 3 and 4 hours respectively. Lane 7 is whole cell lysate and lane 8 is supernatant.

2.3.3 Expression and purification of EsxO/EsxP complex

The pLEICS-5-esxO and pLEICS-1-esxP constructs were used to produce EsxO and EsxP with His₆-tag in *E.coli BL21star* (DE3) host strains. The target proteins were expressed as insoluble products because of changes in the concentration of IPTG from 0.5 mM to 1 mM, which drove most of the proteins to insoluble form (Figure 2.3.6). The inclusion bodies were then resolubilized and co-refolded, as detailed in section 2.2.5.

As described in Section 2.2.5, both EsxO and EsxP were present as insoluble protein and were isolated as inclusion bodies. The inclusion body of both proteins were resolubilized in 30 ml of a 25 mM NaH₂PO₄, 6 M guanidine HCl buffer (pH 8). Then a ratio of 1:1.5 (EsxP with His₆-tag to EsxO without His₆-tag) was used for mixing both proteins at a protein concentration of 0.5 mg/ml, followed by dialysis against the same buffer without the denaturant at 4°C.

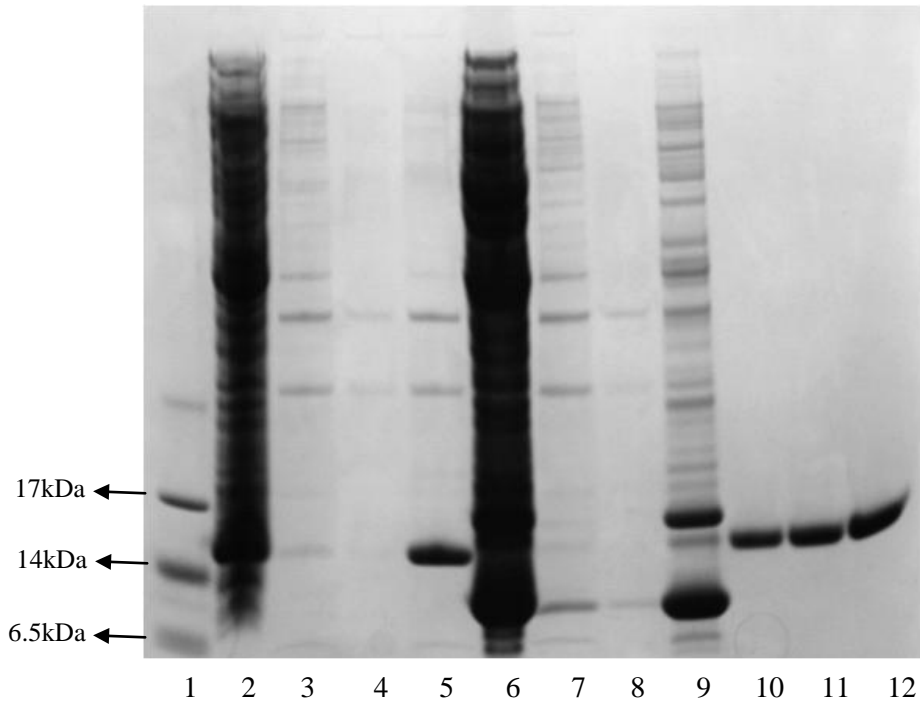


Figure 2.3.6 SDS-PAGE gel shows the steps involved in washing inclusion bodies for both EsxO without His₆-tag and EsxP with His₆-tag. Lane 1 is a low molecular weight marker. Lane 2 is the whole cell lysate fraction of EsxP with His₆-tag (from 500 ml culture). Lanes 3-4 are supernatant of wash steps 1 and 2. Lane 5 is whole inclusion bodies of the last wash step of EsxP with its tag protein (in 30 ml of wash buffer). Lane 6 is the whole cell lysate fraction of EsxO without His₆-tag. Lanes 7-8 are supernatant of wash steps 1 and 2 for EsxO without His-tag and lane 9 is whole inclusion bodies of last wash step of EsxP with His-tag protein (in 30 ml of wash buffer). Lanes 10, 11 and 12 are lysozyme the concentrations of these fractions are 0.1 mg/ml, 0.2 mg/ml and 0.3 mg/ml respectively.

The His₆-tagged EsxP containing, the N-terminal hexa-histidine tag allowed the His₆-tagged EsxO-EsxP complex to be purified by affinity chromatography, as shown in figure 2.3.7. Fractions containing the His₆-tagged EsxO/EsxP complex were pooled and treated with TEV protease to remove the N-terminal His₆-tag, as described in section 2.2.5. The cleaved His₆-tag was separated from the EsxO/EsxP complex by a second Ni²⁺-NTA affinity chromatography step, as shown in figure 2.3.8. The protein was finally subjected to a purification step by gel filtration, as shown in figure 2.2.9. The purified protein was found to be 95% pure by SDS-PAGE. The yield of the purified complex was determined to be approximately 7.4 mg in 10 ml of sample (0.74mg/ml), yielded from 500 ml culture for both types of proteins.

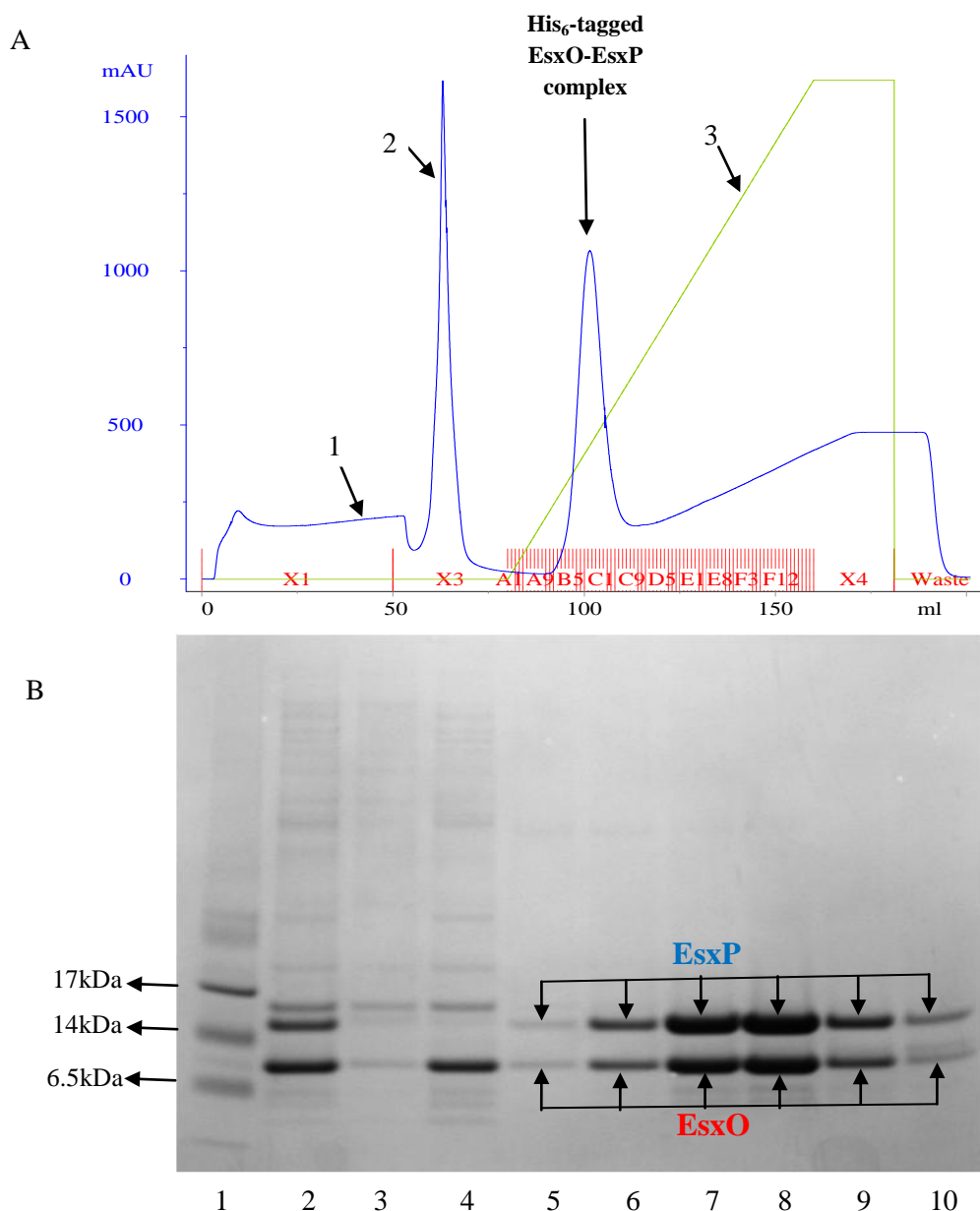


Figure 2.3.7 Purification of His₆-tag EsxO/EsxP complex. Panel (A) shows a typical FPLC profile attained for Ni²⁺-NTA column fractions of eluted His₆-tagged EsxO-EsxP as a complex. The complex was eluted over a gradient concentration of imidazole from 0 mM to 500mM (linear gradient indicated by 3). The wavelength was monitored on 280 nm. The first flow-through is indicated by 1 and the second flow-through, containing EsxO without His₆-tag, is indicated by 2. The His₆-tagged EsxO/EsxP as a complex elution peak is labelled. Panel (B) shows SDS-PAGE gel results for FPLC elution fractions, which contain His₆-tagged EsxO-EsxP without His₆-tag, as a complex (fractions B7, B11, C6, C7, C10 and D1). Lane 1 is a low molecular weight marker. Lane 2 is a loading sample. Lane 3 is X1 (flow-through). Lane 4 is X3 (flow-through). Lanes 6-10 are fractions of His₆-tagged EsxO/EsxP, as complex.

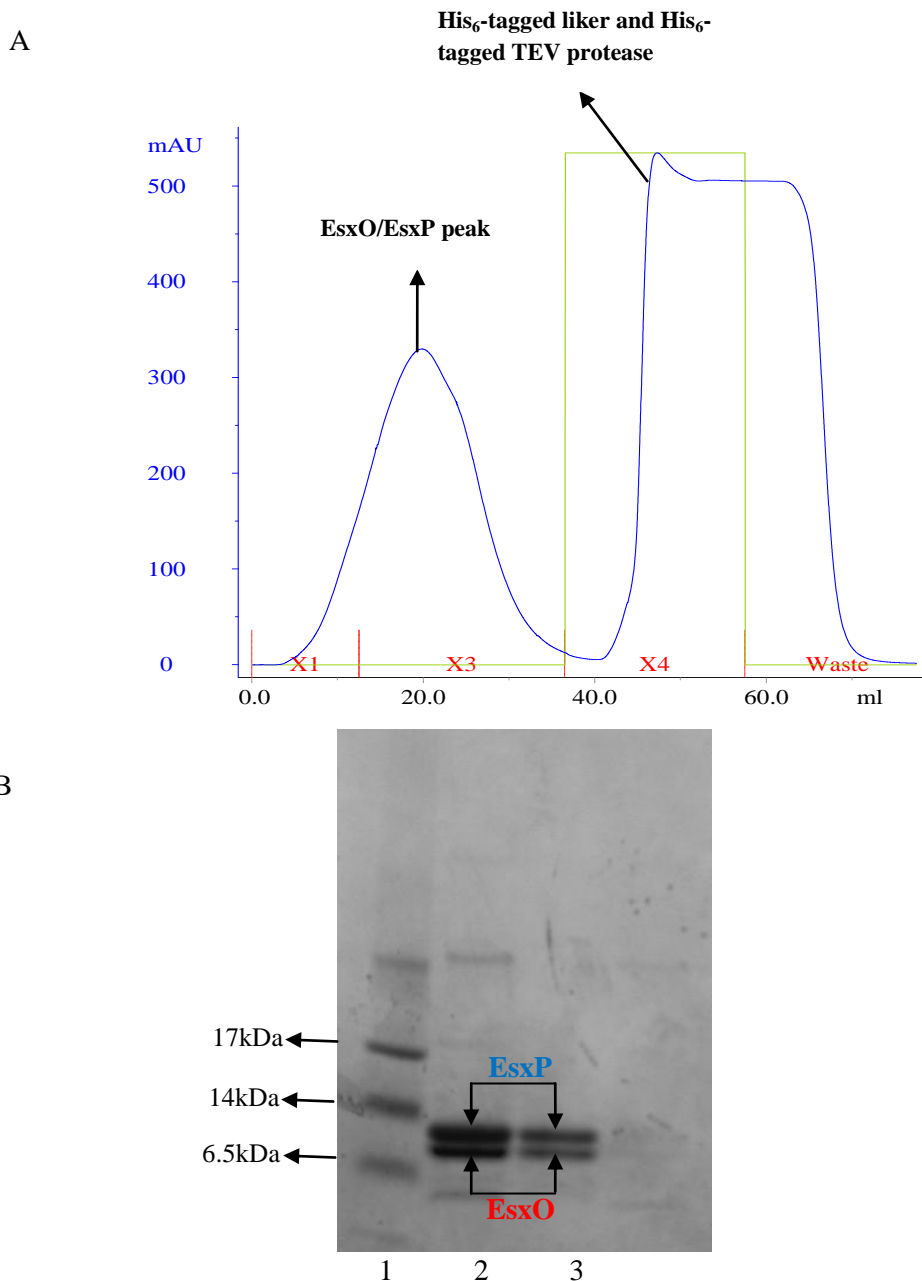


Figure 2.3.8 Purification of EsxO and EsxP, as complex by Ni²⁺ column following treatment with TEV protease. Panel (A) shows Ni²⁺-NTA elution profile of the treated protein sample. The protein complex without the His₆-tag was collected in fraction X1 and X3. The X4 contains His₆-tagged linker and His₆-tagged TEV protease which are eluted from Ni²⁺-NTA column in the 20 mM Tris-HCL buffer containing 500 mM Imidazole (the stepwise gradient of Imidazole from 0 to 500 mM is shown in green). Panel (B) SDS-PAGE gel shows Ni²⁺-NTA column fraction of eluted EsxO/EsxP complex following treatment with TEV protease. Lane 1 is a low molecular weight marker. Lane 2 is loading sample. Lane 3 is fraction of EsxO/EsxP as complex without the His₆ tag terminal.

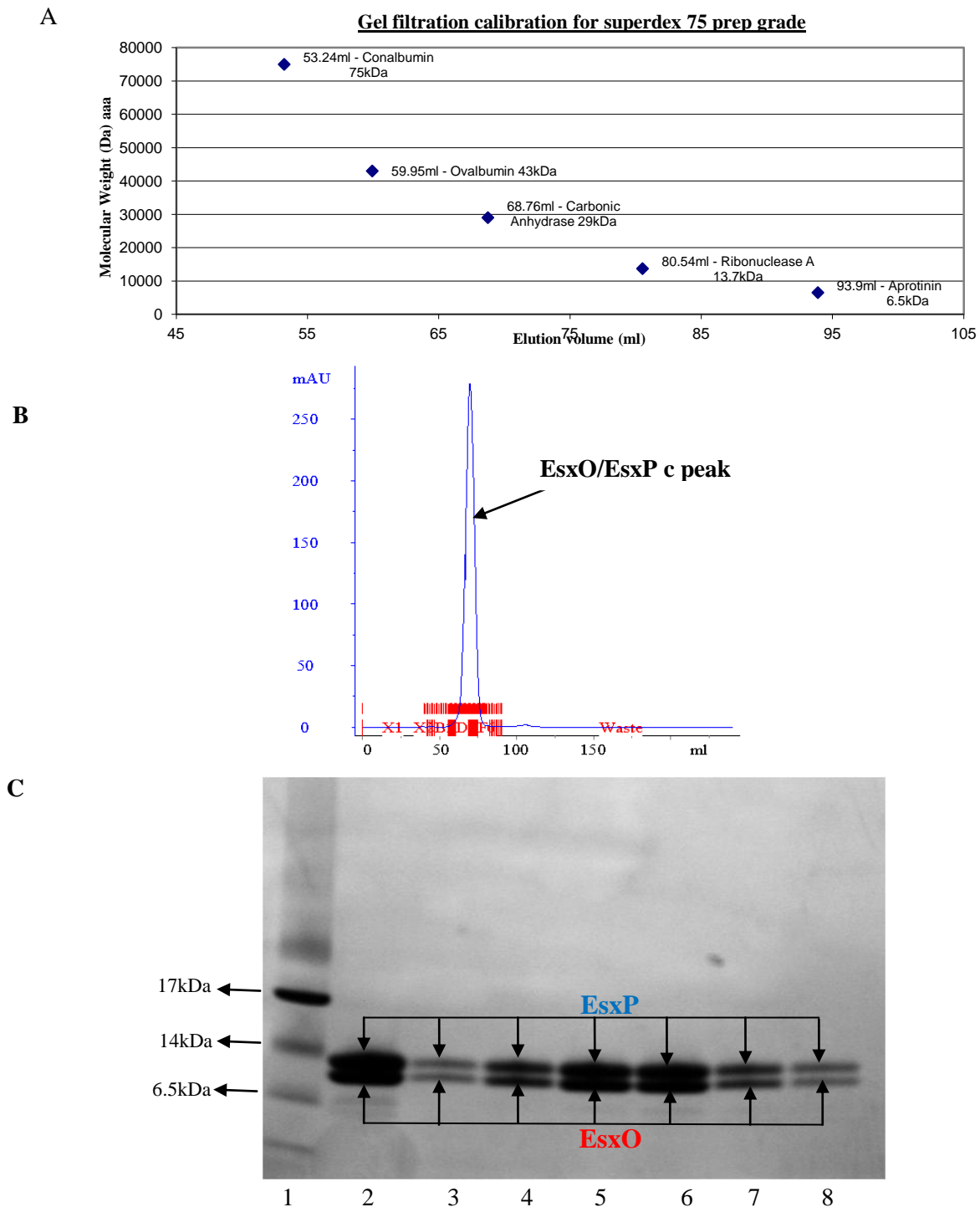


Figure 2.3.9 Purification of the EsxO/EsxP complex by gel filtration. Panel (A) shows a calibration curve for the standard proteins on a 120-ml Superdex 75 16/60 preppacked column. Panel (B) shows a typical FPLC elution profile attained by gel filtration Superdex 75 16/60 column. The EsxO/EsxP complex elution peak is labelled. The target protein complex leaves the column at about 70 ml, suggesting a dimer form for the protein (the expected Mw of protein about 20 kDa). Panel (C) SDS-PAGE gel showing fractions containing EsxO/EsxP complex. Lane 1 is a low molecular weight marker. Lane 2 is loading sample. Lanes 3-8 are peak fractions of the EsxO/EsxP as complex.

The gel filtration experiment shows that EsxO and EsxP form a stable heterodimer. This is because the elution volume of the complex was 70 ml, which is equal to a molecular mass of approximately 20 kDa, twice that of a monomer. Furthermore, relative staining shown on the SDS PAGE suggests that proteins form a 1:1 heterodimer complex (Figure 2.3.9).

In addition, previous studies have demonstrated that two other members of the ESX family including EsxA and EsxB interact with each other to form a tight heterodimer complex, and EsxG interacts with EsxH to form a tight dimer, as well. These findings provide additional supporting evidence for the formation of a tight complex of EsxO/EsxP proteins (117, 118, 162, 163).

2.3.4 Structural characterization of EsxO/EsxP as a complex

2.3.4.1 Far UV circular-dichroism spectrum for the EsxO/EsxP complex

The secondary structure of the EsxO/EsxP complex was determined using far UV circular dichroism (CD) spectroscopy. The spectra obtained for the EsxO/EsxP complex showed that the proteins contained a high percentage of helical structures, as clearly indicated by two intense negative (CD) peaks at approximately 208 and 221 nm, as shown in figure 2.3.10. Analysis of the CD data of the EsxO/EsxP complex was carried out using the CD Pro package, which reported values of 53.2% helix, 11.9% beta sheet, 14% turns and 21.3% unstructured (61). The spectra recorded for EsxO/EsxP as a complex indicate clearly that the majority (53%) of the complex contained a helical structure. Similarly, the spectra obtained by quantitative analysis for the EsxA/EsxB complex has shown that it contains 66% of helical structure, with significant sequence similarity to EsxO/EsxP complex. This suggests that both complexes might form similar structure. In previous studies, it has been shown that the structure of EsxA/EsxB and EsxG/EsxH complexes contained 4 helix bundles (118, 162, 163), suggesting that EsxO/EsxP complex might also contains 4 helix bundles.

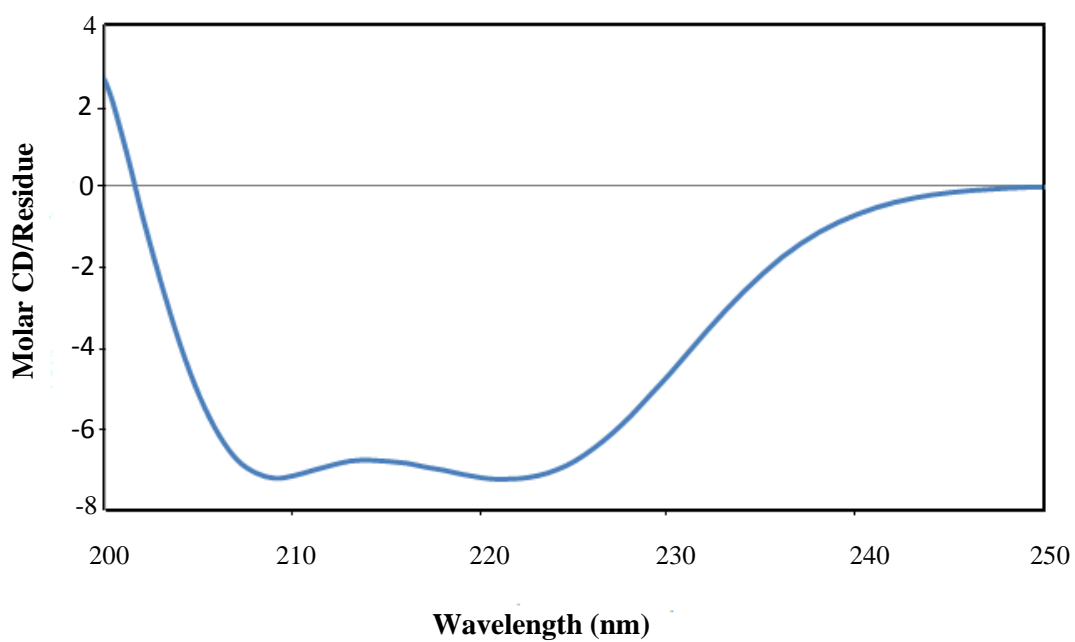


Figure 2.3.10 Far UV CD spectra are shown for the EsxO/EsxP complex at 25°C. The spectra obtained for EsxO/EsxP complex show clear negative bands at about 208 and 221 nm, which is characteristic of proteins with high helical content.

2.3.4.2 The effect of thermal variation on EsxO/EsxP as complex

The effect of temperature on the structural integrity of EsxO/EsxP as a complex was studied by following the change in the CD spectra over a range of temperatures, from 5 to 90°C in increments of 5°C, as shown in figure 2.3.11. All CD spectra were obtained from protein samples dissolved in 25 mM phosphate buffer (pH 6.5) containing 100 mM NaCl with a protein concentration of 15-25 µM, allowed to equilibrate at each temperature before data collection. The stability of the EsxO/EsxP complex was determined by measuring its resistance to heat-induced denaturation. The thermal denaturation curve obtained for the EsxO/EsxP complex was a cooperative type curve, which suggests the stable folded structure of this complex (Figure 2.3.11). The complex is stable up to at least 45°C, with a midpoint around 55°C, which is similar to the midpoint of the EsxA/EsxB complex (69, 102). These similarities between the EsxO/EsxP complex and the EsxA/EsxB complex in sequence, secondary structure content and resistance to heat-induced denaturation strongly suggest that the two complexes may have similar structures.

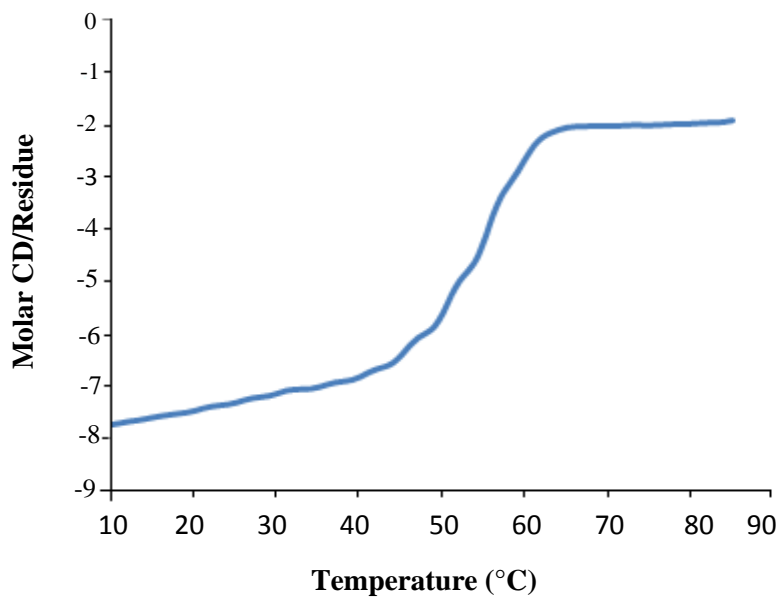


Figure 2.3.11 Illustration of the ability of EsxO/EsxP complex to resist temperature-induced denaturation, in 100 mM NaCl and 25 mM NaH₂PO₄ buffer at pH 6.5. The curve is clearly showing resistance to at least 45 °C, with a denaturation midpoint of around 55 °C. The sigmoidal cooperative curve obtained for this complex suggests that complex is stable and folded complex.

2.3.4.3 1D ^1H NMR analysis of the EsxO/EsxP complex

1D ^1H NMR experiments were performed in 100 mM NaCl and 25 mM NaH_2PO_4 at pH 6.5 and 35°C. The spectrum for the EsxO/EsxP complex demonstrates significant dispersion, including signals from a number of high field-shifted methyl-resonances ($-\text{CH}_3$) (-1 to 0 ppm) and backbone amide group (NH) (6.5 to 9.5 ppm), both of, which are characteristic features of a folded protein (Figure 2.3.12).

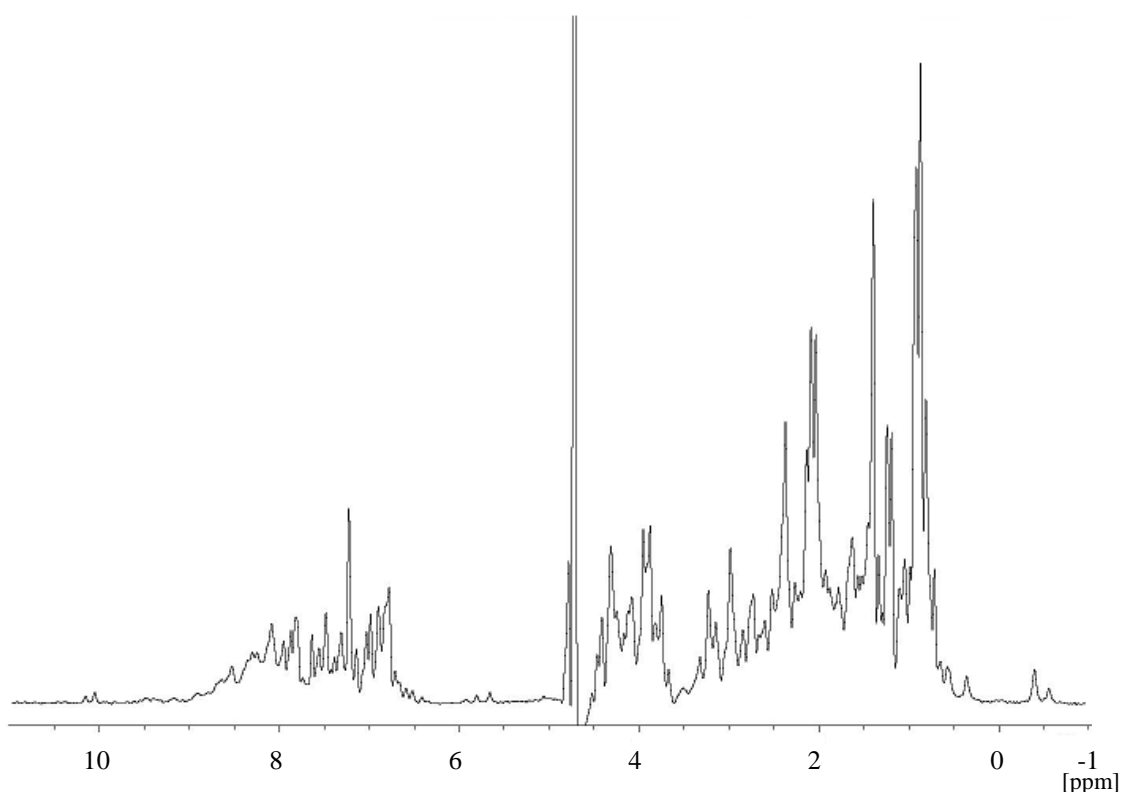


Figure 2.3.12 One-dimensional ^1H NMR spectrum of 80 μM sample of EsxO/EsxP as complex in 100 mM NaCl and 25 mM NaH_2PO_4 at pH 6.5 and 35°C. The spectrum shows chemical shift dispersion of CH_3 and NH which indicate the protein is folded.

2.3.4.4 MALDI-TOF mass spectroscopy of the EsxO/EsxP complex

The molecular mass of EsxO and EsxP proteins was determined by matrix-assisted laser desorption/ionisation-time of flight mass spectrometry (MALDI-TOF). The predicted mass of EsxO is 9954 Da but when measured by this method it was found to be 9821.81 Da. This is because the protein lacks the N-terminal methionine. The predicted mass of EsxP is 10977 Da, but the actual measured mass by MALDI-TOF, was shown to be 11061.93 Da. This may be due to an additional serine resulting from the TEV cleavage of the N-terminal His-tag (Figure 2.3.13).

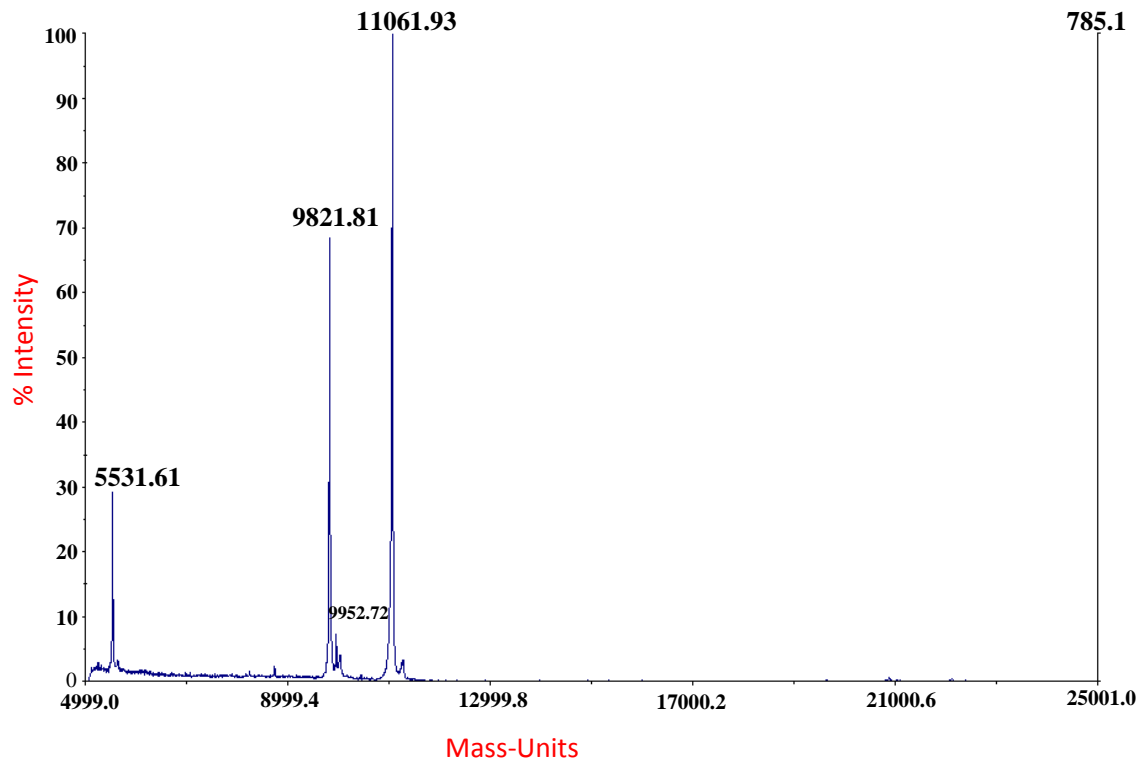


Figure 2.3.13 Mass spectroscopy shows molecular weight of EsxO/EsxP complex. The data indicate that molecular weight of the purified EsxO was 9821.81 Da, which corresponds to EsxO protein lacking the N-terminal methionine. The molecular weight of EsxP was 11061.93 Da which corresponds to this protein and an additional serine resulting from TEV cleavage of the N-terminal histag.

2.3.4.5 Prediction of structure of EsxO/EsxP complex

In this section, the prediction of the structural properties and features of the EsxO/EsxP complex is discussed, using a helical wheel model. It is based on multiple sequence alignments for the members of ESX family proteins and the solution structure of both EsxA/EsxB and EsxG/EsxH complexes (Figures 2.3.14 and 2.3.15) (117, 162). The helical wheel representation provides a suitable approach for predicting the interaction between the helices, where, the residues at positions a and d within the heptad repeat (a-b-c-d-e-f-g) for helix bundle structures are usually expected to form the hydrophobic interface between the helices (117). Analysis of multiple sequence alignments for the members of the ESX family proteins reveals that over half of the interface residues are conserved in the majority of sequences. Solution structure of the EsxA/EsxB and EsxG/EsxH complexes reveals that both complexes form four helix bundles, which indicates that the overall backbone fold of the complexes are similar (Figure 2.3.15). This, together with known complex formation for several genome pairs, strongly suggests that all pairs of these proteins will form similar four helix bundle structures (117, 162).

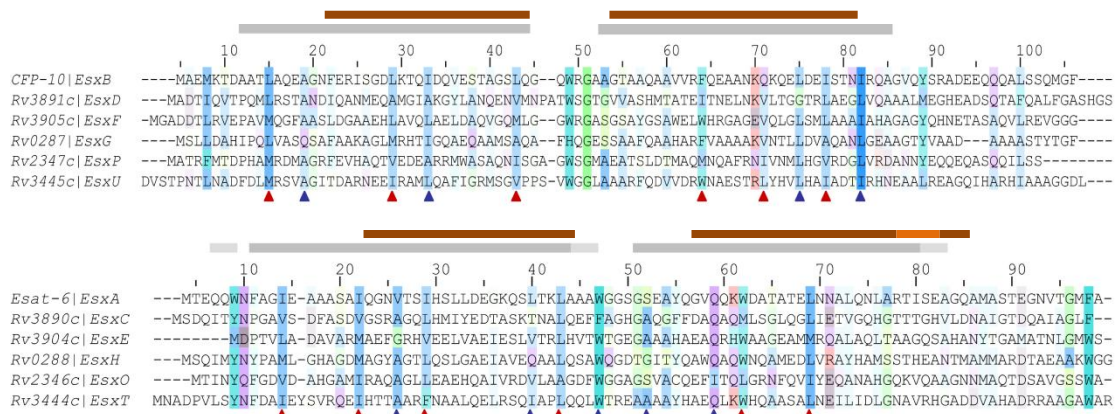


Figure 2.3.14 Multiple sequence alignment illustrating the conservation of the amino acid in members of ESX family proteins, with EsxB related proteins at the top and EsxA related proteins at the bottom. MTINY (EsxI, EsxL, EsxN, EsxO and EsxV) and QILSS (EsxJ, EsxK, EsxM, EsxP and EsxW) proteins are highly related (>90% identity) and are represented by EsxO and EsxP. EsxR/EsxS are closely related proteins (>80% identity) represented here by EsxG and EsxH. The residues are denoted here as follows: aliphatic residues with hydrophobic side chains (Ala, Ile, Met and Val) highlighted in dark blue, aromatic residues (His, Phe, Trp and Tyr) in light blue, the negatively charged residues (Asp and Glu) in dark purple, polar residues (Asn and Gln) are in light purple, the positively charged residues (Arg and Lys) in red, and the small polar residues (Cys, Ser and Thr) are represented by green. ClustalW with Gonnet scoring matrix was used to align the sequence. The positions of helices of EsxA/EsxB and EsxG/EsxH are shown by bars above the sequences (α -helices in dark grey and 3_{10} in light grey indicate EsxA/EsxB and α -helices in dark brown and 3_{10} in light brown indicate EsxG/EsxH). The residues are conserved at position “a” and “d” within the helical wheel diagrams are indicated by triangles coloured blue and red, respectively. Reproduced from Lightbody *et al.*, 2008.

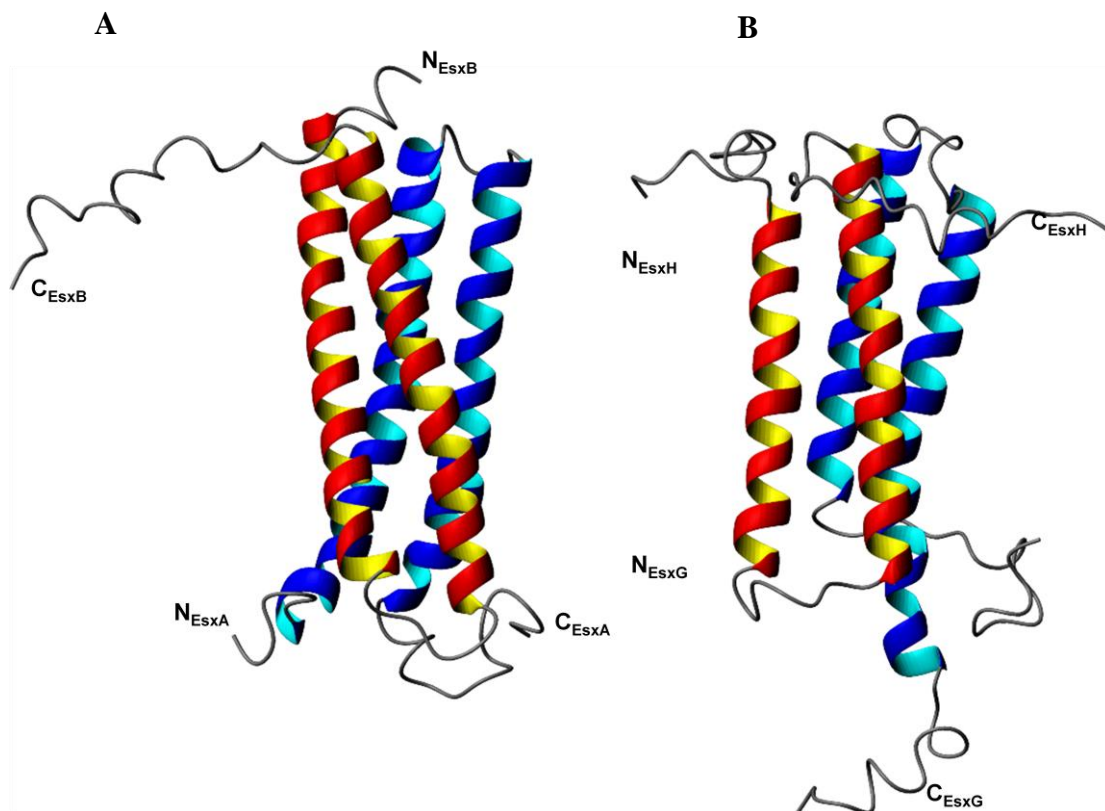


Figure 2.3.15 The solution structures of EsxA/EsxB and EsxG/EsxH complexes. Panels A and B show ribbon representations of the backbone of EsxA/EsxB and EsxG/EsxH complexes respectively, which illustrate the two helix-turn-helix hairpin structures formed by the individual proteins in each complex. Both complexes form four helix bundles, showing that the overall backbone fold for the complexes is similar. Reproduced from Renshaw *et al.*, 2005 and Ilghari *et al.*, 2011.

As previously mentioned, *esxO* and *esxP* are found as tandem in the *Mycobacterium tuberculosis* genome, in common with *esxA/esxB* and *esxG/esxH*. The work reported in this chapter clearly demonstrates that EsxO/EsxP form a tight 1:1 complex, which is mainly helical in structure and is predicted to be closely related to the EsxA/EsxB and EsxG/EsxH complexes. The analysis of a multiple sequence alignment of ESX family members has shown that the hydrophobic residues either found or predicted to be found at positions a and d are highly conserved throughout the family, suggesting that these key interface residues stabilize the formation of the helix-turn-helix structures of the individual family members and suggest that the pairs are likely to adopt a four helix bundle (Figure 2.3.16). Together, these findings suggest that EsxO/EsxP is likely to adopt a four helix bundle structure similar to that EsxA/EsxB and EsxG/EsxH complexes. On the other hand, the residues involved in forming the interface between EsxB and EsxA are poorly conserved throughout the ESX family proteins, which indicates the specificity of the complex formation.

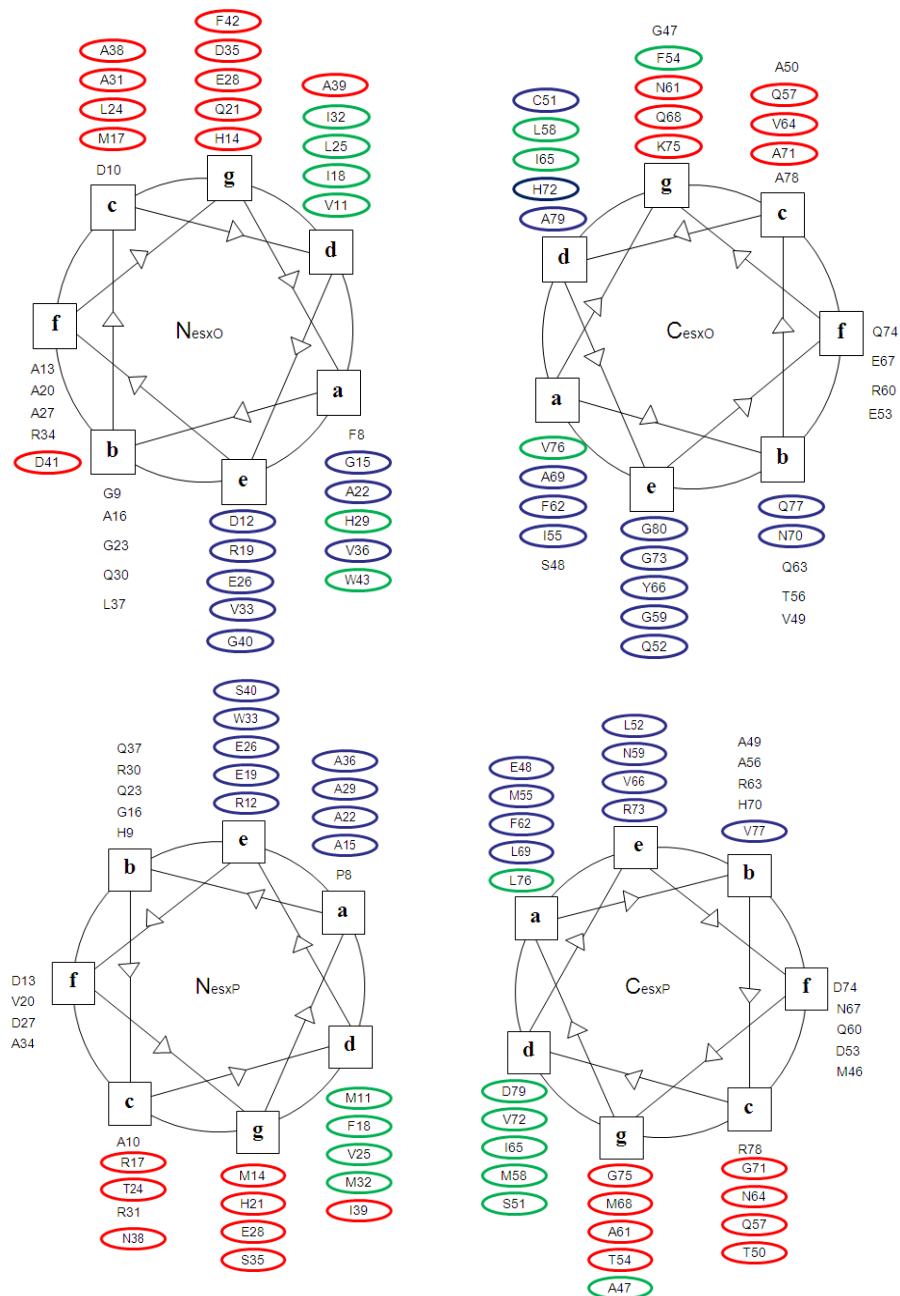


Figure 2.3.16 Helical wheel presentation of the EsxO/EsxP complex. The prediction of the intra and intermolecular interface between helices on the EsxO/EsxP are based on multiple sequence alignments across EsxA/EsxB family members and the knowledge of structures of EsxA/EsxB and EsxG/EsxH complexes. Residues highlighted in blue are predicted to be implicated in intramolecular interactions between helices in EsxO/EsxP and residues that are expected to form part of the intermolecular interface between EsxO and EsxP are depicted by red. Residues in green are expected to be involved at both intra and intermolecular interfaces.

In conclusion, the results presented in this chapter strongly suggest that the EsxO/EsxP complex forms a stable heterodimeric complex. The complex showed a significant resistance to heat-induced denaturation, and the curve was a sigmoidal type, which indicates a stable folded structure. In addition, the 1D¹H NMR studies of the complex clearly showed chemical shift dispersion mainly in the region corresponding to the protons of the backbone amide and methyl groups, suggesting that this complex has a stable folded structure. Furthermore, the elution profile of this complex from a gel filtration column showed that its molecular mass is approximately 20 kDa, which is approximately equal to the complex when it is in dimer form. The EsxO/EsxP complex has a similar helical content CD analysis to that found in other studies of the Esx family complexes. Finally, the helical wheel representation shows that the residues involved in the formation of the intramolecular interface between helices are conserved throughout the EsxO/EsxP complex, suggesting that this complex might form a four helix-bundle structure similar to EsxA/EsxB and EsxG/EsxH complexes. Moreover, the residues at the intermolecular interface may play a role in specificity with regard to complex formation. As previously noticed, these residues are not conserved either throughout the EsxO/EsxP complex or throughout the EsxA/EsxB family members. From these observations, one may expect that changes in these residues might have an effect on the stability and specificity of the complex.

Chapter 3

Specific interaction of the EsxO/EsxP complex with host cells

3.1 Introduction

Although the importance of the EsxA/EsxB family of proteins in mycobacterial virulence and pathogenesis is clear, the precise molecular functions and cellular mechanisms of these proteins have not been fully defined. Several studies have demonstrated that the ESX-1/RD1 locus secretes the effectors EsxA and EsxB. It has been implicated in the spread of infection, granuloma formation and the prevention of phagosome maturation, because when this region is deleted, it results in attenuated infection and the poor formation of granulomas (45, 196, 212, 230). These studies have provided clues to the proteins that participate in related virulence roles or pathogenesis. This is of central importance and therefore, we need to determine the localisation of these proteins on the host cells to identify the basic functional role of these virulence factors.

A microarray study has shown that *esxA* and *esxB* are downregulated when macrophage cells internalise *Mycobacterium tuberculosis* by phagosomes, which indicates that the function of this complex might occur before the phagocytosis of *Mycobacterium tuberculosis* by phagocytic cells (177). It has been suggested that the EsxA/EsxB complex is likely to bind to a target on the surface of host cells. Confirmation of this suggestion has been made in previous microscopy study using a fluorescence microscope assay that included different cells (monocytes, macrophages and fibroblasts) and labelling of complex with Alex Fluor 546 dye (162). The

fluorescence microscopy study of the EsxA/EsxB complex revealed specific interaction between EsxA/EsxB and monocyte and macrophage cells. The specific binding was confirmed by incubating the U937 cells with labelled EsxA/EsxB complex in the presence of an excess of the unlabelled complex. This resulted in a significant reduction of fluorescence intensity which indicates that the interaction is mediated by the complex not by the fluorophores (Figure 3.1.1). Therefore, the fluorescence microscopy assay strongly suggests that the EsxA/EsxB complex binds to a specific target on monocyte and macrophage cells (162).

On the other hand, studies have suggested that the EsxA/EsxB complex causes lysis of the host cell by the formation of pores in the cell membrane (91). However, there are strong arguments against this suggestion in terms of the structure of the EsxA/EsxB complex because the surface of the complex has a uniform distribution of positive and negative charges and no hydrophobic patches, which is incompatible with a membrane spanning pore. Furthermore, in aqueous solution the EsxA/EsxB complex is soluble to over 2 mM with no indication of aggregation, which is not typical of pore forming proteins (162).

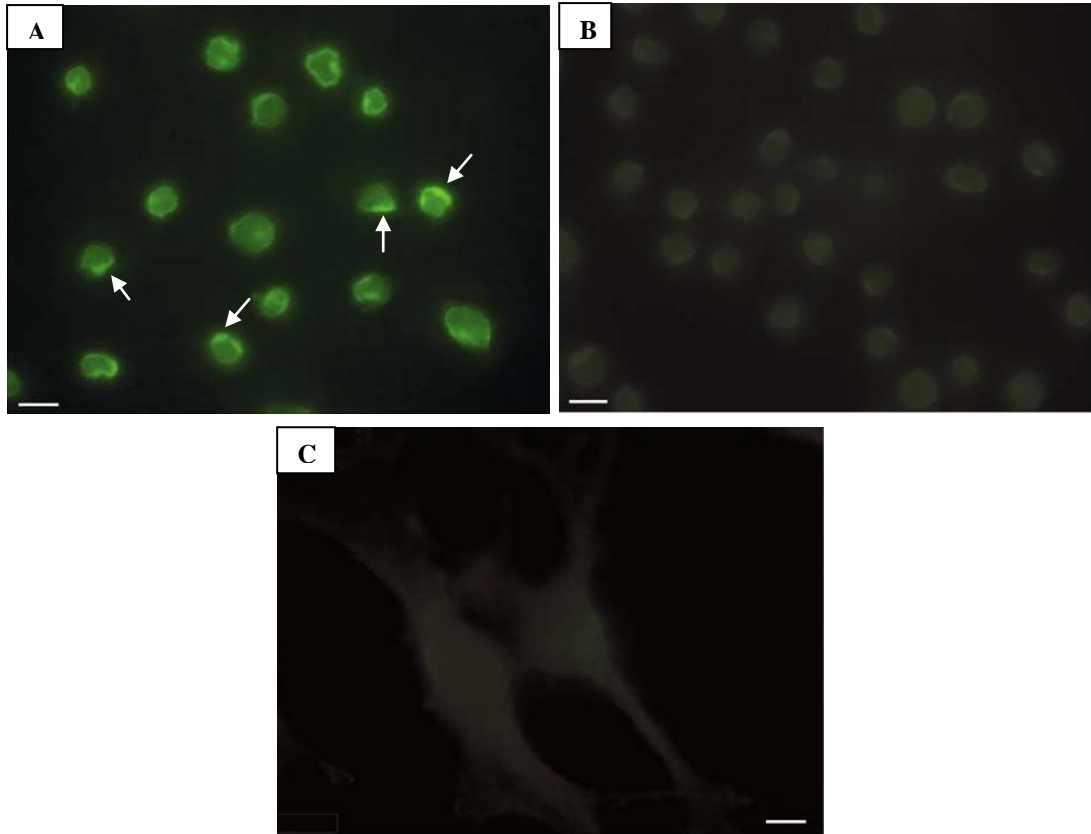


Figure 3.1.1 The interaction of fluorescently labelled EsxA/EsxB complex with the surface of U937 monocyte cells and NIH-3T3 fibroblast cells. All of these cells were exposed to 1 μM Alexa Fluor 546 labelled EsxA/EsxB complex. (A) The labelling is focused on the surface of U937 cells (indicated by arrows) (100 ms exposure). (B) The fluorescence intensity is significantly reduced when U937 cells are exposed to 1 μM labelled EsxA/EsxB complex and 20 μM unlabelled EsxA/EsxB complex. (C) No significant labelling is present on the cell surface of NIH-3T3. The size bars shown correspond to 5 μm . Reproduced from Renshaw *et al.*, 2005.

The work described in this chapter was focussed on assessment of EsxO/EsxP complex by fluorescence microscopy, whether the complex might mediate its function by binding to the surface of the host cells. This suggestion would be consistent with the finding of Schnappinger *et al.* (2003) that expression of EsxO and EsxP are down-regulated by *Mycobacterium tuberculosis* cells internalised within the macrophage phagosome. This indicates that the function of the EsxO/EsxP complex might occur before the take-up of *Mycobacterium tuberculosis* by the macrophage (177).

To investigate this suggestion, I used a fluorescence microscopy approach to assess the potential binding of the EsxO/EsxP complex to various types of cells including human monocytic cell lines U937, J774 macrophage and NIH3T3 fibroblast cell lines. A confocal microscope was used to confirm the localisation of the labelled protein to the surface of the host cells.

3.2. Method and Materials

3.2.1 Purification of the EsxO/EsxP complex

Purification of the EsxO/EsxP complex was carried out as described in section 2.2.5

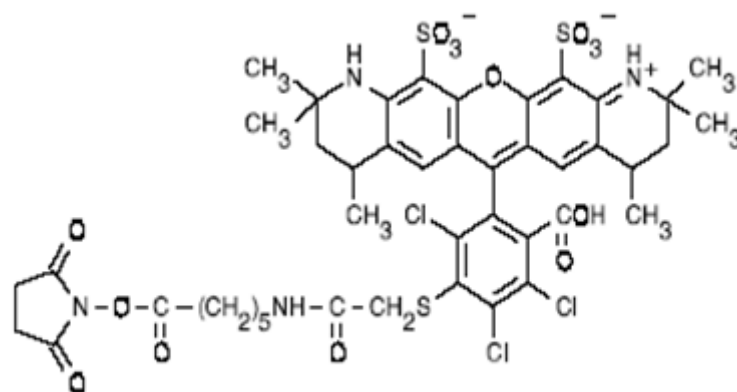
3.2.2 Fluorescent labelling of EsxO/EsxP complex

The EsxO/EsxP complex was labelled with the succinimidyl ester bound of Alexa Fluor 546. Alexa Fluor 546 is one member of the Alexa Fluor dyes that has an excitation at 546 nm and E_{\max} fluorescence emission is recorded at 573 nm (89, 148) (Figure 3.2.1).

The EsxO/EsxP complex was prepared by dialysis against 100 mM NaCl and 25 mM NaH_2PO_4 buffer at pH 7.5 before labelling with Alexa Fluor 546 (Molecular probes). The reaction was performed at pH 7.5 to allow the N-terminal amino groups of EsxO/EsxP complex to react with Alexa Fluor dye, but not charged lysine side chain amino groups. A molar ratio of 10:1 (dye to protein) was used for labelling and the mixture incubated overnight, in the dark at room temperature with continuous rocking. The excess fluorophore was removed by dialysis against 100 mM NaCl and 25 mM NaH_2PO_4 buffer (pH 7.5). Finally, the degree of labelling was determined by measuring the absorbance of the protein-dye conjugate at 280 nm and 556 nm, (absorbance maximum of protein and dye respectively). The degree of labelling was calculated using the following formula (89):

$$\text{Degree of labelling} = \frac{A_{\max} \times \text{dilution factor} \times \text{M.W of protein}}{\text{Concentration of protein} \times \epsilon_{\text{dye}}}$$

A



B

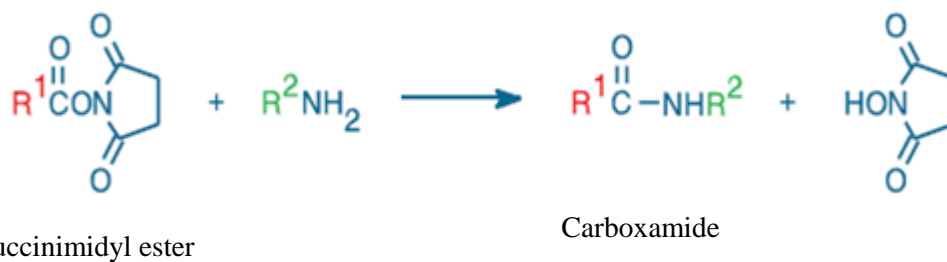


Figure 3.2.1 The reaction of Alexa Fluor 546 succinimidyl ester with a primary amine (B). The structure of Alexa Fluor 546 (A). The primary amine binds to succinimidyl group by the formation of stable amide bond. Reproduced from Haugland *et al.*, 2005.

3.2.3 Cell culture

3.2.3.1 Monocytic cell line:

U937 human monocytic cell line was grown in suspension in RPMI1640 media (Invitrogen) supplemented with 10% (v/v) foetal calf serum (FCS), 2 mM glutamine. The cells were incubated at 37°C and 5 % CO₂.

3.2.3.2 Macrophage cell line:

J774 mouse macrophage cell line was cultured in Dulbecco's modified Eagle's medium (DMEM) (Invitrogen) supplemented with 10 % (v/v) FCS and 2 mM glutamine. Cells were grown at 37°C and 5 % CO₂.

3.2.3.3 Fibroblast cell line:

NIH-3T3 mouse cell line was grown in Dulbecco's modified Eagle's medium (DMEM) (Invitrogen) supplemented with 10% (v/v) FCS and 2 mM glutamine. Cells were incubated 37°C and 5 % CO₂.

3.2.4. Fluorescence microscopy

The U937 cells were initially cultured in a suspension containing 10% FCS and 2 mM glutamine. The FCS was then removed by washing the cells in RPMI without FCS, the cells then allowed to adhere to glass coverslips precoated with 5 ug/ml Fibronectin for 5 minutes at 37°C and 5 % CO₂. Excess cells were removed by washing the coverslips twice using (PBS) buffer. However, J774 cells and NIH-3T3 cell were grown directly on glass coverslips in appropriate media. To analyse whether the EsxO/EsxP complex could bind to the surface of host cells adhered to glass coverslips, they were exposed to 1 µM Alexa Fluor 546 labelled complex for 15 minutes at 4°C on a rocker in the dark. Non-bound complex was removed by washing the cells with PBS before fixing with 4 % (w/v) paraformaldehyde (PFA), cells were permeabilised with 0.2% (v/v) TritonX-100 when required. Prolong antifade reagent (Molecular Probes) was used to mount the coverslips onto slides that were stored at room temperature in dark until dry. A Nikon TE300 inverted microscope was used to visualise the cells, with images captured using an OCRAECCD camera (Hamamatsu) and open lab software (Improvision).

Blocking experiments were performed by incubating U937 cells with 1 µM Alexa Fluor labelled EsxO/EsxP complex in the presence of 20-fold molar excess of unlabelled EsxO/EsxP complex for 15 minutes at 4°C. Nonbound protein was removed by washing the cells with PBS, cells were then fixed and visualised as described above.

To investigate whether the EsxO/EsxP complex was internalised into the cells time course studies were carried out. U937 cells were incubated with complex for 5, 15, 20 and 60, minutes at 37°C and 5% CO₂. Unbound protein was removed by washing the cells with PBS, prior to visualisation under the microscope. The same approach was used to determine whether incubation with the complex had any significant effect on cell morphology or viability.

3.2.5 Confocal fluorescence Microscopy

Cells were imaged with a Leica TCS SP5 laser scanning confocal microscope using the LAS AF software package. I used the same slides of U937 cells and J774 cells that were prepared for fluorescence microscopy to determine the localisation of labelled EsxO/EsxP complex on the surface of host cells line. Imaris software was used to analyse the images obtained.

3.3 Results

3.3.1 Labelling of the EsxO/EsxP complex with Alexa Fluor 546

The EsxO/EsxP complex was shown react with Alexa Fluor 546 at a 10:1 dye to protein molar ratio. Unbound dye was removed by dialysis and the labelling of protein was determined by measuring the absorbance of the protein-dye conjugate at 556 nm, (absorbance of the dye) and 280 nm (absorbance of the protein). The degree of labelling for the EsxO/EsxP complex was between 1.5-1.7:1, which indicates that one-to-two fluorophore molecules bind with the protein complex, which is consistent with the modification of one or both of the N-terminals in the complex (Figure 3.3.1).

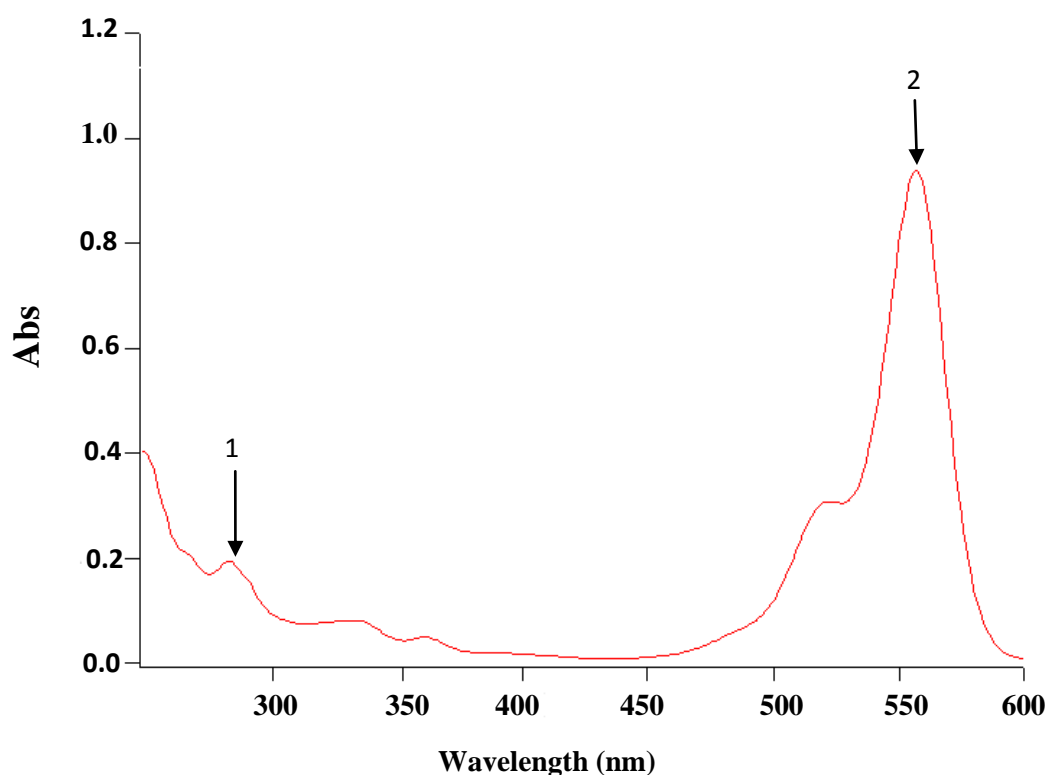


Figure 3.3.1 Absorbance spectra of Alexa Fluor 546 labelled EsxO/EsxP complex. The degree of labelling was typically between 1.5-1.7. The absorbance of protein at 280 nm is indicated by 1 and the absorbance of Alexa Fluor 546 at 556 nm is indicated by 2.

3.3.2 Fluorescence Microscopy

3.3.2.1 Binding of the EsxO/EsxP complex to specific host cells

The fluorescently labelled EsxO/EsxP complex was used to assess whether the complex binds specifically to different types of host cells including U937 monocytes, J774 macrophage cells and NIH-3T3 fibroblast cell lines. The U937 monocyte cell line and J774 macrophage cell line both showed intense fluorescence at the cell surface, indicating binding of EsxO/EsxP complex. Labelling is focused at the cell surface and often is observed in patches for both the U937 monocytic cell line and J774 macrophage cell line. In contrast, the EsxO/EsxP complex shows dramatic reduction of fluorescent labelling on the cell surface of NIH-3T3 fibroblast cell line and low level of background (Figure 3.3.2).

Under identical experimental conditions, when the incubation of permeabilised U937 monocyte and J774 macrophage cells with fluorescently labelled EsxO/EsxP complex was performed, no significant difference in fluorescent labelling on the cell surface when compared with the non-permeabilised cells was observed. Time course studies were used to determine whether incubation with complex had any noticeable effect on cell morphology and to investigate whether the complex is internalised into the cells. U937 monocyte and J774 macrophage cells were incubated with EsxO/EsxP complex for 20, 30 and 60 minutes at 37°C in the incubation buffer in presence of 5 % CO₂. There was no significant difference in the morphology of the cells at 20 min, 30 min and 60 min. The identical experiments were performed using the labelled complex with J774 cells, resulting in the same type of results of fluorescence binding on surface of these cells.

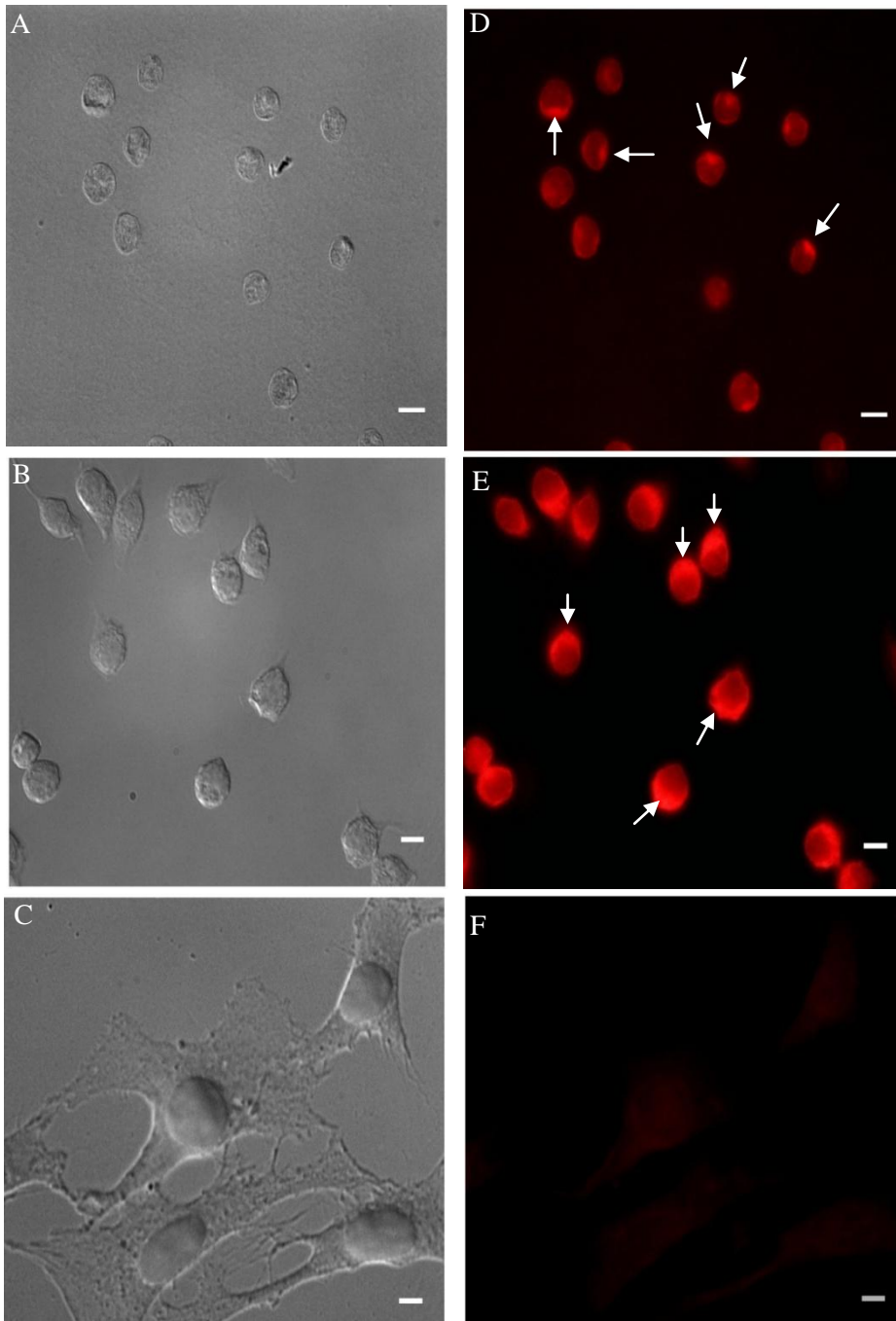


Figure 3.3.2 Binding of fluorescently labelled EsxO/EsxP complex on the surface of U937 monocyte and J774 macrophage cells. Panels (A-C) show bright field microscopy of U937 cells, J774 cells and NIH-3T3 fibroblast cells respectively. Panels (D-F) show U937 cells, J774 cells and NIH-3T3 fibroblast cells exposed to 1 μ M Alexa Fluor 546 labelled EsxO/EsxP complex, 200 ms exposure time. The images of U937 cells, J774 cells show binding of fluorescently labelled EsxO/EsxP complex on the surface of both U937 cells and J774 cells. Labelling is focused at the surface and is often observed in patches (indicated by arrows). However, the image of NIH-3T3 fibroblast cells has shown significant reduction of fluorescent labelling on the cell surface of NIH-3T3 fibroblast cell line and low level of background. This indicates that the EsxO/EsxP complex binds to the specific host (U937 and J774) cells. The size bars shown correspond to 5 μ m.

3.3.2.2 Specificity of EsxO/EsxP complex binding to a host cell

The specific interaction of the EsxO/EsxP complex with U937 monocytic and J774 macrophage cells suggests that this interaction is due to a specific target on the cell surface membrane rather than to non-specific binding between the EsxO/EsxP complex or the fluorophore and the cell surface. Specificity of the interaction was confirmed by fluorescence microscopy experiments in the presence of 20-fold molar excess of unlabelled complex to create competition with Alexa Fluor 546 labelled EsxO/EsxP complex. The dramatic reduction in fluorescence at the surface of both U937 monocytic cells and J774 macrophage cells exposed to an excess of unlabelled complex clearly indicates that binding to the cell surface is mediated by the protein complex not by the fluorophore. Figure 3.3.3 shows significantly different pixel intensity between the blue and red charts which represents the cells exposed to 1 μM labelled complex and those exposed to 1 μM labelled complex and 20 μM unlabelled complex, respectively. Therefore, it is confirmed that the labelled EsxO/EsxP complex binds to the target on the surface of monocyte and macrophage cells and the results of this binding is not mediated by the dye. In addition, it is noticed that the level of labelling or intensity in J774 macrophage cells was greater than that of U937 monocytic cells, suggesting that these types of cells express more of the putative target for EsxO/EsxP complex.

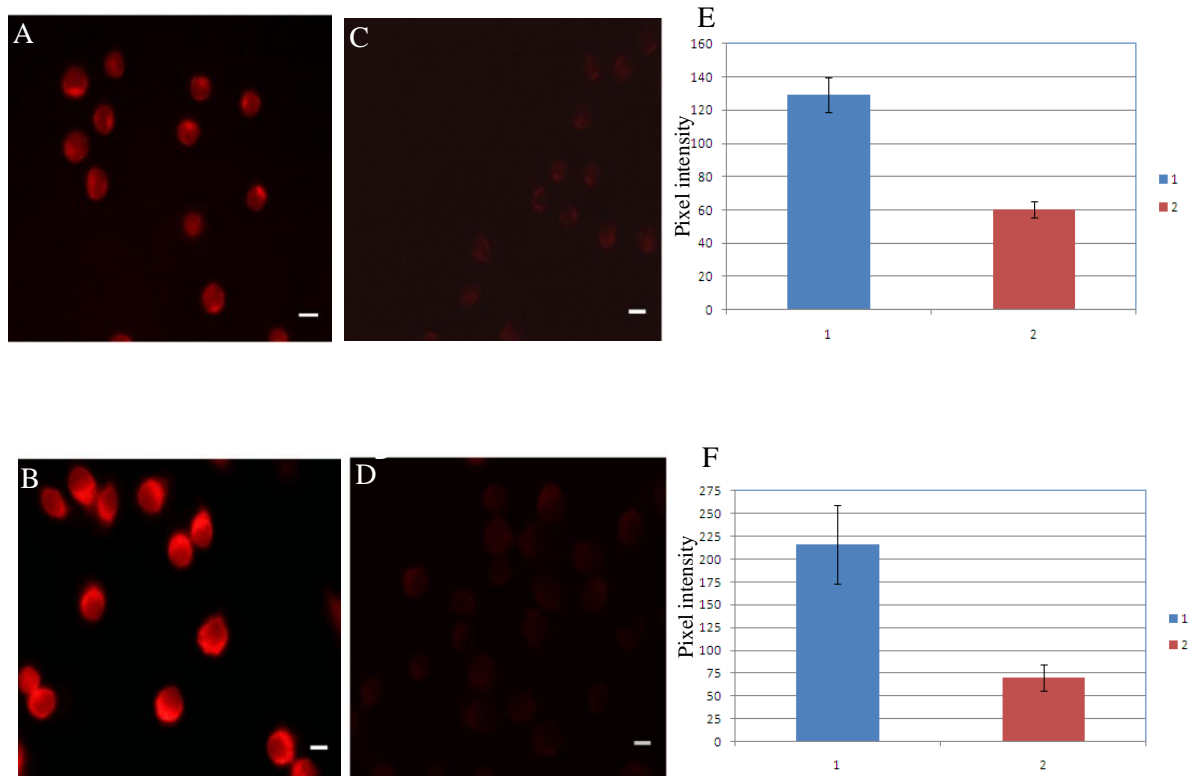


Figure 3.3.3 Inhibiting the binding of fluorescently labelled EsxO/EsxP complex to U937 and J774 cells by competition with unlabelled complex. (A-B) Typical labelling of U937 and J774 cells respectively with 1 μ M labelled EsxO/EsxP complex. (C-D) U937 and J774 cells exposed to 1 μ M labelled EsxO/EsxP and 20-fold molar excess of unlabelled complex, 200 ms exposure time. The size of bars shown corresponds to 5 μ m. (E-F) The mean pixel intensity levels of U937 and J774 cells were analysed by openlab software. The chart shows that there is significant change in the level of intensity between U937 and J774 cells exposed to 1 μ M labelled complex (blue bars) and U937 and J774 cells exposed to 1 μ M labelled complex and 20 μ M unlabelled complex (red bars). It is clear that fluorescence labelling in the presence of unlabelled complex is drastically reduced, indicating that the interaction between the complex and host cell surface is not fluorophore mediated.

3.3.2.3 The location of the EsxO/EsxP complex in specific host cells

Fluorescence microscopy has been used to show a specific interaction between the EsxO/EsxP complex and monocyte and macrophage cells. Here I assess whether the the esxO/esxP complex is present at the cell surface, or within the cell. Confocal microscopy was used to investigate the location of the complex on host cells by obtaining high resolution images to allow the production of three dimensional reconstructions. Imaris software was used to analyse these images. The analysis of the images of both U937 monocyte and J774 macrophage cells showed that the labelled complex was present on the surface of cells in patches. Figure 3.3.4, illustrates that the binding between EsxO/EsxP complex and host cells is present on the cell surface, which is likely mediated by targets on the membrane. I conclude that the position of EsxO/EsxP complex is on the surface of both U937 monocyte and J774 macrophage cells and not within the cell.

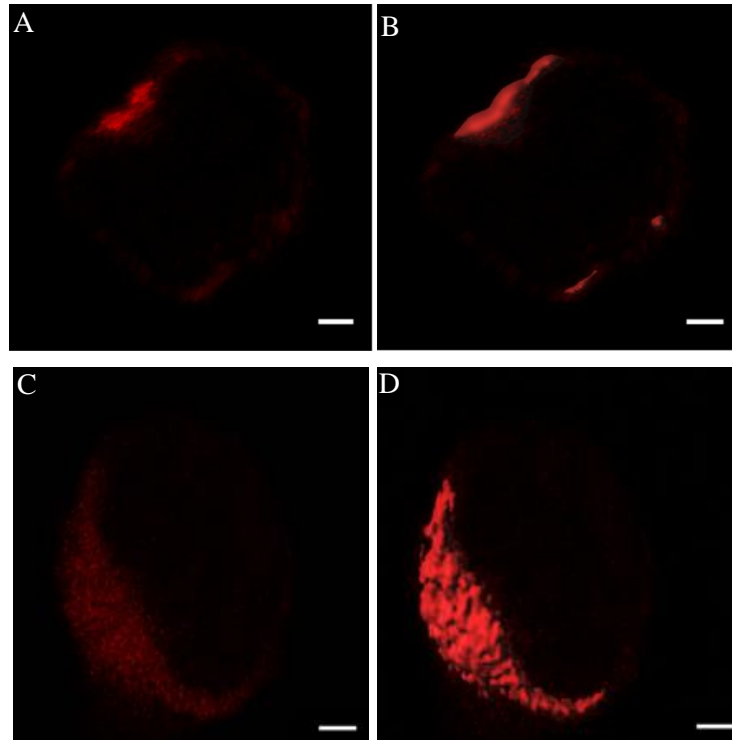


Figure 3.3.4 Imaris 3D surface representation of EsxO/EsxP complex form patches on U937 and J774 macrophage cells. The location of EsxO/EsxP complex was determined by scanning U937 and J774 cells with the confocal microscope and by using Imaris software to analyse the images respectively. (A and C) raw data (pixel image) of surface of cell for U937 and J774 macrophage cell. (B) and (D) is the same image as (A) and (C) respectively, with surface rendered 3D to show the localisation more clearly in a 3D image. The scanning of both cell lines shows the position of binding between host cell and labelled complex present on surface of the cell based in three dimensions. The size of bars shown corresponds to 2 μm for U937 and 3 μm for the J774 macrophage cell.

3.4 Discussion

The host cell binding assays showed significant differences in the fluorescence labelling on the host cell surfaces; between monocyte/macrophage cell lines compared to the fibroblast cell line, indicating that the EsxO/EsxP complex specifically interacts with monocyte/macrophage cell lines (Figure 3.3.2). The fluorescence labelling was concentrated in patches, which appeared to be associated with the target being on the cell membrane. Furthermore, the level of intensity of the binding on the surface of J774 macrophage cells was higher compared to U937 monocyte cells, indicating that the macrophage cells probably express more of a putative target for the EsxO/EsxP complex. This fluorescence microscopy study indicates that the EsxO/EsxP complex likely binds to targets that are present on the surface membranes of monocyte and macrophage cells, but not to fibroblast cell lines. The specificity of the interaction between the labelled EsxO/EsxP complex and the monocyte and macrophage cells was mediated by the complex and was not due to nonspecific interactions with the fluorophore, based on the results obtained from blocking experiments, where U937 and J774 cells were incubated with fluorescently labelled complex and a 20-fold molar excess of unlabelled EsxO/EsxP complex, which showed a dramatic reduction in fluorescence intensity.

The EsxO/EsxP complex showed no sign of lysing cells when U937 and J774 cells were exposed to the complex. Besides, the complex is soluble to over 1.3 mM in aqueous solution with no sign of aggregation, which is not typical of a pore forming protein. In addition, the time course studies by exposing U937 and J774 cells to labelled EsxO/EsxP complex for 15 minutes, 20 minutes, 1 h and up to 24 h showed

no evidence of cell lysis. Therefore, this observation shows clearly that the EsxO/EsxP complex is not associated with cytolytic activity, which is similar to the EsxA/EsxB complex, as mentioned previously (162).

Capping formation or the clustering of cell surface receptors can occur when the surface comes into contact with specific ligands. This phenomenon has been reported in various receptors, such as the insulin, epidermal growth factor, L-selectin, immunoglobulin and immune cell receptors. Previous studies have shown that the formation of the antigen/receptor cluster might be essential for initiating physiological responses in lymphocytes (T-cell and B-cells), such as transcription of genes, release of cytokines and progression of the cell cycle, migration, cell proliferation and antigen-receptor triggered apoptosis (105, 112, 185).

During capping formation, host surface receptors interact with complementary ligands, which might result in the activation of signalling pathways and aggregation of receptors into patch-like structures. These patch-like structures then assemble in one pole of the cell and form a cap (10, 93). The ligands that induce cap formation might be essential for the transduction of extracellular signals through the aggregation of different signalling elements. Several studies have indicated that the assembly of molecules in caps is specific for ligand/receptor combinations and may be significant for signal transduction (56, 93, 112). The observation from the confocal microscopy results demonstrated that the EsxO/EsxP complex forms patches on the surface of both U937 and J774 cells, therefore, suggesting that a tight binding occurs between the complex and target protein on the cell surface (Figure 3.3.4). Furthermore, the

EsxA/EsxB complex has been shown to form patches on the cell surfaces of host cells (162). Taken together, these results are consistent with the observation of Schnappinger *et al.* (2003), who reported that both complexes are downregulated upon bacterial internalisation into the phagosome, which suggests that both complexes probably trigger the induction of cell signalling pathways and modulation of host cell behaviour.

Chapter 4

Assessment of potential Biological Roles of EsxO/EsxP complex

4.1 Introduction

The work described in the previous chapter clearly shows that the EsxO/EsxP complex binds to specific targets on the surface of monocyte and macrophage cells, leading to the formation of distinct cap-like structures, which might be an indication of a signalling pathway. The work described in this chapter focused on determining of whether cell signalling results in changes in cell motility or gene expression.

Davis and Ramakrishnan reported that macrophages in zebrafish embryos infected with Δ RD1 *M. marinum* showed reduced motility and spread in comparison to wild type *M. marinum* containing the RD1 region (45). This perhaps suggests that RD1 secreted factors such as EsxA/EsxB may play a role in macrophage motility and spread, and possibly other Esx complexes which have been found to bind to the surface of host cells, such as the EsxO/EsxP complex. The work described in this section of the thesis investigated whether EsxA/EsxB (which is secreted by RD1) and EsxO/EsxP complexes play a role in motility.

A so called Transwell migration assay has been commonly used for studying the migration of different types of cells, including immunity cells such as macrophages in response to an external signal. The assay is found useful in screens for compounds that act as chemoattractants or inhibitors of chemotaxis. The main idea of this assay relies on cells which are placed on the upper layer of a permeable membrane whereas the solution containing the test agent is placed below the cell permeable membrane.

Following an incubation period of typically 3–18 hours, the cells that have moved through the membrane are stained and subsequently counted. In practice, the membrane is usually coated with some extracellular matrix component, such as collagen, which acts to facilitate both adherence and migration (100, 197). If the external signal is thought to be a motility factor rather than a chemoattractant, then a live cell imaging approach, as used here is considered an appropriate way to determine motility (86, 104, 209, 83, 78).

Lipopolysaccharide (LPS) accounts for the majority of the lipid component of the outer membrane of gram negative bacteria. LPS is a known endotoxin which can trigger immune response at sub-nanogram levels (125). This reaction is even more prevalent in monocytes and macrophages, due to the secretion of various proinflammatory mediators, such as TNF α , IL-6 and IL-1 β . Therefore, removal of LPS from recombinant proteins is essential to prevent any biological response from LPS being attributed to the recombinant protein of choice (22, 125).

4.2 Methods and Materials

4.2.1 Protein purification and removal of LPS

Initially, the EsxO/EsxP complex was purified by affinity chromatography followed by gel filtration purification as described previously. To remove LPS from the sample, ion exchange chromatography was utilised, where, LPS-free water was used in the preparation of buffers, and a new 5 ml HiTrap Q sepharose column, as well as pyrogen-free sterile plastics were used. The column was then washed with 5 column

volumes of pyrogen free water, and equilibrated with 5 column volumes of 20 mM sodium phosphate at pH 7.4 that was left overnight. At the same time, the EsxO/EsxP complex was dialysed against 2L of the same buffer overnight. Then the complex was loaded onto a column, followed by washing with 5 column volumes of 20 mM sodium phosphate at pH 7.4. Then the EsxO/EsxP complex was eluted by washing the column with 5 column volumes of a buffer containing 75 mM NaCl and 1 ml of each fraction was collected. The column was then washed with 150 mM and 500 mM NaCl buffers to ensure that all the protein was eluted. This protocol was repeated twice to remove as much LPS as possible from the sample. LPS levels were tested using an endosafe-PTS spectrophotometer and cartridges (Charles River Laboratories). This is based on the activation of pro-enzyme by LPS which generate a colour producing substrate that can be easily detected (95). Protein samples with low levels of LPS were used in subsequent investigations of the cell motility and microarray experiments.

4.2.2 Cell Motility Assays

J774 macrophage cells were seeded directly onto 6 well plates (6-well flat-bottom Nuclon MultiDish) at density of 1.4×10^6 cells/ml. The cells were allowed to adhere and grow for 24 hours at 37°C and 5 % CO₂, before replacing the old media with fresh media containing 1 µM of LPS free EsxO/EsxP complex. Three regions were selected in each well and imaged using brightfield by time-lapse fluorescence microscopy, with a 10X objective on a Nikon Eclipse TE2000 inverted microscope in an atmosphere of 5 % CO₂ at 37°C. The images were captured with a Hamamatsu ORCA-ER (C4742-95) digital camera every 15 minutes over a period of 24 hours.

The migration of 22 cells for 8 hours was analysed using the manual tracking plugin of ImageJ (NIH, Bethesda, MD, USA), and track plots following the path of individual cells were created using the chemotaxis tool plugin for ImageJ (78, 83, 86, 104, 209). Then, the directionality of the cells was determined. Directionality is defined as the Euclidean distance between the starting and end point divided by the accumulated distance (total distance moved). Directionality is calculated by dividing the average of all the cells' Euclidian distances by their average accumulated distance and represents a measure of their trajectories' directness. A directness (D) equal to or near 1 means a straight-line migration from start to endpoint. D equal to or near 0 means strong meandering and turns. An average migration speed and distance were obtained from the raw data using the manual tracking plugin and the results are represented here (198).

4.2.3 Microarray

In the microarray experiments, approximately 9×10^7 U937 cells in 10 ml RPMI medium were exposed to either 1 μ M LPS free EsxO/EsxP complex in 25 mM NaH_2PO_4 , 100 mM NaCl (pH 7.4) or to an equivalent volume of buffer alone for either 30 or 120 minutes. Following exposure to the protein complex or the control buffer, the cells were harvested by centrifugation at 1000 rpm for 5 minutes. Total RNA was extracted using the RNase Mini Kit (QIAGEN) according to the manufacturer's instructions, with the cells homogenised by passing the cell lysate through a 20-gauge needle until a homogeneous lysate was achieved. The concentration of RNA was measured using a spectrophotometer at 260 nm.

The expression profile of samples was determined by using a whole human genome microarray from Affymetrix with our collaborators at the National Institute of Medical Research (Dr Roger Buxton and colleagues). ArrayTrack was used to analyse and process the six datasets that were generated in the experiment (200, 201). The raw data was imported into the ArrayTrack database, normalised by Mean/Median Scaling and then t-test was selected, to identify genes with significant changes in expression levels between treated and non-treated samples. Significant genes were identified by applying three criteria; T-test which estimates p-value, fold change and genes that have demonstrated a mean channel intensity reading higher than the determined noise level which was 250. Significant genes were identified with cut off ($p \leq 0.05$ and fold change ≥ 1.5). Selected genes were further analysed using KEGG (Kyoto Encyclopedia of Genes and Genomes) and GOFFA (Gene Ontology for Functional Analysis) (96, 190, 200). GOFFA software within the array track uses a standard vocabulary (terminology) derived by the Gene of Ontology Consortium to generate gene ontology information. The ontology provides standard vocabularies for description of the molecular function, biological process and cellular component of gene products (191, 201).

4.3 Results

4.3.1 Purification of EsxO/EsxP complex and removal LPS

LPS was removed from EsxO/EsxP complex samples using ion exchange chromatography after initial purification by affinity chromatography and gel filtration. EsxO/EsxP was eluted at 100 mM of NaCl and the amount of protein for each fraction was estimated and then samples were analysed by SDS-PAGE (Figure 4.3.1). Finally, the amount of LPS was estimated using an Endosafe-PTS spectrophotometer. The level of LPS found in the sample prior to the purification was 700 pg/ml but after purification, it decreased to about 1 pg/ml, which is considered a low concentration of LPS and this could then be used in the subsequent experiments. This consideration was based on the US Food and Drug Administration (FDA) findings, which suggested 50 pg/ml of LPS as the threshold required to induce any response of the cells (127).

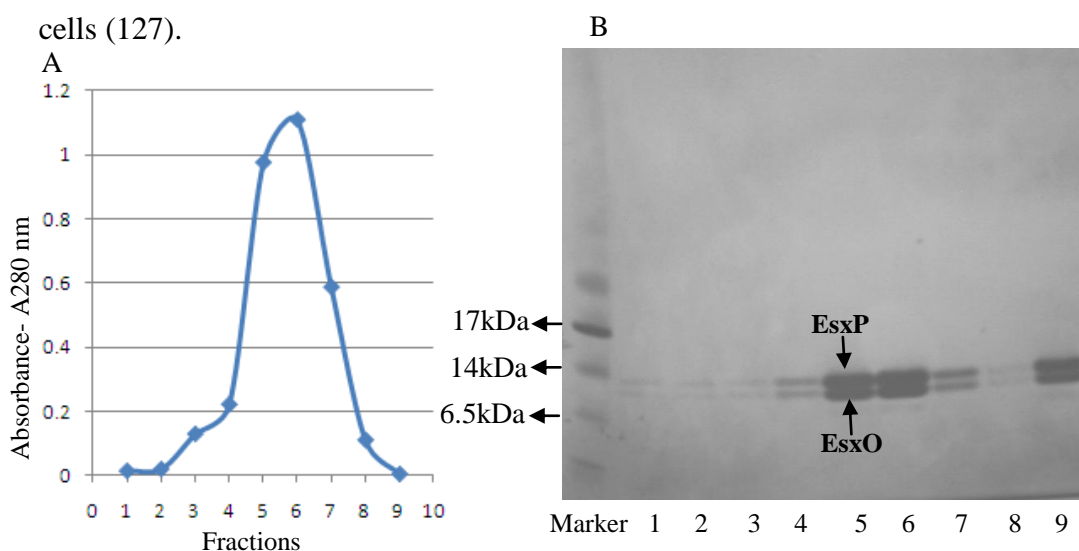


Figure 4.3.1. The EsxO/EsxP complex elution profile and LPS removal. Panel A shows a plot of elution profile fractions of EsxO/EsxP complex at 100 mM salt buffer. Panel B shows SDS-PAGE gel displaying the ion exchange column fractions of eluted EsxO/EsxP as a complex. The bands on the left hand side of the gel represent a low molecular weight marker. Lanes 1-9 are fractions of the eluted EsxO/EsxP complex. Lane 1-6 represent fraction 1-6 (as seen in panel A) respectively. Lanes 9, 7, 8 represent fraction 7, 8, 9 respectively.

4.3.2 Assessment of the effects of Esx complexes on cell the motility

J774 cells were exposed to either EsxA/EsxB or EsxO/EsxP complexes to investigate whether they have any effect on cell motility. Movies were generated by brightfield images taken every 15 minutes and a track was created for each cell using the manual tracking plugin of ImageJ (NIH, Bethesda, MD, USA) (78, 83, 86, 104, 209). The data of velocity and distance obtained from manual tracking of each cell track over duration of eight hours was entered into the chemotaxis tool from plugin of ImageJ to create track plots following the path of individual cells (Figure 4.3.2). This method was used to measure the accumulated distances, which were $67.75 \pm 24.5 \mu\text{m}$, $60.01 \pm 18.1 \mu\text{m}$ and $64.75 \pm 22.03 \mu\text{m}$ for the untreated cells, treated cells with esxA/esxB complex and with EsxP/EsxO complex, respectively. The velocity results were $0.14 \pm 0.051 \mu\text{m/minute}$, $0.12 \pm 0.037 \mu\text{m/minute}$ and $0.13 \pm 0.042 \mu\text{m/minute}$ for the untreated cells, treated cells with EsxA/EsxB complex and with EsxP/EsxO complex, respectively. Previous studies have reported a comparable velocities; $0.43 \mu\text{m/minute}$ and $0.67 \mu\text{m/minute}$ for J774 cells control and wild-type mouse bone marrow-derived macrophages (BMMS) cells respectively (108, 216). However, the slight differences might be as result of different cells or experimental conditions used.

The data of the average distance and velocity for all the cells generated from the analysis of cell motility showed no significant difference in terms of distance and velocity between the control cells and cells treated with EsxA/EsxB or EsxO/EsxP complexes (Figure 4.3.3). Also, the Euclidean distance was $4.04 \mu\text{m}$, $5.01 \mu\text{m}$ and $4.31 \mu\text{m}$ for untreated cells, treated cells with EsxA/EsxB complex and with EsxP/EsxO complex respectively. In the experiment, the directionality of the control

cells and cells exposed to EsxA/EsxB or to EsxO/EsxP complex were 0.06, 0.08 and 0.07 respectively. These results indicate that the cells do not migrate in a straight-line motion but many of turns and changes of the track of cells was observed, because directionality of cell was near 0 and the directionality of straight-line migration should be equal to or near 1(198).

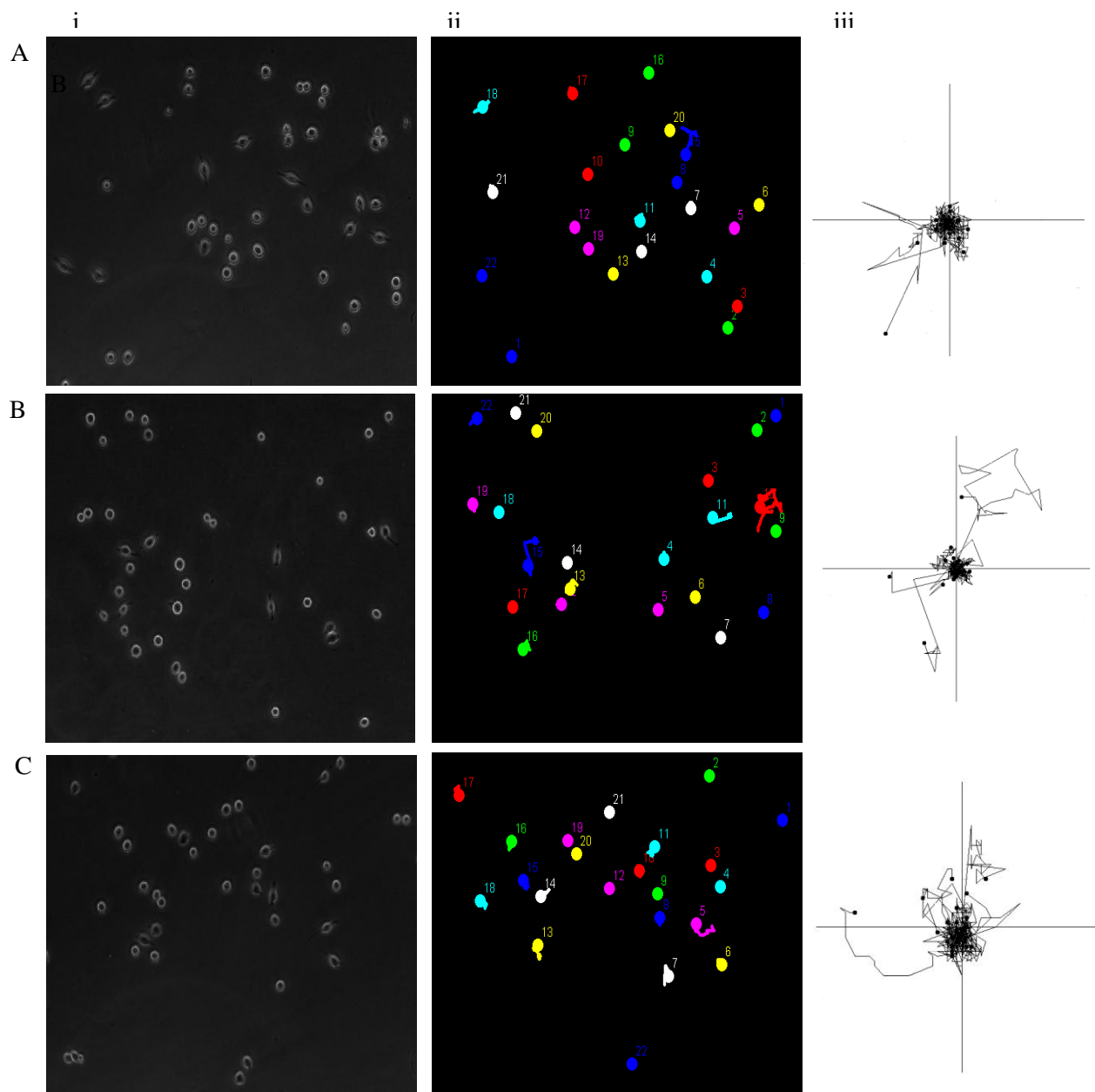


Figure 4.3.2 The migration tracks of 22 cells of untreated and treated cells with either EsxA/EsxB complex or EsxO/EsxP complex. Panels A, B and C respectively represent untreated, cells exposed to EsxA/EsxB complex and cells exposed to EsxO/EsxP complex. (i) shows all the raw images of J774 cells, (ii) shows the dot and track for each cell created by the manual tracking plugin of imageJ (NIH, Bethesda, MD, USA) and (iii) shows track plots created by following the path of individual cells using the chemotaxis tool plugin of imageJ(migration path) (78, 83, 86, 104, 209). 22 cells were used for each experiment.

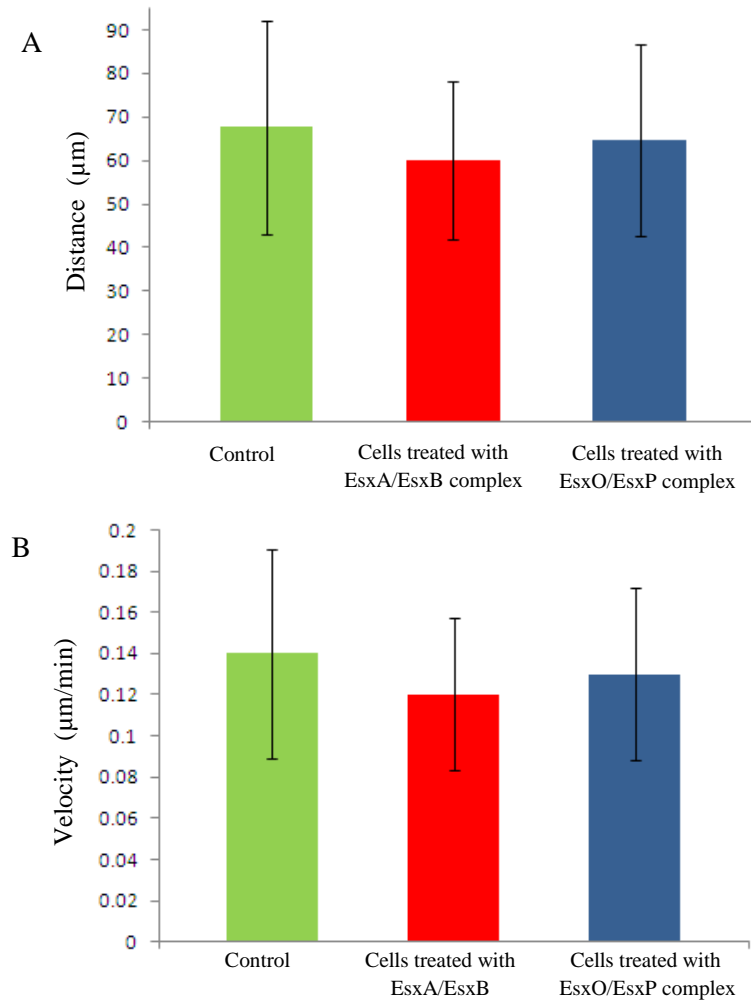


Figure 4.3.3 Cell migration was analysed using the manual tracking plugin of imageJ to identify any differences between the control cells and cells exposed to EsxA/EsxB or EsxO/EsxP complex in terms of distance and velocity. As illustrated by the bar charts, panel A shows that there is no significant change in accumulated distance for J774 macrophage cells when treated with EsxA/EsxB complex (red bar), EsxO/EsxP complex (blue bar) versus control cells (green bar). Panel B shows that no significant difference in the velocity of J774 macrophage cells when treated with EsxA/EsxB complex (red bar), EsxO/EsxP complex (black bar) and control (green bar). The Standard Deviation is calculated for each experimental condition. Note that 22 cells were used for each experiment.

4.3.3 Microarray analysis of gene expression change of U937 cells treated with EsxO/EsxP complex at different time points

T-test was used to determine whether there was any significant difference in the gene expression profiles between the untreated U937 cells and those treated with EsxO/EsxP complex for 30 minutes and 120 minutes. The principle component analysis (PCA) within array track was used to carry out an examination of the relationship among the samples. PCA showed that the untreated samples were grouped together as well as the treated samples were grouped together for both 30 minutes and 120 minutes treatments. In addition, the PCA analysis showed a clear differentiation between the treated and untreated groups, therefore it could be concluded that the data is of good quality and the genes are certainly differentially expressed between the treated group and the control group (Figure 4.3.4 panels A-B) (103, 167).

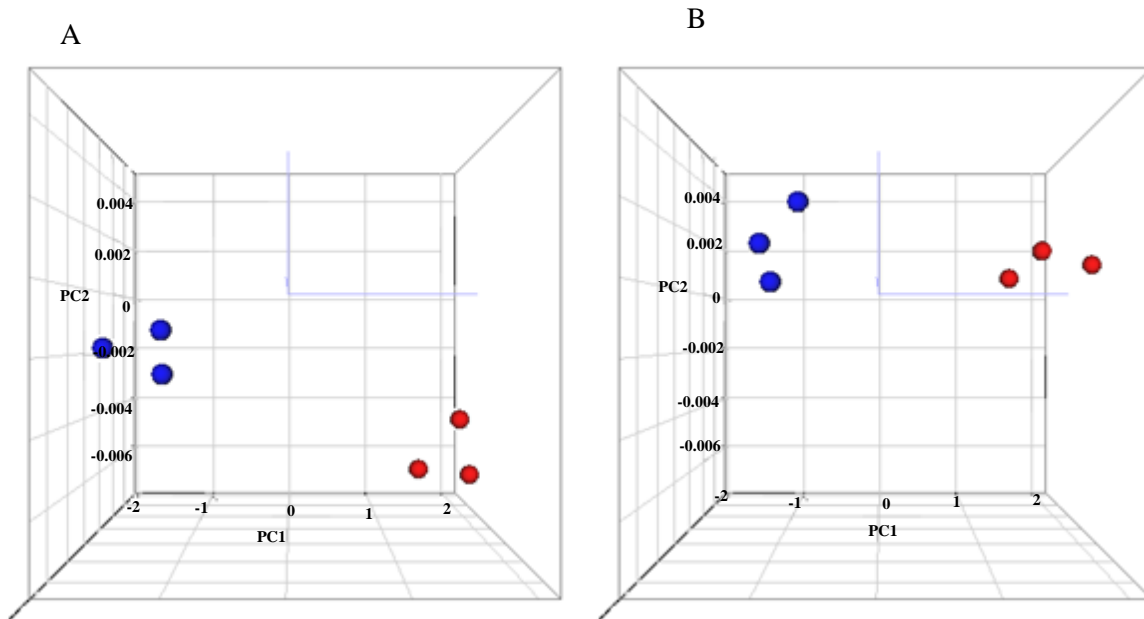


Figure 4.3.4 Panels A–B show Principal Component Analysis (PCA) 3D view for genes expression profile of three EsxO/EsxP complex-treated U937 cells samples (red dots) and three control samples (blue dots) for 30 minutes and 2h hour treatment experiments respectively. Three principle components (PC1, PC2 and PC3, the label is not show) are plotted. This analysis shows the samples were grouped together according to the untreated and treated samples. The separation between the untreated (controls) samples and the EsxO/EsxP treated samples indicates the good quality of the microarray experiment (103, 167).

Microarray data were visualized using a volcano plot and significant gene lists were generated using $p\text{-value} \leq 0.05$ and fold change ≥ 1.5 as criteria for significance. A volcano plot for differentially expressed genes between treated and untreated U937 cells is shown in figure 4.3.5 panels A-B (31, 62). The expression profiles of treated and control cells were analysed based on $p\text{-value} \leq 0.05$ and fold change ≥ 1.5 . A group of 6 genes were found to be differentially expressed by cells exposed to 30 minutes of treatment with the EsxO/EsxP complex, including 5 genes that were up-regulated and one gene that was down-regulated. On the other hand, the expression pattern for a group of 14 genes was found to be significantly changed after the 120 minutes treatment with the complex. Out of these 14 genes 9 genes were up-regulated while 5 genes were down-regulated. A complete list of these genes in both experiments (30 minutes and 120 minutes treatment with EsxO/EsxP complex) can be found in tables 4.3.1 and 4.3.2 respectively. There were 274 genes whose $p\text{-value}$ was less or equal 0.05 with fold change < 1.5 (pink dots), 60 genes that have fold change > 1.5 without considering the $p\text{-value}$ (yellow dots) and 14,123 non-significant genes whose fold change < 1.5 and $p\text{-value}$ more than 0.05 (black dots) after 30 minutes treatment. Whereas after 120 minutes treatment, there were 223 genes that have $p\text{-value}$ less than 0.05 with fold change < 1.5 (pink dots), 107 genes whose fold change > 1.5 without considering the $p\text{-value}$ (yellow dots) and 11,967 genes that fold change < 1.5 and $p\text{-value}$ more than 0.05 (black dots).

Hierarchical cluster analysis was used to group entities and conditions based on the similarity on their expression profile as demonstrated in this analysis, where distinct groupings of the controls and treated samples were observed, as shown in figure 4.3.5 panels C-D. These results indicated that EsxO/EsxP complex induced a distinct

pattern of gene expression changes (103). This cluster pattern shows that most similar profiles are joined together into a group, which suggests similarity within the untreated samples as well as the treated ones that were also grouped together into a separate cluster. In addition, the cluster pattern formation indicates variation between the expression profiles of the untreated group and the treated group clusters.

The selected genes of both treatments after 30 minutes and 120 minutes were analysed by Kyoto Encyclopedia of Genes and Genomes (KEGG), which provides information on metabolic and regulatory pathways in order to identify a disease or processes that were associated with the differentially expressed genes (DEGs) (97). However, functional analysis with KEGG showed that there was no significant gene cluster involved in any specific pathway. The 6 genes that were identified from the 30 minutes treatment with EsxO/EsxP complex, 2 genes were mapped to pathways collected by the KEGG database and found in two different pathways. The PDXK gene is involved in the vitamin B6 metabolism pathway and DAXX gene is involved in the MAPK signalling pathway. While, from the 14 genes identified in the 120 minutes treatment, 2 genes were also mapped to the pathway collected by the KEGG and found to be involved in different pathways. The HSPD1 gene is involved in the RNA degradation pathway and the ZYX gene is involved in the focal adhesion pathway.

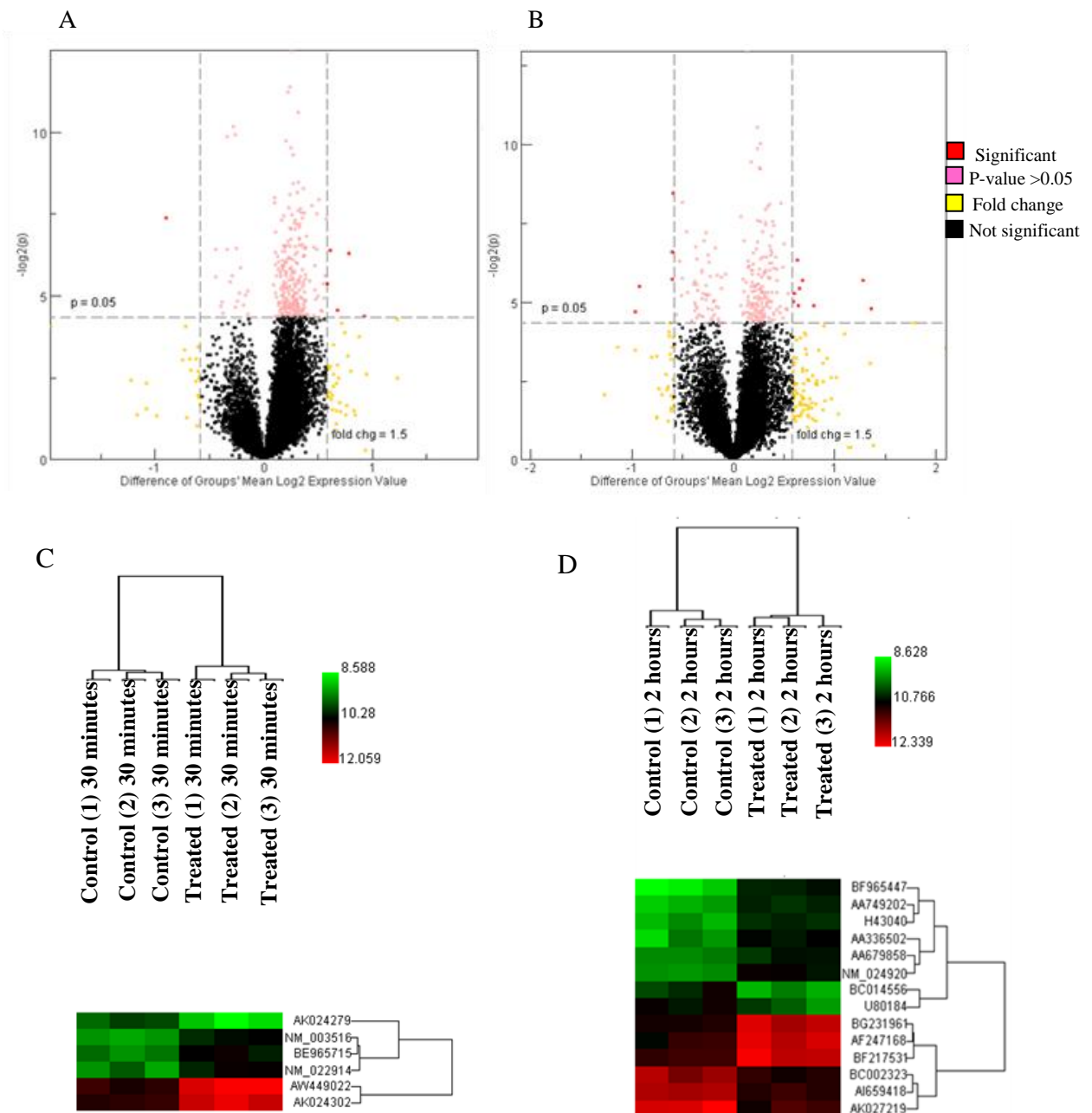


Figure 4.3.5 panels A and B show volcano plot of the significant gene expression change in the U937 cells when treated with EsxO/EsxP complex for 30 minutes and 120 minutes respectively. The plot is based on log₂ fold change versus log₂ *p*-value. The change in gene expression was identified as significant if the *P*-value was equal or less than 0.05 and the fold change equal or greater than 1.5. Red dots indicate significant genes (5 up-regulated and 1 down regulated after 30 minutes treated, 9 genes up-regulated and 5 genes down regulate after 120 minutes treated), features in pink dots indicate genes that have *p* < 0.05 and fold change < 1.5, features in yellow dots indicate genes that genes have *p* > 0.05 and fold change > 1.5, features in black dots indicate genes that have *p* > 0.05 and fold change < 1.5. Panels C–D hierarchical cluster analysis shows a significant change in gene expression profile for 6 genes and 14 genes at 30 minutes and 2 hours respectively which repeated three times for each experimental condition. The unique groupings of treated samples and controls indicated that EsxO/EsxP complex treatment induced a distinct pattern of genes expression change.

Table 4.3.1 Significant gene expression in U937 cells after treatment with EsxO/EsxP for 30 minutes ($p \leq 0.05$, fold change ≥ 1.5).

	GENEBANKACC	Gene name	<i>p</i> -value	Fold change	Description
1	AK024279	WIPI2	0.0061	0.5377	WD repeat domain phosphoinositide-interacting protein 2
2	NM_022914	ACD	0.0121	1.525	Adrenocortical dysplasia protein homolog
3	BE965715	DAXX	0.0129	1.7266	Death domain-associated protein
4	NM_003516	HIST2H2AA3	0.0245	1.5036	Histone H2A type 2-A (H2A.2) (H2A/o)
5	AK024302	OCIAD1	0.043	1.6063	OCIA domain-containing protein 1 (Ovarian carcinoma immunoreactive antigen)
6	AW449022	PDXK	0.0485	1.8983	Pyridoxal kinase (EC=2.7.1.35) (Pyridoxine kinase)

Table 4.3.2 Significant changes in expression when U937 cells exposed to EsxO/EsxP complex for 2 hours ($p \leq 0.05$, fold change ≥ 1.5).

	Genbank Acc	Gene name	<i>p</i> -value	Fold change	Description
1	BC002323	ZYX	0.003	0.6616	Zyxin (Zyxin-2)
2	U80184	FLII	0.0106	0.6608	Protein flightless-1 homolog
3	AA679858	SFRS2IP	0.0126	1.5489	Splicing factor, arginine/serine-rich, 2-interacting protein
4	AI659418	RCSD1	0.0195	0.6593	RCSD domain-containing protein 1
5	BF965447	HSPD1	0.0196	2.4304	
6	BG231961	MIRHG2	0.0199	1.6099	
7	AK027219		0.0228	0.5271	
8	AF247168	C1orf63	0.0235	1.5753	Chromosome 1 open reading frame 63
9	BF217531	TMEM181	0.0262	1.5208	Transmembrane protein 181
10	H43040	FUS	0.0316	1.5044	RNA-binding protein FUS (fused in sarcoma)
11	AA749202		0.0344	1.5554	
12	NM_024920	DNAJB14	0.0347	1.731	DnaJ homolog subfamily B member 14
13	AA336502	SMCHD1	0.0371	2.5698	
14	BC014556	FLJ35390	0.039	0.5124	

□ Unknown

The significant gene lists of 30 minutes treatment and 120 minutes treatment were compared using Venn diagrams to determine the number of common differentially expressed genes. Using this approach, no differentially expressed genes were identified as common between the 30 minutes treated and 120 minutes treated experiments (Figure 4.3.6).

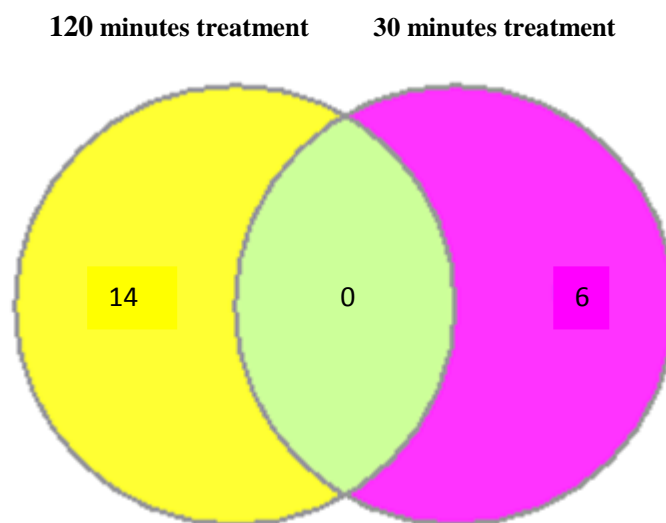


Figure 4.3.6 Venn diagrams comparing the differentially expressed genes between 30 minutes and 120 minutes treated U937 cells with EsxO/EsxP complex. This diagram shows no overlap between 30 minutes and 120 minutes EsxO/EsxP complex treated U937 cells.

The lists of significant genes found in both 30 minutes treatment and 2 hours treatment were directly utilized for GOFFA analysis (191). Biological process in GOFFA terms was examined for genes of 30 minute and 2 hour treatment individually. Terms that are significantly altered ($p < 0.05$) are summarised in Tables 4.3.3 and 4.3.4. Out of the 6 genes found to be differentially expressed in 30 minutes treatment experiment, 4 genes were identified in the GOFFA database. Two of these genes (ACD and HIST2H2AA3) were found to be involved in chromosome organization. In contrast, 5 genes were identified by the GOFFA database from 14 genes whose expression changes after 2 hour treatment experiment. However, the GOFFA analysis indicated no apparent relationship between these 5 genes in terms of biological processes.

Table 4.3.3 Significant biological processes created with GOFFA terms of U937 cells treated with EsxO/EsxP complex for 30 minutes ($p < 0.05$).

Gene name	GO ID	Go term	<i>p</i>-value
DAXX	GO:0051347	positive regulation of transferase activity	0.002835
	GO:0043085	negative regulation of nucleobase, nucleoside, nucleotide and nucleic acid metabolic process	0.013015
	GO:0044093	positive regulation of molecular function	0.016396
	GO:0000910	cytokinesis	0.016875
	GO:0031324	negative regulation of cellular metabolic process	0.02086
	GO:0070302	induction of programmed cell death	0.024861
	GO:0030522	regulation of cellular process	0.030995
PDXK	GO:0042823	pyridoxal phosphate biosynthetic process	0.000369
	GO:0042819	vitamin B6 biosynthetic process	0.001108
ACD	GO:0051347	telomere maintenance	0.002835
	GO:0034502	protein localization to chromosome	0.002952
	GO:0043085	positive regulation of catalytic activity	0.013015
	GO:0033554	chromosome organization	0.016843
	GO:0051716	telomere assembly	0.034714
	GO:0051101	regulation of DNA binding	0.04281
HIST2H2AA3	GO:0031497	chromatin assembly	0.027752
	GO:0065004	protein-DNA complex assembly	0.029555
	GO:0022607	chromosome organization	0.042439

Table 4.3.4 Significant biological processes create GOFFA terms of U937 cells treated with EsxO/EsxP complex for 2 hours ($P < 0.05$).

Gene name	GO ID	Go term	<i>p</i> -value
HSPD1	GO:0002368	B cell cytokine production	0.000493
	GO:0002840	regulation of T cell mediated immune response to tumor cell	0.000985
	GO:0032727	positive regulation of interferon-alpha production	0.001477
	GO:0043032	positive regulation of macrophage activation	0.001969
	GO:0042026	protein refolding	0.00246
	GO:0032733	positive regulation of interleukin-10 production	0.00246
	GO:0032735	positive regulation of interleukin-12 production	0.00246
	GO:0002836	toll-like receptor signaling pathway	0.007855
	GO:0002221	pattern recognition receptor signaling pathway	0.009322
	GO:0045088	regulation of innate immune response	0.026775
DNAJB14	GO:0006457	protein folding	0.002565
FUS	GO:0008380	cellular process	0.00823
ZYX	GO:0044419	biological regulation	0.008732
SFRS2IP	GO:0034622	cellular macromolecular complex assembly	0.011381
	GO:0006396	RNA processing	0.029231

4.4 Discussion

Recently, it has been shown by Davis and Ramakrishnan that in the initial phases of granuloma formation macrophages are in a high state of motility. Therefore, the early stages of granuloma formation might offer selective advantage to the pathogens as it would promote recruitment of macrophages into the sites of infection (45). In addition, infected macrophages are killed during the granuloma formation, which leads to active recruitment of uninfected macrophages to the site of infection. The recruited macrophages then phagocytose infected cell remnants and their bacterial contents. Davis and Ramakrishnan have demonstrated that the mycobacterial RD1 locus is essential for efficient recruitment of macrophages into the site of *M. marinum* infection. They have reported that RD1-deficient *M. marinum* could not properly execute the recruitment process and facilitate bacterial growth, thus, minimizing the rate of death of the infected cell and phagocytosis action of the uninfected cells (45). However, the molecular basis for RD-1-dependent recruitment of uninfected cells remains to be determined. Whether this is due to a direct effect of a product of ESX-1 secretion (such as EsxA and EsxB) or because of the stimulation of host chemokines or reaction to products of dying cells (such as uric acid) remains to be elucidated (19, 74, 133). There is an increasing effort to understand the role of ESX-1 proteins in mycobacterial virulence (45, 58, 196, 212). This might unveil essential information regarding the involvement of this virulence system in the survival of *M. marinum* (and presumably, *Mycobacterium tuberculosis*). The cell motility assays described in this chapter showed no significant difference in terms of distance and velocity between the control macrophages and macrophages exposed to EsxA/EsxB or EsxO/EsxP complexes, which suggests that macrophages motility might not be

altered by EsxA/EsxB or EsxO/EsxP complexes (Figure 4.3.3). Therefore, RD-1 dependent recruitment of uninfected cells may not be linked to EsxA and EsxB proteins, but might related to other proteins secreted by the RD1 region or the activation of host chemokines or response to the released contents of dying cells. However, as appropriate positive control for this motility assay, IL-4 has been shown to increase the motility of macrophages (55). IL-4 activates several signalling pathways, including the Akt pathway, which plays a key role in many cellular processes, such as cell motility (37, 217). Therefore, IL-4 would be an appropriate positive control for the motility assay described in this section to confirm that the motility assay is working.

In addition, in this study, it has been observed that the macrophages move in a random motion but not directed motion. Previous findings have revealed that random and directed motion together play a part in the movement process (45). It has been proposed that the signal generated by the infected macrophages resident in the granuloma stimulates new cell recruitment and random motion whereas another signal is produced by the dying cells which attract the nearby macrophages for phagocytosis. Therefore, both types of movements are hypothesized to be essential for effective phagocytosis of nascent granulomas (45).

Microarray analysis was used to determine whether exposure of U937 cells to EsxO/EsxP complex results in changes in gene expression. After the treatment of the cells with EsxO/EsxP complex for 30-minute, the expression of 6 genes was found to be significantly altered between untreated and treated samples. Five genes were up-regulated and one gene was down-regulated. Interestingly, half of the significant

genes found in the 30 minutes treatment could be involved in the regulation of chromatin structure and telomeres in the host. One of these genes is the death domain-associated protein (Daxx), which recently has emerged as a scaffold protein that directs the assembly of several nuclear complexes contributing to major aspects of the control of gene expression, such as the repression of several transcriptional activators (106, 119, 121, 175, 219). In addition, recent work has revealed that the ATRX–Daxx complex was attached to telomeric chromatin and that both components of the complex are essential for H3.3 deposition at telomeres; thus, both ATRX and H3.3 were required in maintaining telomere chromatin (52, 116). The second gene is HIST2H2AA3, which encodes histone H2AO; a variant of H2A, which is a member of the octamer of core histones; H3, H4, and H2B. Histones are now understood to play multiple roles in eukaryotic biology beyond the common function of DNA compaction for packaging into the nuclei. To this effect, histones were shown to recruit other DNA-associated proteins, mark genes for silencing and play a role in DNA repair and replication (24, 26). The third gene is *ACD*, which has been shown in several investigations to be essential in the protection of telomeres. This suggestion is supported by the evidence from the finding that *ACD* mutant mice showed telomere dysfunction and genomic instability (57, 98, 210). Together, these findings suggest that the EsxO/EsxP complex might indirectly mediate changes to host cell chromatin structure. In contrast, the 2 hour treatment with EsxO/EsxP complex showed 14 significant genes, but no link between these genes in any biologically significant way was observed. In addition, no overlap was seen between significant genes reported for both time-course treatments.

It has been demonstrated that LPS interacts with Toll-like receptor 4 (TLR4) on monocytes/macrophages, leading to a plethora of biological responses required for shaping both the innate and adaptive arms of the immune response (184, 192, 231). These effects are mediated through activation of many transcription factors, especially the nuclear factor NF- κ B, which induces a wide variety of cellular responses. The spectrum of these cellular responses covers the induction or repression of a wide range of genes that regulate inflammation, cell proliferation, migration and cell survival (16, 25, 77, 218, 223). Together, these studies indicate that LPS stimulates gene expression of immune cells. A number of studies have used LPS as a positive control in experiments involving the investigation of changes in gene expression in macrophages and untreated cells, to confirm the changes are induced or due to some other factor (67, 120). Therefore, LPS would be an appropriate positive control for the microarray experiments described here to confirm that the cells and arrays are working well.

Chapter 5

Conclusions and Future Work

5.1 Conclusions

5.1.1 Interactions of secreted *M. tuberculosis* factors with host cells

The structural analysis of the EsxA/EsxB complex suggests that its role is consistent with a receptor-mediated interaction with host cells (136). In addition, fluorescently tagged EsxA/EsxB binds human monocyte/macrophage tissue culture cells and this interaction is mediated by a long, flexible C-terminal arm on EsxB (136, 162). Experiments using monocyte/macrophage cell lines derived from mice have identified TLR2 as a receptor for EsxA (150). During *M. marinum* infection of zebrafish, macrophage aggregation is dependent upon RD-1 determinants, further supporting a receptor-mediated interaction of EsxA/EsxB with host cells (193).

The fluorescence microscopy work described in chapter 3 provides clear evidence that the EsxO/EsxP complex specifically binds to the surface of monocyte and macrophage cells. The results show the complex binding to the surface of U937 monocytes cells and J744 macrophages cells but not to fibroblast cell lines, which strongly suggests that the EsxO/EsxP complex specifically binds to a target on the surface of monocytic cells. The addition of excess unlabelled EsxO/EsxP complex inhibited the fluorescence labelling of monocytes and macrophages, thus confirming that binding is protein specific and not mediated by the fluorophore. It is also important to note that treatment of U937 and J774 cells with EsxO/EsxP complex

resulted in no significant cell lysis. Detailed confocal microscopy analysis revealed that the EsxO/EsxP complex forms cap-like structures on the surface of both U937 and J774 cells, which strongly suggests that the function of this complex involves a receptor-mediated interaction with host cells.

5.1.2 Escape of *M. tuberculosis* from the phagolysosome to the cytoplasm

Van der Wel *et al* demonstrated that the EsxA/EsxB complex helped the translocation of *M. tuberculosis* from phagolysosomes to the cytoplasm in myeloid cells. This work involved the use of mutant strains of *M. tuberculosis* (Tn::*esxB*) and *M. bovis* BCG, which are both unable to produce the EsxA/EsxB complex and failed to enter the host cytosol, indicating an important role for the EsxA/EsxB complex in this process (206). In contrast, an ESX-5 compromised mutant of *M. tuberculosis* retained the ability to escape from phagolysosomes into cytosol, which points to distinct roles for EsxA/EsxB and EsxO/EsxP complexes (3). One possibility is that the EsxA/EsxB complex is needed for cytosolic localization of mycobacteria to allow ESX-5 effectors molecules, such as the EsxO/EsxP complex to be secreted in the cytosol.

5.1.3 *M. tuberculosis* induced cell death

Van der Wel *et al* reported that *M. tuberculosis* infected dendritic cells (DC) showed significantly increased cell death. In contrast, *M. tuberculosis* Tn::*esxB* infected DC cells demonstrated lower apoptotic cell death, suggesting that EsxA/EsxB has some role in the induction of cell death following infection (206). Similarly, wild-type *M. marinum* infected cells showed increased cell death compared to ESX-5

compromised mutants, suggesting a potential role for ESX-5 secreted proteins, such as EsxO and EsxP, in inducing cell death (3).

It has been proposed that the EsxA/EsxB complex acts as a pore-forming molecule, however, incubation of the complex with monocyte and macrophage cells for up to 24 hours for fluorescence microscopy studies provided no evidence of cytolysis (91, 162). In addition, analysis of the surface features of the complex reveals no obvious hydrophobic patches essential for spanning the membrane during pore formation. In the same way, incubation of the EsxO/EsxP complex with monocyte and macrophage cells for up to 24 hours showed no evidence of cell lysis (chapter 3). Therefore, the structural and surface features of both ESX family complexes, together with specific binding to host cells, seems more consistent with a cell signaling role requiring interactions with one or more cell surface proteins.

5.1.4 ESX-mediated granuloma formation and early dissemination of *M. tuberculosis*

Studies have produced evidence that RD-1 proteins, including EsxA/EsxB, might mediate both the enhanced motility of uninfected macrophages in granuloma and their attraction to dead infected cells (45). More recent work, involving leukocytes derived from cattle has identified a specific interaction between the EsxA/EsxB complex and CD172a (SIRP α)-producing cells (215). Treating peripheral blood mononuclear cell cultures derived from *M. bovis*-infected calves with EsxA/EsxB complex led to specific expansion of SIRP α ⁺ cells, with binding of the complex to the surface of SIRP α ⁺ cells (215). The interaction with SIRP α -CD47 was shown to be

critical for effective migration of dendritic cells to the secondary lymphoid organs and skin (80, 207). Therefore, it has been suggested that EsxA/EsxB complex induced expansion of SIRP α -expressing cells might promote relocation of DCs/macrophages to the site of infection, encouraging effective granuloma formation and early dissemination of *M. tuberculosis*.

Investigation of the possible role of EsxO/EsxP or EsxA/EsxB on macrophage motility using live cell imaging (Section 4.3.2) showed no difference between treated and untreated cells in terms of either speed or distance. This suggests that there is no evidence that EsxA/EsxB or EsxO/EsxP directly affect macrophage motility.

5.1.5 *M. tuberculosis*-modulation of proinflammatory cytokine expression

The EsxA/EsxB complex has been shown to inhibit reactive oxidative species (ROS) production, as well as interfere with LPS-induced ROS production, which resulted in a downregulation of the production of various proinflammatory cytokines, such as TNF α , IL-2, INF- γ and nitric oxide synthase 2 (69, 101, 115). Interestingly, Misher *et al* have reported that EsxA is essential for stimulating caspase-1 activity within *M. tuberculosis* infected macrophages. Caspase-1 is a proteolytic enzyme that plays a central role in cell death by apoptosis (113), but it is also involved in the activation and release of IL-1 β , which is one of the key pro-inflammatory cytokines initiating the inflammatory response. In addition, activation of IL-1 β leads to the release of mature cytokines into extracellular space. These observations suggest a potential role for EsxA alone in apoptosis, as well as in inflammatory response (137). In contrast, previous studies have demonstrated that ESX-5-secreted proteins as complexes

suppress the expression of IL-12, TNF α and IL-6 in human macrophages infected with wild-type *M. marinum*. Surprisingly, infection of human macrophages with an ESX-5 mutant of *M. marinum* resulted in enhanced production of those proinflammatory cytokines (3). The data appear to suggest a role for ESX family proteins in modulating cytokine expression, but precise details remain unclear.

5.2 Future Works

5.2.1 Identification of Host cell Receptors for the EsxO/EsxP complex

Following the results reported in this thesis, one of the main aims for future work would be to identify the cell surface receptor that interacts with EsxO/EsxP. Several methods could be used to attempt to identify the EsxO/EsxP receptor, including affinity purification and photo-activated cross-linking.

The EsxO/EsxP complex containing an N-terminal His-tag on EsxP is purified by affinity purification. N-terminal His-tag on EsxP allows the EsxO/EsxP complex to be immobilized on a Ni-NTA (nickel-nitrilotriacetic acid) column, to which a U937 membrane fraction could be applied. After washing with buffer, bound proteins are eluted by increasing the concentration of imidazole. SDS-PAGE analysis of the eluted fractions from the complex exposed to the membrane fraction and the complex exposed to a buffer as a control could be compared. Proteins detected only in the presence of bound EsxO/EsxP complex could then be identified by mass spectroscopy (13, 71).

Previous studies using a cross-linking approach have demonstrated the specific binding of the mycobacterial proteins Rv2536 and Rv2560 to membrane proteins on U937 cells (70, 151), therefore similar methods using the photo-activated cross-linking agent, 4-benzoylbenzoic acid, succinimidyl ester (Molecular Probes), could be used to identify the host cell binding partner of the EsxO/EsxP complex. U937 cells would be exposed to a labelled EsxO/EsxP complex and upon UV illumination, it is expected that the cross-linking agent would covalently bind to U937 proteins interacting with the complex. Following the cross-linking event, the membrane

protein fraction from the U937 cells could be analysed by SDS-PAGE and bands containing EsxO/EsxP complex could be identified by western blotting, using specific antibodies. N-terminal sequencing or electrospray mass spectrometry of trypsin digested fragments could be use to identify the host cell partner bound to the EsxO/EsxP complex.

5.2.2 Cytokine assays

A recent study has used enzyme-linked immunosorbent assays (ELISA) to measure the level of interferon gamma (IFN- γ), which is produced by T-lymphocytes after stimulation by early secretory antigen target 6 (EsxA) and culture filtrate protein 10 (EsxB)(54). The ELISA assay is widely used for detecting and quantifying the concentration of cytokine proteins. This assay is highly specific, reliable and is relatively low cost and easy to use. These factos make ELISA a good option for assessing cytokine levels. The principle of ELISA in detecting cytokine is based on its recognition by capture and detection antibodies. However, the quality of these antibodies determines the assay sensitivity and specificity (161).

Previous studies have demonstrated that infection of human macrophages with wild-type *M. marinum* resulted in suppressed expression of IL-12, TNF- α and IL-6, but infection with an ESX-5 mutant resulted in strongly induced production of these proinflammatory cytokines (2, 3). This result suggests that ESX-5 plays a critical role in the modulation of immune cytokine secretion by human macrophages (3). As mentioned in chapter 2, the ESX-5 region is likely to be responsible for exporting several closely related pairs of Esx family complexes, including the EsxO/EsxP

complex. In addition, the fluorescence microscopy work described in chapter 3 provides clear evidence that the EsxO/EsxP complex specifically binds to the surface of monocyte and macrophage cells. Therefore, one possibility is that whether the expression of these cytokines (IL-12, TNF α and IL-6) is affected by the EsxO/EsxP complex, could be investigated using ELISA, comparing cells exposed to the EsxO/EsxP complex with non-exposed cells.

Appendix-1

Regents and culture Media

1.1 Selected Reagents

1.1.1 1 % (W/V) Agarose

1 g agarose in 100 ml of 1x TAB buffer. Heat until the agarose is fully dissolved.

Once cool, add ethidium bromide to a final concentration of 0.5 µg/ml.

1.1.2 Coomassie Brilliant Blue Staining

Dissolve 2.5 g/l coomassie brilliant blue in 40% methanol (v/v) and 10% acetic acid (v/v). Stir overnight at room temperature. Make up to 1 litre with dH₂O and filter through 0.2 µm filter.

1.1.3 Antibiotics

1.1.3.1 Ampicillin

Ampicillin stock solution: 100 mg/ml in dH₂O and filter sterilised through 0.2 µm syringe filter. Store at -20°C. Add to LB media to a final concentration of 100 µg/ml.

1.1.3.2 Kanamycin

Stock solution was prepared at 20 mg/ml in dH₂O and filter sterilised through 0.2 µm syringe filter. Store for one month at -20°C. Add to LB media to a final concentration of 40 µg/ml.

1.1.4 MES SDS running buffer

20x stock solution, 60.6 Tris base, 10.0 g sodium dodecyl sulphate (SDS). 97.8 g 2-(N-morpholino) ethanesulphonic acid (MES), 3.0 g EDTA in ultrapure water to 500 ml(Initrogen)

1.1.5 Bacterial Culture Media

1.1.5.1 Luria-Bertani (LB) Media

10 g/l tryptone, 5 g/l yeast extract, 10 g/l NaCl. Make up to volume with de-ionized H₂O and autoclave. Add appropriate antibiotic when cool.

1.1.5.2 Luria-Bertani (LB) agar

LB agar prepared as described above for LB broth with addition of 15 g/l bacteriological agar. Flasks were autoclaved and allowed to cool, with appropriate antibiotic added immediately prior pouring into plates.

Appendix-2

Competent Cell Preparation, Transformation Protocol

2.1 Preparation of Competent Cells

Reagents:

LB Medium - 10 ml sterile LB medium with no antibiotic (Appendix 1).

SOB Medium- 2 g tryptone, 0.5 g yeast extract, 0.05 g NaCl. Make up to 95 ml with dH₂O. Add 1 ml 250 mM KCl and adjust pH to 7.0. Make up to 100 ml with dH₂O, divide into 2 x 50 ml in 250 ml flasks and autoclave. Add 0.5 ml sterile 2 M MgCl₂ prior to use.

50% Glycerol Solution- Prepare 50% (v/v) glycerol in dH₂O and sterilise by autoclaving. Store at 4°C. Use at a final concentration of 15%.

50 mM CaCl₂ solution- Prepare 50 mM CaCl₂ in dH₂O, filter sterilise through 0.2 µm syringe filter into a sterile container.

Method :

Streak out *E.coli* (BL21 DE3) onto LB agar without antibiotic (Appendix 1). Incubate at 37°C overnight.

Inoculate one colony from the culture plates into 10 ml sterile LB (minus antibiotic).

Incubate at 37°C with shaking at 200 rpm overnight.

Use 1 ml of this culture to inoculate 50 ml SOB. Incubate at 37°C with shaking at 200 rpm until the absorbance reads at 600 nm is 0.5 (1 cm path length cell). Pellet cells by centrifugation, 5000 rpm at 4°C for 10 minutes. Resuspend pellet cells very gently in 25 ml ice- cold 50 mM CaCl₂ and incubate on ice for 30 minutes. Spin down cells as before and very gently in 2.1 ml ice-cold 50 mM CaCl₂, keeping cells on ice. Add 900 µl ice-cold 50% glycerol and mix gently by inversion, do not vortex. Aliquot 100 µl cells into sterile cryogen tubes and flash freeze in liquid nitrogen. Store at -80°C until required.

2.2 Transformation of Competent Cells

Reagents:

Prepare LB agar plates with the appropriate antibiotic as described in appendix 1

Prepare LB broth minus antibiotic marker (appendix 1).

Method:

Aliquot 50 µl competent cells into sterile 1.5 ml eppendorf tubes. Add 4 µl of plasmid mixture and then mix gently. Incubate the mixture on ice for 30 minutes. Heat shock at 42°C for 45 seconds and then leave on ice for 5 minutes. Add 300 µl LB broth (no antibiotic) and incubate for 45 minutes at 200 rpm and 37°C, with the tubes placed horizontally in the incubator. Plate out cells 50, 100 and 200 µl aliquots onto LB agar (with appropriate marker) and incubate at 37°C overnight.

References

- 1- Aagaard, C.I., Brock, A., Olsen, T.H., Ottenhoff, K., and Weldingh. (2004) Mapping of the immune reactivity of Rv2653 and Rv2654; two novel low molecular mass antigens found specifically in the *Mycobacterium tuberculosis* complex. *Journal of Infectious Diseases*. **189**, 812-819.
- 2- Abdallah, A.M., Gey, van Pittius, N.C., Champion, P.A., Cox, J., Luirink, J., Vandenbroucke-Grauls, C.M., Appelmelk, B.J. and Bitter, W. (2007) Type VII secretion-mycobacteria show the way. *Nature Reviews Microbiology*. **11**, 883-891.
- 3- Abdullah, A.M., Savage, N.D., van Zon, M., Wilson, I., and Vandenbroucke-Grauls, C.M, et al. (2008) The ESX-5 secretion system of *Mycobacterium marinum* modulates the macrophage response. *The Journal of Immunology*. **181**, 7166-7157.
- 4- Abdallah, A.M., Verboom, T., Hannes, F., Safi, M., and Strong, M., et al. (2006) A specific secretion system mediates PPE41 transport in pathogenic mycobacteria. *Molecular Microbiology*. **62**, 662-679.
- 5- Abramo, C., Meijgaarden, KE., Garcia, D., Franken, KL., Klein, MR., Kolk, AJ., Oliveira, SC., Ottenhoff, TH., Teixeira, HC. (2006) Monokine induced by interferon gamma and IFN- γ response to a fusion protein of *Mycobacterium tuberculosis* ESAT-6 and CFP-10 in Brazilian tuberculosis patients. *Microbes and Infection*. **1**, 45–51.

- 6- Ahmad, S. (2011) Pathogenesis, immunology, and diagnosis of latent Mycobacterium tuberculosis infection. *Clinical Developmental Immunology*. **2011**, 814943–814960.
- 7- Alderson, B., Bement, T., Day, C., Zhu, L., Molesh, D., Skeiky, W., Coler, R., Lewinsohn, D., Reed, S., and Dillon, D. (2000) Expression cloning of an immunodominant family of Mycobacterium tuberculosis Antigens Using Human CD4+ T Cell. *Journal of Experimental Medicine*. **191**, 551-559.
- 8- Aliprantis, A.O., Yang, R.B., Mark, M.R. (1999) Cell activation and apoptosis by bacterial lipoproteins through Toll- like receptor-2. *Science*. **285**, 736–739.
- 9- Andersen, P., Munk, ME., Pollock, J.M., and Doherty, T.M. (2000) Specific immune-based diagnosis of tuberculosis. *Lancet*. **92**, 1048-9.
- 10- Arhets, P., Olivo, J.C., Gounon, P., Sansonetti, P., and Guillén, N. (1999) Virulence and functions of myosin II are inhibited by overexpression of light meromyosin in Entamoeba histolytica. *Molecular Biology of the Cell*. **6**, 1537-47.
- 11- Aslanidis, C., and Jong, P. (1990) Ligation independent cloning of PCR products (LIC-PCR). *Nucleic acids Research*. **18**, 6069-6074.

- 12- Bafica, A., Scanga, CA., Feng, CG., Leifer, C., Cheever, A., Sher, A. (2005) TLR9 regulates Th1 responses and cooperates with TLR2 in mediating optimal resistance to Mycobacterium tuberculosis. *Journal of Experimental Medicine*. **202**, 1715–1724.
- 13- Baldwin, M. (2004) Protein Identification by Mass Spectrometry Issues to be Considered. *Molecular & Cellular Proteomics*. **6**, 143-48.
- 14- Barry, E.B., Boshoff, H., Dartois, V., Dick, T., Ehrt, S., Flynn, J., Schnappinger D., Wilkinson, R., and Young D. (2009) The spectrum of latent tuberculosis: rethinking the biology and intervention strategies. *Nature Reviews Microbiology*. **7**, 845-855.
- 15- Bao, L., Chen, W., Zhang, H., Wang, X. (2003) Virulence, immunogenicity, and protective efficacy of two recombinant Mycobacterium bovis bacillus Calmette-Guerin strains expressing the antigen ESAT-6 from Mycobacterium tuberculosis. *Infection and Immunity*. **71**, 1656–1661.
- 16- Babu, AN., Meng, X., Zou, N., Yang, X., Wang, M., Song, Y., Cleveland, JC., Weyant, M., Banerjee, A., Fullerton, DA. (2008) Lipopolysaccharide stimulation of human aortic valve interstitial cells activates inflammation and osteogenesis. *Annals of Thoracic Surgery*. **1**, 71-6.

17- Bass, J.B., Farer, L.S, Hopewell, P.C., Brien, R., Jacobs, R.F., Snider, D.E., and Thornton, G. (1994) Treatment of tuberculosis and tuberculosis infection in adults and children. American Thoracic Society and the Centers for Disease Control and Prevention. *Journal of Respiratory and Critical Care Medicine*. **149**, 1359-1374.

18- Behr, M.A., Wilson, M.A., Gill, W.P., Salamon, H., Schoolnik, G.K., Rane, S., and Small, P.M. (1999) Comparative genomics of BCG vaccines by whole-genome DNA microarray. *Science*. **284**, 1520-3.

19- Behrens, M.D., Wagner, W.M., Krco, C.J., Erskine, C.L., Kalli, K.R., Krempski, J., Gad, E.A., Disis, M.L., and Knutson, K.L. (2008) The endogenous danger signal, crystalline uric acid, signals for enhanced antibody immunity. *Blood*. **3**, 1472-9.

20- Berthet, F.X., Ramussen, P.B., Rosenkrands, I., Andersen, P., and Gicquel, B. (1998) A Mycobacterium tuberculosis operon encoding ESAT-6 and a novel low-molecular-mass culture filtrate protein (CFP-10). *Microbiology*. **144**, 3195-3203.

21- Berthet, FX., Rasmussen, PB., Rosenkrands, I., Andersen, P., Gicquel, B. (1998) A Mycobacterium tuberculosis operon encoding ESAT-6 and a novel low-molecular-mass culture filtrate protein (CFP-10). *Microbiology*. **144** , 3195-203.

22- Beutler, B and Rietschel, T. (2003) Innate immune sensing and its roots: the story of endotoxin. *Nature review*. **3**, 169-174

23- Bitter, W., Houben, E.N., Bottai, D., Brodin, P., Brown, E.J., Cox, J.S., Derbyshire, K., Fortune, S.M., Gao, L.Y., Liu, J., Gey van Pittius, N.C., Pym, A.S., Rubin, E.J., Sherman, D.R., Cole, S.T., Brosch, R. (2009) Systematic genetic nomenclature for type VII secretion systems. *PLoS Pathogens*. **5**, e1000507.

24- Bonenfant, D., Coulot, M., Towbin, H., Schindler, P., van Oostrum, J. (2006) Characterization of histone H2A and H2B variants and their post-translational modifications by mass spectrometry. *Molecular & Cellular Proteomics*. **3**, 541-52.

25- Bonizzi, G., Karin, M. (2004) The two NF-kappaB activation pathways and their role in innate and adaptive immunity. *Trends Immunol*. **25**, 280-288.

26- Boyne, M.T., Pesavento, J.J., Mizzen, C.A., Kelleher, N.L. (2006) Precise characterization of human histones in the H2A gene family by top down mass spectrometry. *Journal of Proteome Research*. **2**, 248-53.

27- Brandt, L., Cunha, J.F., Olsen, A.W., Chilima, B., Appelberg, R.H. and Andersen, P. (2002) Failure of the *Mycobacterium bovis* BCG Vaccine: Some Species of Environmental Mycobacteria Block Multiplication of BCG and Induction of Protective Immunity to Tuberculosis. *Infection and Immunity*. **70**, 672-678.

28- Brennan, M.J., Delogu, G. (2002) The PE multigene family: a 'molecular mantra' for mycobacteria. *Trends Microbiol*. **10**, 246-9.

- 29- Brightbill, H.D., Libraty, D.H., Krutzik, S.R. (1999) Host defense mechanisms triggered by microbial lipoproteins through toll-like receptors. *Science*. **285**, 732–736.
- 30- Brodin, P., de Jonge, M.I., Majlessi, L., Leclerc, C., Nilges, M., Cole, S.T., and Brosch, R. (2005) Functional Analysis of Early Secreted Antigenic Target-6, the Dominant T-cell Antigen of *Mycobacterium tuberculosis*, Reveals Key Residues Involved in Secretion, Complex Formation, Virulence, and Immunogenicity. *The Journal of Biological Chemistry*. **280**, 33953-33959
- 31- Brosch, R., Pym, A.S., Gordon, S.V., and Cole, S.T. (2001) The evolution of mycobacterium pathogen city: clues from comparative genomics. *Trends Microbiol.* **45**, 452- 458.
- 32- Brusasca, P.N., colangeli, R., Lyashchenko, K.P., Zhao, X., Vogelstein, M., Spencer, J.S., McMurray, D.N. and Gennaro, M.L. (2001) Immunological characterization of antigens encoded by the RD1 region of the *Mycobacterium tuberculosis* genome. *Infection and Immunity*. **70**, 6996-7003.
- 33- Camacho, L.R., Constant, P., Raynaud, C., Laneelle, M.A., Triccas, J.A., Gicquel, B., Daffe, M., and Guilhot, C. (2001) Analysis of the phthiocerol dimycocerosate locus of *Mycobacterium tuberculosis*. Evidence that this lipid is involved in the cell wall permeability barrier. *The Journal of Biological Chemistry*. **276**, 19845-19854.

- 34- Camus, J.C., Pryor, M.J., Médigue, C., and Cole, S.T. (2002) Re-annotation of the genome sequence of *Mycobacterium tuberculosis* H37Rv. *Microbiology*. **10**, 2967-73.
- 35- Champion, P.A., Stanley, S.A., Champion, M.M., Brown, E.J., and Cox J.S. (2006) C-terminal signal sequence promotes virulence factor secretion in *Mycobacterium tuberculosis*. *Science*. **313**, 1632–1636
- 36- Chenna, R., Sugawara, H., Koike, T., Lopez, R., Gibson, T.J., Higgins, DG and Thompson, J.D. (2003) Multiple sequence alignment with the Clustal series of programs. *Nucleic Acids Res.* **31**, 3497-500.
- 37- Chin, YR., Toker, A. (2009) Function of Akt/PKB signaling to cell motility, invasion and the tumor stroma in cancer. *Cell Signal*. **4**, 470-6.
- 38- Clamp, M., Cuff, J., Searle, S.M., and Baton, G.J. (2004) *Bioinformatics*. **20**, 426-427.
- 39- Cole, S.T., Brosch, R., Parkhill, J., Garnier, T., Churcher, C., Harris, D., Gordon, S.V., Eiglmeier, K., Gas, S., Barry, C.E., Tekaiia, F., Badcock, K., Basham, D., Brown, D., Chillingworth, T., Connor, R., Davies, R., Devies, K., Feltwell, T., Gentles, S., Hamlin, N., Holroyd, S., Hornsby, T., Jagels, K., Krogh, A., McLean, J., Moule, S., Murphy, L., Oliver, K., Osborne, J., Quail, M.A., Rajandream, M.A., Rogers, J., Rutter, S., Seeger, K., Skelton, J., Squares, R., Squares, S., Sulton,

J.E., Taylor, K., Whitehead, S., and Barrell, B.G. (1998) Deciphering the biology of *Mycobacterium tuberculosis* from the complete genome sequence. *Nature*. **393**, 537-544.

40- Collins, T.J. (2007) ImageJ for microscopy. *Biotechniques*. **43**, 25-30.

41- Cordelieres, F. (2004) Manual Tracking. *Institut Curie, Orsay (France)*. First version.

42- Coulombe, F., Divangahi, M., Veyrier, F., de, Léséleuc L., Gleason, JL., Yang, Y., Kelliher, MA., Pandey, AK., Sasseti, CM., Reed, MB.,Behr,MA. (2009) Increased NOD2-mediated recognition of N-glycolyl muramyl dipeptide. *Journal of Experimental Medicine*. **206**, 1709–1716.

43- Cox, H.S., Morrow, and Deutschmann, P.W. (2008) Long term efficacy of DOTS regimens for tuberculosis. *systematic review*. **336**, 485-487.

44- Cui, X., Churchill, G.A. (2003) Statistical tests for differential expression in cDNA microarray experiments. *Genome Biology*. **4**, 210-221.

45- Davis, J., and Ramakrishnan, L. (2009) The Role of the Granuloma in Expansion and Dissemination of Early Tuberculous Infection. *Cell*. **136**, 37-49.

- 46- Derrick, SC., Morris, SL. (2007) The ESAT6 protein of *Mycobacterium tuberculosis* induces apoptosis of macrophages by activating caspase expression. *Cellular Microbiology*. **9**, 1547–1555.
- 47- Deutscher, M. (2006) Degradation of RNA in bacteria: comparison of mRNA and stable RNA. *Nucleic Acids Research*. **34**, 659-666.
- 48- Dietrich, J., Weldingh, K., Andersen, P. (2006) Prospects for a novel vaccine against tuberculosis. *Veterinary Microbiology*. **112**, 163-169.
- 49- DiGiuseppe Champion, P.A., and Cox, J.S. (2007) Protein secretion systems in Mycobacteria. *Cell Microbiol*. **9**, 1376-84
- 50- Dillon, D., Alderson, M., Day, C., Bement, T., Campos-Neto, A., Skeiky, Y., Roberts, A., Steen, S., Dalemans. W., Badaro, R., Reed, S., Vedvick, T., and Houghton, R. (2000) Molecular and Immunological Characterization of *Mycobacterium tuberculosis* CFP-10, an Immunodiagnostic Antigen Missing in *Mycobacterium bovis* BCG . *Journal of Clinical Microbiology*. **38**, 3285-3290.
- 51- Divangahi, M., Mostowy, S., Coulombe, F., Kozak, R., Guillot, L., Veyrier, F., Kobayashi, KS., Flavell, RA., Gros, P., Behr, MA. (2008) NOD2-deficient mice have impaired resistance to *Mycobacterium tuberculosis* infection through defective innate and adaptive immunity. *Journal of Immunology*. **181**, 7157–7165.

52- Drané, P., Ouararhni, K., Depaux, A., Shuaib, M., and Hamiche, A.(2010) The death-associated protein DAXX is a novel histone chaperone involved in the replication-independent deposition of H3.3. *GENES & DEVELOPMENT*. **12**, 1253-65.

53- Drennan, MB., Nicolle, D., Quesniaux, VJ., Jacobs, M., Allie, N., Mpagi, J., Frémond, C., Wagner, H., Kirschning, C., Ryffel, B. (2007) Tolllike receptor 2-deficient mice succumb to *Mycobacterium tuberculosis* infection. *American Journal of Pathology*. **164**, 49–57.

54- DS,V., Souza, D., Cabral, M., Rego, J., Balbino, V., Saad, MH., Schindler, HC., Abath, FG., Montenegro,S. (2010) Immunological diagnosis of tuberculosis based on recombinant antigens ESAT-6 and CFP-10 in children from an endemic area in northeast Brazil. *Scandinavian Journal of Immunology*. **72**, 460-8.

55- Dugast, C., Gaudin, A., Toujas, L. (1997) Generation of multinucleated giant cells by culture of monocyte-derived macrophages with IL-4. *Journal of Leukocyte Biology*. **4**, 517-21.

56- Eda, S., Yamanaka, M., and Beppu, M. (2004) Carbohydrate-mediated phagocytic recognition of early apoptotic cells undergoing transient capping of CD43 glycoprotein. *The Journal of Biological Chemistry*. **7**, 5967-74.

57- Else, T., Theisen, B.K., Wu, Y., Hutz, J.E., Keegan, C.E., Hammer, G.D., and Ferguson, D.O. (2007) Tpp1/Acd maintains genomic stability through a complex role in telomere protection. *Chromosome Res.* **8**, 1001-13.

58- Ernest, J., Trevejo-Nunez, G., and Banaiee, N. (2007) Genomics and the evolution, pathogenesis, and diagnosis of tuberculosis. *The Journal of Clinical Investigation.* **117**, 1738–1745.

59- Fenhalls, G., Stevens, L., Bezuidenhout, J., Amphlett, G.E., Duncan, K., Bardin, P., Lucky, P.T. (2002) Distribution of IFN-gamma, IL-4 and TNF-alpha protein and CD8 T cells producing IL-12p40 mRNA in human lung tuberculous granulomas. *Immunology.* **105**, 325-335.

60- Fenhalls, G., Stevens, L., Moses, L., Bezuidenhout, J., Betts, J.C., Helden, P.V. P., Lukey, P.T., Duncan, K. (2002) In situ detection of Mycobacterium tuberculosis transcripts in human lung granulomas reveals differential gene expression in necrotic lesions. *Infection and Immunity.* **70**, 6330-6338.

61- Fenton, M.J., Vermeulen, M.W. (1996) Immunopathology of tuberculosis: roles of macrophages and monocytes. *Infection and Immunity.* **64**, 683-90.

62- Fine, P.E.M., Carneiro, I.A.M., Milstein, J.B. and Clements, C.J. (1999) Issues related to the use of BCG in immunization programmes: a discussion document.

World Health Organization, Geneva, Switzerland. *WHO/V&B*. **23**, 1-44.

63- Flynn, J.L., Chan, J. (2005) what's good for the bug. *Trends Microbiol.* **13**, 98-102.

64- Fremont, C.M., Togbe, D., Doz, E., Rose, S., Vasseur, V., Maillet, I., Jacobs, M., Ryffel, B., Quesniaux, VF. (2007) IL-1 receptor-mediated signal is an essential component of MyD88-dependent innate response to Mycobacterium tuberculosis infection. *Journal of Immunology*. **179**, 1178–1189.

65- Fortune, S.M., Jaeger, A., Sarracino, D.A., Chase, M.R., Sasseti, C.M., Sherman, D.R., Bloom, B.R., and Rubin, E.J. (2005) Mutually dependent secretion of proteins required for mycobacteria virulence. *PNAS*. **102**, 10676-10681.

66- Fulton, SA., Reba, SM., Pai, RK., Pennini, M., Torres, M., Harding, CV., Boom, WH. (2004) Inhibition of major histocompatibility complex II expression and antigen processing in murine alveolar macrophages by mycobacterium bovis BCG and the 19-kilodalton mycobacterial lipoprotein. *Infection and Immunity*. **72**, 2101–2110.

67- Galindo, CL., Fadl, AA., Sha, J., Pillai, L., Gutierrez, C. Jr., Chopra, AK. (2005) Microarray and proteomics analyses of human intestinal epithelial cells treated with the *Aeromonas hydrophila* cytotoxic enterotoxin. *Infection and Immunity*. **5**, 2628-43.

68- Garnier, T., Eiglmeier, K., Camus, J.C., Medina, N., Mansoor, H., Pryor, M., Duthoy, S., Grondin, S., Lacroix, C., Monsempe, C., Simon, S., Harris, B., Alkin, R., Doggett, J., Mayes, R., Keating, L., Wheeler, P.R., Parkhill, J., Barrell, B.G., Cole, S.T., Gordon, S.V., and Hewinson, R.G. (2003) The complete genome sequence of *Mycobacterium bovis*. *PNAS*. **100**, 7877-7882.

69- Ganguly, N., Giang, PH., Gupta, C., Basu, SK., Salunke, DM., Sharma, P. (2008) *Mycobacterium tuberculosis* proteins CFP-10, ESAT-6 and the CFP10:ESAT6 complex inhibit lipopolysaccharide-induced NF- κ B transactivation by downregulation of reactive oxidative species (ROS) production. *Immunology and Cell Biology*. **86**, 98-106.

70- García, J., Puentes, A., Rodríguez, L., Ocampo, M., Curtidor, H., Vera, R., Lopez, R., Valbuena, J., Cortes, J., Vanegas, M., Barrero, C., Patarroyo, MA., Urquiza, M., Patarroyo, ME. (2005) *Mycobacterium tuberculosis* Rv2536 protein implicated in specific binding to human cell lines. *Protein Science*. **14**, 2236-45

71- Gingras, A., Aebersold, R., Raught, B. (2005) Advances in protein complex analysis using massspectrometry. *Journal Physiol*. **563**, 11-21.

72- Gehring, AJ., Dobos, KM., Belisle, JT., Harding, CV., Boom, WH.(2004) *Mycobacterium tuberculosis* LprG (Rv1411c): a novel TLR-2 ligand that inhibits human macrophage class II MHC antigen processing. *The Journal of Immunology*. **173**, 2660–2668.

73- Gey Van Pittius, N.C., Gamielien, J., Hide, W., Brown, G.D., Siezen, R.J., Beyers, A.D. (2001) The ESAT-6 gene cluster of *Mycobacterium tuberculosis* and other high G+C Gram-positive bacteria. *Genome Boil.* **2**, 1334-45.

74- Green, DR., Ferguson, T., Zitvogel, L., Kroemer, G. (2009) Immunogenic and tolerogenic cell death. *Nat Rev Immunol.* **5**, 353-63.

75- Greenfield, N.J. (2006) Using circular dichroism spectra to estimate protein secondary structure. *Nature protocols.* **6**, 2876-2890.

76- Gringhuis, SI., den Dunnen, J., Litjens, M., van der Vlist, M., Geijtenbeek, TB. (2009) Carbohydrate-specific signaling through the DC-SIGN signalosome tailors immunity to *Mycobacterium tuberculosis*, HIV-1 and *Helicobacter pylori*. *Nature Immunology.* **10**, 1081-1088.

77- Guha, M., O'Connell, MA., Pawlinski, R., Hollis, A., McGovern, P., Yan, SF., Stern, D., Mackman, N. (2001) Lipopolysaccharide activation of the MEK-ERK1/2 pathway in human monocytic cells mediates tissue factor and tumor necrosis factor alpha expression by inducing Elk-1 phosphorylation and Egr-1 expression. *Blood.* **5**, 1429-39.

78- Guryanova, OA., Drazba, JA., Frolova, EI., Chumakov, PM. (2011) Actin Cytoskeleton Remodeling by the Alternatively Spliced Isoform of PDLIM4/RIL Protein. *The Journal of Biological Chemistry*. **30**, 26849-59.

79- Guinn, KM., Hickey, MJ., Mathur, SK., Zakel, KL., Grotzke, JE., Lewinsohn, DM., Smith, S., Sherman, DR. (2004) Individual RD1 -region genes are required for export of ESAT-6/CFP-10 and for virulence of *Mycobacterium tuberculosis*. *Molecular Microbiology*. **51**, 359–370.

80- Hagnerud, S., Manna, PP., Cella, M., Stenberg, A., Frazier, WA., Colonna, M., Oldenborg, PA. (2006) Deficit of CD47 results in a defect of marginal zone dendritic cells, blunted immune response to particulate antigen and impairment of skin dendritic cell migration. *Journal of Immunology*. **176**, 5772–5778.

81- Harding, C.V., Boom, W.H. (2010) Regulation of antigen presentation by *Mycobacterium tuberculosis*: a role for Toll-like receptors. *Nature Reviews Microbiology*. **8**, 296-307.

82- Harries, A.D., Jahn, A., Zachariah, R., and Enarson, D. (2008). "Adapting the DOTS framework for tuberculosis control to the management of non-communicable diseases in sub-Saharan Africa". *PLoS Medicine*. **5**, e124.

- 83- Harris, SJ., Parry, RV., Foster, JG., Blunt, MD., Wang, A., Marelli-Berg F, Westwick, J., Ward, SG. (2011) Evidence that the lipid phosphatase SHIP-1 regulates T lymphocyte morphology and motility. *Journal Immunol.* **8**, 4936-45.
- 84- Hannig, G., Makrides, S.C., (1998) Strategies for optimizing heterologous protein in Escherichia coli. *Trends Biotechnol.* **16**, 54-60.
- 85- Heldwein, KA., Liang, MD., Andresen, TK., Thomas, KE., Marty, AM., Cuesta, N., Vogel, SN., Fenton, MJ. (2003) TLR2 and TLR4 serve distinct roles in the host immune response against Mycobacterium bovis BCG. *Journal of Leukocyte Biology.* **74**, 277–286.
- 86- Henry, SC., Traver, M., Daniel, I X., Indaram, M., Oliver, T., Taylor, GA. (2010) Regulation of macrophage motility by Irgm1. *J Leukoc Biol.* **2**, 333-43.
- 87- Hölscher, C., Reiling, N., Schaible, UE., Hölscher, A., Bathmann, C., Korbel, D., Lenz, I., Sonntag, T., Kröger, S., Akira, S., Mossmann, H., Kirschning, CJ., Wagner, H., Freudenberg, M., Ehlers, S. (2008) Containment of aerogenic Mycobacterium tuberculosis infection in mice does not require MyD88 adaptor function for TLR2, -4 and -9. *European Journal of Immunology.* **38**, 680–694.
- 88- Horwitz, M.A. (2005) Recombinant BCG expressing Mycobacterium tuberculosis major extracellular proteins. *Microbes and Infection.* **31**, 7 947-954.

89- Haugland, R. (2005) *The Handbook: A Guide to Fluorescent Probes and Labeling Technologies. Invitrogen.* p 10-32.

90- Hemmi, H., Takeuchi, O., Kawai, T., Kaisho, T., Sato, S., Sanjo, H., Matsumoto, M., Hoshino, K., Wagner, H., Takeda, K., Akira, S.(2000) A Toll-like receptor recognizes bacterial DNA. *Nature.* **7**, 740-5.

91- Hsu, T., Hingley-Wilson, S., Chen, M., Dai, A., Morin, P., Marks, C., Padiyar, J., Goulding, C., Gingery, M., Eisenberg, D., Russell, R., Derrick, S., CollinsSheldon, L., Morris, C., and Jacobs, W. (2003) The primary mechanism of attenuation of bacillus Calmette–Guérin is a loss of secreted lytic function required for invasion of lung interstitial tissue. *Proc.Natl.Acad.Sci. USA.* **100**, 12420-12425

92- <http://medlib.medlib.med.utah.edu/WebPath/HISTHTML/STAINS/STAINO17.html>.

93- Ilghari, D., Lightbody, KL., Veverka, V., Waters, LC., Muskett , FW., Renshaw, PS., Carr, MD. (2011) Solution structure of the M. tuberculosis EsxG-EsxH complex: functional implications and comparisons with other M. tuberculosis Esx family complexes. *The Journal of Biological Chemistry.* Published on July 5, 2011 as Manuscript M111.248732.

94- Imamura, Y., Oda, A., Katahira, T., Bundo, K., Pike, K.A., Ratcliffe, M.J., Kitamura, D. (2009) BLNK binds active H-Ras to promote B cell receptor-mediated capping and ERK activation. *The Journal of Biological Chemistry*. **15**, 9804-13.

95- Interim Guidance for Human and Veterinary Drug Products and Biologicals, U.S. Dept. of Health and Human Services, Center for Drug Evaluation and Research, July 15, 1991.

96- Ishikawa, E., Ishikawa, T., Morita, Y.S., Toyonaga, K., Yamada, H., Takeuchi, O., Kinoshita, T., Akira, S., Yoshikai, Y., Yamasaki, S. (2009) Direct recognition of the mycobacterial glycolipid, trehalose dimycolate, by C-type lectin Mincle. *Journal of Experimental Medicine*. **206**, 2879–2888.

97- Kanehisa, M., Goto, S. (2000) KEGG: kyoto encyclopedia of genes and genomes. *Nucleic Acids Res.* **1**, 27-30.

98- Keegan, C.E., Hutz, J.E., Krause, A.S., Koehler, K., Metherell, L.A., Boikos, S., Stergiopoulos, S., Clark, A.J., Stratakis, C.A., Huebner, A., and Hammer, G.D. (2007) Novel polymorphisms and lack of mutations in the ACD gene in patients with ACTH resistance syndromes. *Clin Endocrinol (Oxf)*. **2**, 168-74.

99- Kelly, S.M., Jess, T.J., Price, N.C. (2005) How to study proteins by circular dichroism. *Biochim Biophys Acta*. **1751**, 119-139.

100- Khademhosseini, A., Borenstein, J., Toner, M., and Takayama, S. (2008) Micro and nanoengineering of the cell microenvironment *Technologies and Applications. Artech House Publishers.* **7**, 627-631.

101- Kim, E., Kim, SH., Kim, S., Kim, TS. (2006) The novel cytokine p43 induces IL-12 production in macrophages via NF-kappaB activation, leading to enhanced IFN-gamma production in CD4+ cells. *Journal Immunol.* **176**, 256-264.

102- Kinkhikar, AG., Verma, I., Chandra, D., Singh, KK., Weldingh, K., Andersen, P., Hsu, T., Jacobs, WR. Jr., Laal, S. (2010) Potential role for ESAT6 in dissemination of *M. tuberculosis* via human lung epithelial cells. *Mol Microbiol.* **75**, 92–106.

103- Knudsen, S. (2004) Guide to analysis of DNA microarray data, second edition. *WILEY-LISS.* p63-80.

104- Kopp, PM., Bate, N., Hansen, TM., Brindle, NP., Praekelt, U., Debrand, E., Coleman, S., Mazzeo, D., Goult, BT., Gingras, AR., Pritchard, CA., Critchley, DR., Monkley, SJ. (2010) Studies on the morphology and spreading of human endothelial cells define key inter- and intramolecular interactions for talin1. *Eur J Cell Biol.* **9**, 661-73.

105- Krawczyk, C., Penninger, J.M. (2001) Molecular motors involved in T cell receptor clusterings. *Journal of Leukocyte Biology.* **3**, 317-30

106- Kuo, H.Y., Chang, C.C., Jeng, J.C., Hu, H.M., Lin, D.Y., Maul, G.G., Kwok, R. P.S., and Shih, H.M. (2005) SUMO modification negatively modulates the transcriptional activity of CREB-binding protein via the recruitment of Daxx. *PNAS*. **102**, 16973-16978.

107- Jarlier, V., Nikaido, H. (1990) Permeability barrier to hydrophilic solutes in *Mycobacterium chelonae*. *J Bacteriol.* **172**, 1418-23.

108- Jayachandran, R., Gatfield, J., Massner, J., Albrecht, I., Zanolari, B., Pieters, J. (2008) RNA interference in J774 macrophages reveals a role for coronin 1 in mycobacterial trafficking but not in actin-dependent processes. *Molecular Biology of the Cell.* **3**, 1241-51.

109- Jo, E-K. (2008) Mycobacterial interaction with innate receptors: TLRs, C-type lectins, and NLRs. *Current Opinion in Infectious Diseases.* **21**, 279–286.

110- Jo, EK., Yang, CS., Choi, CH., Harding, CV. (2007) Intracellular signalling cascades regulating innate immune responses to mycobacteria: branching out from Toll-like receptors. *Cellular Microbiology.* **9**, 1087–1098.

111- Jones, GJ., Hewinson, RG., Vordermeier, HM. (2010) Screening of predicted secreted antigens from *Mycobacterium bovis* identifies potential novel differential diagnostic reagents. *Clinical and Vaccine Immunology.* **9**, 1344-8.

112- Junge, S., Brenner, B., Lepple-Wienhues, A., Nilius, B., Lang, F., Linderkamp, O., Gulbins, E. (1999) Intracellular mechanisms of L-selectin induced capping. *Cell Signal*. **11**, 301-8.

113- Launay, S., Hermine, O., Fontenay, M., Kroemer, G., Solary, E., Garrido, C. (2005) Vital functions for lethal caspases. *Oncogene*. **33**, 5137-48.

114- Leber, JH., Crimmins, GT., Raghavan, S., Meyer-Morse, NP., Cox, JS., Portnoy, DA. (2008) Distinct TLR- and NLR-mediated transcriptional responses to an intracellular pathogen. *PLoS Pathogens*. **4**, article e6.

115- Lee, SB., Schorey, JS. (2005) Activation and mitogen-activated protein kinase regulation of transcription factors Ets and NF-kappaB in *Mycobacterium* -infected macrophages and role of the factors in tumor necrosis factor alfa and nitric oxide synthase 2 promoter function. *Infection and Immunity*. **10**, 6499-507.

116- Lewis, P.W., Elsaesser, S.J., Noh, K.M., Stadler, S.C., Allis, C.D. (2010) Daxx is an H3.3-specific histone chaperone and cooperates with ATRX in replication-independent chromatin assembly at telomeres. *PNAS*. **32**, 14075-80.

117- Lightbody, K.L., lighari, D., Waters, L.C., Carey, G., Bailey, M.A., Williamson, R.A., Renshaw, P.S., and Carr, M.D. (2008) Molecular features governing the stability and specificity of functional complex formation by *Mycobacterium*

tuberculosis ESAT-6/CFP-10 family proteins. *Journal of Biological Chemistry*. **283**, 17681-17690.

118- Lightbody, K., Renshaw, P., Collins, M., Wright, R., Hunt, D., Gordon, S., Hewinson, R., Buxton, R., Williamson, R., and Carr, M.D. (2004) Characterisation of complex formation between members of the *Mycobacterium tuberculosis* complex CFP-10/ESAT-6 protein family: towards an understanding of the rules governing complex formation and thereby functional flexibility. *FEMS Microbiology*. **238**, 255-262.

119- Lin, D.Y., Huang, Y.S., Jeng, J.C., Kuo, H.Y., Chang, C.C., Chao, T.T., Ho, C.C., Chen, Y.C., Lin, T.P., Fang, H.I., Hung, C.C., Suen, C.S., Hwang, M.J., Chang, K.S., Maul, G.G., and Shih, H.M. (2006) Role of SUMO-interacting motif in Daxx SUMO modification, subnuclear localization, and repression of sumoylated transcription factors. *Molecular Cell*. **3**, 341-54.

120- Li, Y., Schutte, R.J., Abu-Shakra, A., Reichert, W.M. (2005) Protein array method for assessing in vitro biomaterial-induced cytokine expression. *Biomaterials*. **10**, 1081-5.

121- Lin, D.Y., Fang, H.I., Ma, A.H., Huang, Y.S., Pu, Y.S., Jenster, G., Kung, H.J., and Shih, H.M. (2004) Negative modulation of androgen receptor transcriptional activity by Daxx. *Molecular and Cellular Biology*. **24**, 10529-41.

122- Lodish, B., Matsudaira, K., Krieger, S., Zipursky, D. (2004) Molecular cell biology . Fifth edition. *Freeman*. 94-95

123- Louise, R., Skjøt, V., Agger, E.M., Andersen, P. (2001) Antigen discovery and tuberculosis vaccine development in the post-genomic era. *Scand J Infect Dis*. **9**, 643-7.

124- Macgum, J.A., Raghavan, S., Stanley, S.A., and Cox, L.S. (2005) A non-RD1 gene cluster is required for Snm secretion in *Mycobacterium tuberculosis*. *Molecular Microbiology*. **57**, 1653-1663.

125- Magalhães¹, P., Lopes, A., Mazzola, P., Rangel-Yagui, C., Penna, T., Pessoa, A. (2007) Methods of Endotoxin Removal from Biological Preparations: a Review. *J Pharm Pharmaceut Sci*. **10** , 388-404.

126- Mahairas, G.G., Sabo, P.J., Hickey, M.J., Singh, D.C., Stover, C.K. (1996) Molecular analysis of genetic differences between *Mycobacterium bovis* BCG and virulent *M. bovis*. *Journal of Bacteriology*. **178**, 1274-1282.

127- Maitz, M.F., Teichmann, J., Sperling, C., Werner, C. (2009) Surface endotoxin contamination and hemocompatibility evaluation of materials. *Journal Biomedical Materials*. **1**, 18-25.

128- Malen, H., Berven, F., Fladmark, K., and Wiker, H. (2007) Comprehensive analysis of exported proteins from *Mycobacterium tuberculosis* H37Rv. *Proteomics*. **7**, 1702-1718.

129- Marmiesse, M., Brodin, P., Buchrieser, C., Gutierrez, C., Simoes, N., Vincent, V., Glaser, P., Cole, S., and Brosch, R. (2004) Macro-array and Bioinformatic analyses reveal mycobacterial core genes variation in the ESAT-6 genes family and new phylogenetic markers for the *Mycobacterium tuberculosis* complex. *Microbiology*. **150**, 483-496.

130- Mattow, J., Schaible, UE., Schmidt, F., Hagens, K., Siejak, F., Brestrich, G., Haeselbarth, G., Müller, E.C., Jungblut, P.R., Kaufmann, S.H. (2003) Comparative proteome analysis of culture supernatant proteins from virulent *Mycobacterium tuberculosis* H37Rv and attenuated *M. bovis* BCG Copenhagen. *Electrophoresis*. **24**, 3405-20.

131- Majlessi, L., Brodin, P., Brosch, R., Rojas, M.J., Khun, H., Huerre, M., Cole, S.T., Leclerc, C. (2005) Influence of ESAT-6 secretion system 1 (RD1) of *Mycobacterium tuberculosis* on the interaction between mycobacteria and the host immune system. *The Journal of Immunology*. **6**, 3570-9.

132- Master, SS., Rampini, SK., Davis, AS., Keller, C., Ehlers, S., Springer, B., Timmins, GS., Sander, P., Deretic, V. (2008) *Mycobacterium tuberculosis* prevents inflammasome activation. *Cell Host and Microbe*. **3**, 224–232.

133- McDonald, B., Pittman, K., Menezes, G.B., Hirota, S.A., Slaba, I., Waterhouse C.C., Beck, P.L., Muruve, D.A., Kubes, P. (2010) Intravascular danger signals guide neutrophils to sites of sterile inflammation. *Science*. **6002**, 362-6.

134- McKinney, J.D., Honer zu Bentrup, K., Munoz-Elias, E.J., Miczak, A., Chen, B., Chan, W.T., Swenson, D., Sacchettini, J.C., Jacobs, W.R. Jr., Russell, D.G. (2000) Persistence of *Mycobacterium tuberculosis* in macrophages and mice requires the glyoxylate shunt enzyme isocitrate lyase. *Nature*. **406**, 735-738.

135- Meher, A.K., Lella, R.K., Sharma, C., and Arora, A. (2007) Analysis of complex formation and immune response of CFP-10 and ESAT-6 mutants. *Vaccine*. **25**, 6098-111.

136- Meher, AK., Bal, NC., Chary, KV., Arora, A. (2006) *Mycobacterium tuberculosis* H37Rv ESAT-6-CFP-10 complex formation confers thermodynamic and biochemical stability. *FEBS Journal*. **273**, 1445-62.

137- Mishra, BB., Moura-Alves, P., Sonawane, A., Hacohen, N., Griffiths, G., Moita, LF., Anes, E. (2010) *Mycobacterium tuberculosis* protein ESAT-6 is a potent activator of the NLRP3/ASC inflammasome. *Cellular Microbiology*. **12**, 1046-63.

138- Murphy, D., Comer, L., Gormley, E. (2008) Adverse reaction to *Mycobacterium bovis* bacille Calmette–Guérin (BCG) vaccination against tuberculosis in humans, veterinary animals and wildlife species. *Tuberculosis*. **88**, 344-357.

139- North, R.J., Jung, Y.J. (2004) Immunity to tuberculosis. *Annual Review of Immunology*. **22**, 599-623.

140- Noss, EH., Pai, RK., Sellati, TJ., Radolf, JD., Belisle, J., Golenbock, DT., Boom, WH., Harding, CV. (2001) Toll-like receptor 2-dependent inhibition of macrophage class II MHC expression and antigen processing by 19-kDa lipoprotein of *Mycobacterium tuberculosis*. *The Journal of Immunology*. **167**, 910–918.

141- Novy, R., Yaeger, K., and Kolb, K. (2004) Ligation independent cloning: efficient Directional Cloning of PCR Products. *Novagen ,Inc*. **20**, 66-78.

142- Okkels, L.M., and Andersen, P. (2004) Protein-protein interactions of proteins from the ESAT-6 family of *Mycobacterium tuberculosis*. *Journal Bacteriology*. **186**, 2487-91.

143- Okkels, L.M., Brock, I., Follmann, F., Agger, E.M., Arend, S.M., Ottenhoff, T.H., Oftung, F., Rosenkrands, I., and Andersen, P. (2003) PPE protein (Rv3873) from DNA segment RD1 of *Mycobacterium tuberculosis*: strong recognition of both specific T-cell epitopes and epitopes conserved within the PPE family. *Infection and Immunity*. **71**, 6116–6123.

- 144- Olsen, A.W., Pinxteren, L.H., Okkels, L.M., Rasmussen, P.B., Andersen, P. (2001) Protection of Mice with a Tuberculosis Subunit Vaccine Based on a Fusion Protein of Antigen 85B and ESAT-6 . *Infection and Immunity*. **69**, 2773-2778.
- 145- Pai, R.K., Pennini, M.E., Tobian, A.A., Canaday, D.H., Boom, W.H., Harding, C.V. (2004) Prolonged toll-like receptor signaling by *Mycobacterium tuberculosis* and its 19-kilodalton lipoprotein inhibits gamma interferon-induced regulation of selected genes in macrophages. *Infection and Immunity*. **72**, 6603–6614.
- 146- Peter, M., Dalpke, A., Frank, J., Heeg, K. (2006) Activation of toll-like receptor 9 by DNA from different bacterial species. *Infection and Immunity*. **74**, 940-6.
- 147- Pallen, M.J. (2002) The ESAT-6/WXG100 Superfamily -and a new Gram-Positive secretion system ? *Trends Microbiol.* **10**, 209-212.
- 148- Panchuk-Voloshina, N., Haugland, R.P., Bishop-Stewart, J., Bhalgat, M.K., Millard, P.J., Mao, F., Leung, W.Y., and Haugland, R.P. (1999) Alexa dyes, a series of new fluorescent dyes that yield exceptionally bright, photostable conjugates. *J of Histochemistry and Cytochemistry*. **47**, 1179-1188.
- 149- Pandey, A.K., Yang, Y., Jiang, Z., Fortune, S.M., Coulombe, F., Behr, M.A., Fitzgerald, K.A., Sasseti, C.M., Kelliher, M.A. (2009) Nod2, Rip2 and Irf5 play a critical role in the type I interferon response to *Mycobacterium tuberculosis*. *PLoS Pathogens*, **5** , Article ID e1000500.

- 150- Pathak, SK., Basu, S., Basu, KK., Banerjee, A., Pathak, S., Bhattacharyya, A., Kaisho, T., Kundu, M., Basu, J. (2007) Direct extracellular interaction between the early secreted antigen ESAT-6 of *Mycobacterium tuberculosis* and TLR2 inhibits TLR signaling in macrophages. *Nature Immunology*. **6**, 610-8.
- 151- Plaza, D. F., Curtidor, H., Patarroyo, M. A., Chapeton-Montes, J. A., Reyes, C., Barreto, J. and Patarroyo, M. E. (2007) The *Mycobacterium tuberculosis* membrane protein Rv2560 – biochemical and functional studies. *FEBS Journal*. **274**, 6352–6364.
- 152- PELICIC, V., and GICQUEL, B. (1995) expression of the *Bacillus subtilis* sacB Gene confers sucrose sensitivity on *Mycobacteria*. *J. Bacteriology*. **178**, 1197-1199.
- 153- Posey, J.E., Shinnick, T.M., Quinn, F.D. (2006) Characterization of the twin-arginine translocase secretion system of *Mycobacterium smegmatis*. *J Bacteriology*. **188**, 1332-40.
- 154- Pym, A.S., Brodin, P., Majlessi, L., Brosch, R., Demangel, C., Williams, A., Griffiths, K.E., Marchal, G., Leclerc, C., and Cole, S.T. (2003) Recombinant BCG exporting ESAT-6 confers enhanced protection against tuberculosis. *Nature Medicine*. **9**, 533-539.
- 155- Pym, A.S., Brodin, P., Brosch, R., Huerre, M., Cole, S.T. (2002) Loss of RDI contributed to the attenuation of the live tuberculosis vaccines *Mycobacterium bovis* BCG and *Mycobacterium microti*. *Molecular Microbiology*. **46**, 709-717.

156- Quesniaux, V., Fremont, C., Jacobs, M., Parida, S., Nicolle, D., Yermeev, V., Bihl, F., Erard, F., Botha, T., Drennan, M., Soler, MN., Le Bert, M., Schnyder, B., Ryffel, B. (2008) Toll-like receptor pathways in the immune responses to mycobacteria. *Microbes Infect.* **6**, 946-59.

157- Raghavan, S., Manzanillo, P., Chan, K., Dovey, C., and Cox, J.C. (2008) Secreted transcription factor controls *Mycobacterium tuberculosis* virulence. *Nature.* **454**, 717-721.

158- Rasband, W.S., ImageJ, U.S. National Institutes of Health, Bethesda, Maryland, USA, <http://rsb.info.nih.gov/ij/>, 1997-2005.

159- Radosevic, K., Wieland, C.W., Rodriguez, A.C., Weverling, G.J., Mintardjo, R., Gillissen, G., Vogels, R., Skeiky, Y.A., Hone, D.M., Sadoff, J.C., van der Poll, T., Havenga, M., and Goudsmit, J. (2007) Protective Immune Responses to a Recombinant Adenovirus Type 35 Tuberculosis Vaccine in Two Mouse Strains: CD4 and CD8 T-Cell Epitope Mapping and Role of Gamma Interferon. *Infection and Immunity.* **75**, 4105-4115.

160- Reiling, N., Hölscher, C., Fehrenbach, A., Kröger, S., Kirschning, CJ., Goyert, S., Ehlers, S. (2002) Cutting edge: Toll-like receptor (TLR)2- and TLR4-mediated pathogen recognition in resistance to airborne infection with *Mycobacterium tuberculosis*. *Journal of Immunology.* **169**, 3480–3484.

161- Remick, D., and Whiteside, T. (2004) Cytokine Assays. *University of Pittsburgh Cancer Institute, USA*.**17**, 54-81.

162- Renshaw, P.S., Lightbody, K.L., Veverka, V., Muskett, W.F., Kelly, G., Frenkiel, T.A., Gordon, S.V., Hewinson, R.G., Bruke, B., Norman, J., Williamson, R.A., and Carr, M.D. (2005) Structure and function of the complex formed by the tuberculosis virulence factors CFP-10 and ESAT-6. *EMBO Journal*. **24** , 2491-2498.

163- Renshaw, P.S., Panagiotidou, P., Whelan, A., Gordon, S.V., Hewinson, R.G., Williamson, R.A., Carr, M.D. (2002) Conclusive evidence that the major T-cell antigens of the M. tuberculosis complex ESAT-6 and CFP-10 form a tight, 1:1 complex and characterisation of the structural properties of ESAT-6, CFP-10 and the ESAT-6-CFP-10 complex: implications for pathogenesis and virulence. *Journal of Biological Chemistry*. **277**, 21598-21603.

164- Rehren, G., Walters, S., Fontan, P., Smith, I., and Zarrage, M. (2007) Differential gene expression between Mycobacterium tuberculosis and Mycobacterium bovis. *Tuberculosis*. **87**, 347-359

165- Rhoades, E., Hsu, F., Torrelles, J.B., Turk, J., Chatterjee, D., and Russell, D.G. (2003) Identification and macrophage-activating activity of glycolipids released from intracellular Mycobacterium bovis BCG. *Molecular Microbiology*. **48**, 875-888.

166- Rindi, L., Lan, N., and Garzelli, C. (1999) Search for genes potentially involved in Mycobacterium tuberculosis virulence by mRNA differential display. *Biochemical Biophysical Research Communications*. **258**, 94- 101.

167- Ringnér, M. (2008) What is principal component analysis?. *Nature Biotechnology*. **26**, 303-304 .

168- Rocha-Ramírez, LM., Estrada-García, I., López-Marín, LM., Segura-Salinas, E., Méndez-Aragón, P., Van Soolingen, D., Torres-González, R., Chacón-Salinas, R., Estrada-Parra, S., Maldonado-Bernal, C., López-Macías, C., Isibasi, A.(2008) Mycobacterium tuberculosis lipids regulate cytokines, TLR-2/4 and MHC class II expression in human macrophages. *Tuberculosis (Edinb)*. **88**, 212-20.

169- Rosenkrands, I., King, A., Weldingh, K., Moniatte, M., Moertz, E., and Andersen, P. (2000) Towards the proteome of Mycobacterium tuberculosis. *Electrophoresis*. **21**, 3740-3756.

170- Rothfuchs, AG., Bafica, A., Feng, CG., Egen, JG., Williams, DL., Brown, GD., Sher, A. (2007) Dectin-1 interaction with Mycobacterium tuberculosis leads to enhanced IL-12p40 production by splenic dendritic cells. *Journal of Immunology*. **179**, 3463–3471.

171- Rubin, E. (2009) The granuloma in Tuberculosis—Friend or Foe? *The new England Journal of medicine*. **12**, 361-64.

172- Russell, D. G. (2007) Who puts the tubercle in tuberculosis? *Nature Reviews Microbiology*. **5**, 39- 47.

173- Sacchettini, J.C., Rubin, E.J., and Freundlich, J.S. (2008) Drug versus bugs: in pursuit of the persistent predator *Mycobacterium tuberculosis*. *Nature Reviews Microbiology*. **6**, 41-52.

174- Saiga, H., Shimada, Y., Takeda, K. (2011) Innate immune effectors in mycobacterial infection. *Clinical Developmental Immunology*. **2011**, 347594–347602.

175- Salomoni, P., Khelifi, A.F. (2005) Daxx: death or survival protein?. *Trends in Cell Biology*. **2**, 97-104.

176- Samten, B., Wang, X., Barnes, PF. (2009) *Mycobacterium tuberculosis* ESX-1 system-secreted protein ESAT-6 but not CFP10 inhibits human T-cell immune responses. *Tuberculosis (Edinb)*. **89** Suppl 1:S74-6.

177- Schnappinger, D., Ehrt, S., Voskuil, M., Liu, Y., Mangan, J., Monahan, I., Dolganov, G., Efron, B.D., Butcher, P., Nathan, C., and Schoolnik, G. (2003) Transcriptional Adaptation of *Mycobacterium tuberculosis* within macrophages insight into the phagosomal Environment. *Journal of Experimental Medicine*. **198**, 693-704.

- 178- Schroder, K., Tschopp, J. (2010) The Inflammasomes. *Cell*. **140**, 821–832.
- 179- Schoenen, H., Bodendorfer, B., Hitchens, K., Manzanero, S., Werninghaus, K., Nimmerjahn, F., Agger, EM., Stenger, S., Andersen, P., Ruland, J., Brown, GD., Wells, C., Lang, R. (2009) Cutting Edge: Mincle is essential for recognition and adjuvant activity of the mycobacterial cord factor and its synthetic analog trehalose-dibehenate. *Journal of Immunology*. **184**, 2756–2760.
- 180- Scott, J.R., Barnett, T.C. (2006) Surface proteins of gram-positive bacteria and how they get there. *Annual Review Microbiology*. **60**, 397-423.
- 181- Singh, G., Singh, B., Trajkovic, V., Sharma, P. (2005) Mycobacterium tuberculosis 6 kDa early secreted antigenic target stimulates activation of J774 macrophage. *Immunology Letters*. **98**, 180–188.
- 182- Skjot, R.L.V., Brock, S.M.A., Bend, M.E., Munk, M., Theisen, T.H.M., and Andersen, P. (2002) Epitope mapping of the immunodominant antigen TB 10.4 and the two homologous proteins TB 10.3 and TB 12.9, which constitute a subfamily of the esat-6 gene family. *Infection and Immunity*. **70**, 5446-5453.
- 183- Skj, R.I., Oettinger, T., Rosenkrands, I., Ravn, P., Brock, I., Jacobsen, S., and Andersen, P. (2000) Comparative evaluation of low-molecular mass proteins from Mycobacterium tuberculosis identifies members of the ESAT-6 family as immunodominant T-cell antigens. *Infection and Immunity*. **68**, 214-220.

184- Sharif, O., Bolshakov, VN., Raines, S., Newham, P., Perkins, ND. (2007) Transcriptional profiling of the LPS induced NF-kappaB response in macrophages. *BMC Immunology*. **12**, 8-17.

185- Söderström, T.S., Nyberg, S.D., Eriksson, J.E. (2005) CD95 capping is ROCK-dependent and dispensable for apoptosis. *Journal of Cell Science*. **10**, 2211-23.

186- Smith, I. (2003) Mycobacterium tuberculosis pathogenesis and molecular determinants of virulence. *Clinical Microbiology Reviews*. **16**, 463-496.

187- Stanley, S., Raghavan, S., Hwang, W.W., Cox, J.S. (2003) Acute infection and macrophage subversion by Mycobacterium tuberculosis require a specialized secretion system. *PNAS*. **100**, 13001–13006.

188- Stewart, G.R., Robertson, B.D., Young, D.B. (2003) Tuberculosis: a problem with persistence. *Nature Reviews Microbiology*. **1**, 97-105.

189- Sugawara, I., Yamada, H., Li, C., Mizuno, S., Takeuchi, O., Akira, S. (2003) Mycobacterial infection in TLR2 and TLR6 knockout mice. *Microbiology and Immunology*. **47**, 327–336.

190- Sugawara, I., Yamada, H., Kaneko, H., Mizuno, S., Takeda, K., Akira, S. (1999) Role of interleukin-18 (IL-18) in mycobacterial infection in IL-18- gene-disrupted mice. *Infection and Immunity*. **67**, 2585–2589.

191- Sun, H., Fang, H., Chen, T., Perkins, R., Tong, W. (2006) GOFFA: gene ontology for functional analysis--a FDA gene ontology tool for analysis of genomic and proteomic data. *BMC Bioinformatics*. **7**, 20-S23.

192- Suzuki, T., Hashimoto, S., Toyoda, N., Nagai, S., Yamazaki, N., Dong, HY., Sakai, J., Yamashita, T., Nukiwa T, Matsushima K. (2000) Comprehensive gene expression profile of LPS-stimulated human monocytes by SAGE. *Blood*. **7**, 2584-91.

193- Swaim, L.E., Connolly, L.E., Volkman, H.E., Humbert, O., Born, D.E., Ramakrishnan, L. (2006) Mycobacterium marinum infection of adult zebrafish causes caseating granulomatous tuberculosis and is moderated by adaptive immunity. *Infection and Immunity*. **11**, 6108-17.

194- Takeuchi, O., Akira, S. (2010) Pattern recognition receptors and inflammation. *Cell*. **140**, 805–820.

195- Tailleux, L., Neyrolles, O., Honoré-Bouakline, S., Perret, E., Sanchez, F., Abastado, JP., Lagrange, PH., Gluckman, JC., Rosenzweig, M., Herrmann, JL. (2003) Constrained intracellular survival of Mycobacterium tuberculosis in human dendritic cells. *Journal of Immunology*. **170**, 1939–1948.

196- Tan, T., Lee, W., Alexander, D., Grinstein, S., and Liu, J. (2006) The ESAT-6/CFP-10 secretion system of *Mycobacterium marinum* modulates phagosome maturation. *Cellular Microbiology*. **8**, 1417-1429.

197- The scienceAdvisoryboard. (2003) <http://www.scienceboard.net/resources/protocols>.

198- Trap, G., and Horn, E. (2007) Chemotaxis and Migration Tool Version 1.01. Visualization and data analysis of chemotaxis and migration processes based on ImageJ. *Ibidi integrated BioDiagnostics*.

199- Tsai, M.C., Chakravarty, S., Zhu, G., Xu, J., Tanaka, K., Koch, C., Tufariello, J., Flynn, J., Chan, J. (2006) characterization of the tuberculous granuloma in murine and human lungs: cellular composition and relative tissue oxygen tension. *Cellular Microbiology*. **8**, 218-232.

200- Tong, W., Cao, X., Harris, S., Sun, H., Fang, H., Fuscoe, J., Harris, A., Hong, H., Xie, Q., Perkins, R., Shi, L., Casciano, D. (2003) ArrayTrack--supporting toxicogenomic research at the U.S. Food and Drug Administration National Center for Toxicological Research. *Environmental Health Perspectives*. **15**, 1819-26.

201- Tong, W., Harris, S., Cao, X., Fang, H., Shi, L., Sun, H., Fuscoe, J., Harris, A., Hong, H., Xie, Q., Perkins, R., Casciano, D. (2004) Development of public

toxicogenomics software for microarray data management and analysis. *Mutat Res.* **549**, 241-53.

202- Tuberculosis, from basic science to patient care. (2007). 93-112. [www.Tuberculosis-textbook. Com.](http://www.tuberculosis-textbook.com)

203- Tuberculosis update (Health Protection Agency), March (2010) [http's://www.hpa.org.uk/publications/2007/I'B](http://www.hpa.org.uk/publications/2007/I'B).

204- Ulrichs, T., Kaufmann, S.H. (2006) New insights into the function of granulomas in human tuberculosis. *J Pathol.* **208**, 261-9.

205- Ulrichs, T., Kosmiadi, G.A., Trusov, V., Jorg, S., Pradl, L., Mishenko, V., Gushina, N., Kaufmann, S.H. (2004) Human tuberculous granulomas induce peripheral lymphoid follicle-like structures to orchestrate local host defence in the lung. *Journal Pathology.* **204**, 217-228.

206- Van der Wel, N., Hava, D., Houben, D., Fluitsma, D., van Zon, M., Pierson, J., Brenner, M., Peters, P.J. (2007) *M. tuberculosis* and *M. leprae* translocate from the phagolysosome to the cytosol in myeloid cells. *Cell.* **129**, 1287–1298.

207- Van, V., Lesage, S., Bouguermouh, S. (2006) Expression of the self-marker CD47 on dendritic cells governs their trafficking to secondary lymphoid organs. *EMBO Journal*. **25**, 5560–5568.

208- Van Pinxteren, L.A.H., Ravn, P., Agger, E.M., Pollock, J., and Andersen, P. (2000) Diagnosis of Tuberculosis Based on the Two Specific Antigens ESAT-6 and CFP10. *Clinical and Diagnostic Laboratory Immunology*. **7**, 155-160.

209- Vidali, L., Chen, F., Cicchetti, G., Ohta, Y., Kwiatkowski, DJ. (2006) Rac1-null mouse embryonic fibroblasts are motile and respond to platelet-derived growth factor. *Molecular Biology of the Cell*. **5**, 2377-90.

210- Vlangos, C.N., O'Connor, B.C., Morley, M.J., Krause, A.S., Osawa, G.A., Keegan, C.E. (2009) Caudal regression in adrenocortical dysplasia (acd) mice is caused by telomere dysfunction with subsequent p53-dependent apoptosis. *Developmental Biology*. **2**, 418-28.

211- Volkman, HE., Pozos, TC., Zheng, J., Davis, JM., Rawls, JF., Ramakrishnan, L. (2009) Tuberculous granuloma induction via interaction of a bacterial secreted protein with host epithelium. *Science*. **5964**, 466-9.

212- Volkman, H.E., Clay, H., Beery, D., Chang, J.C.W., Sherman, D.R., and Ramakrishnan, L. (2004) Tuberculous granuloma formation is enhanced by a *Mycobacterium* virulence determinant. *PLoS Biology*. **2**, 1946-1956.

213- Voskuil, M.I., Schnappinger, D., Rutherford, R., Liu, Y., Schoolnik, G.K. (2004) Regulation of the Mycobacterium tuberculosis PE/PPE genes. *Tuberculosis (Edinb)*. **84**, 256-62.

214- Wang, X., Barnes, P.F., Dobos-Elder, K.M., Townsend, J.C., Chung, Y.T., Shams, H., Weis, S.E., Samten, B. (2009) ESAT-6 inhibits production of IFN-gamma by Mycobacterium tuberculosis-responsive human T cells. *The Journal of Immunology*. **182**, 3668-77.

215- Waters, W. R., Palmer, M. V., Nonnecke, B. J. (2009) Signal regulatory protein α (SIRP α)⁺ cells in the adaptive response to ESAT-6/CFP-10 protein of tuberculous mycobacteria. *PLoS One*. 4, no. 7 article e6414.

216- Wheeler, A.P., Wells, C.M., Smith, S.D., Vega, F.M., Henderson, R.B., Tybulewicz, V.L., Ridley, A.J. (2006) Rac1 and Rac2 regulate macrophage morphology but are not essential for migration. *Journal of Cell Science*. **13**, 2749-57.

217- Wang, H.W., Joyce, J.A. (2009) Alternative activation of tumor-associated macrophages by IL-4: priming for protumoral functions. *Cell Cycle*. **24**, 4824-35.

218- West, A.P., Koblansky, A.A., Ghosh, S. (2006) Recognition and signaling by toll-like receptors. *Annual Review of Cell and Developmental Biology*. **22**, 409-437.

219- Wethkamp, N., Klempnauer, K.H. (2009) Daxx is a transcriptional repressor of CCAAT/enhancer-binding protein beta. *The Journal Biological Chemistry*. **42**, 28783-94.

220- WHO Report, (2009). Global tuberculosis control - a short update to the 2009 report. World Health Organization, Geneva, Switzerland.

221- WHO. The stop TB strategy, Building on and enhancing DOTS to meet the TB-related millennium development goals. Geneva: WHO, 2006. Report No WHO/HTM/STB/2006.37.

222- Xu, Y., Jagannath, C., Liu, XD., Sharafkhaneh, A., Kolodziejska, KE., Eissa, NT. (2007) Tolllike receptor 4 is a sensor for autophagy associated with innate immunity. *Immunity*. **27**, 135–144.

223- Xue, B., Wu, Y., Yin, Z., Zhang, H., Sun, S., Yi, T., Luo, L. (2005) Regulation of lipopolysaccharide-induced inflammatory response by glutathione S-transferase P1 in RAW264.7 cells. *FEBS Letters*. **19**, 4081-7.

224- Yadav, M., Schorey, JS. (2006) The β -glucan receptor dectin-1 functions together with TLR2 to mediate macrophage activation by mycobacteria. *Blood*. **108**, 3168–3175.

- 225- Yan He, X., Hui Zhuan, Y., Gang Zhang, X., Li Li, G. (2003) Comparative proteome analysis of culture supernatant proteins of *Mycobacterium tuberculosis* H37Rv and H37Ra. *microbes and infection*. **5**, 851-856.
- 226- Yamada, H., Mizumo, S., Horai, R., Iwakura, Y., Sugawara, I. (2000) Protective role of interleukin-1 in mycobacterial infection in IL-1 α/β double-knockout mice. *Laboratory Investigation*. **80**, 759–767.
- 227- Yamasaki, S., Ishikawa, E., Sakuma, M., Hara, H., Ogata, K., Saito, T. (2008) Mincle is an ITAM-coupled activating receptor that senses damaged cells. *Nature Immunology*. **9**, 1179–1188.
- 228- Yang, C.S., Lee, J.S., Song, C.H., Hur, G.M., Lee, S.J., Tanaka, S., Akira, S., Paik, T.H., Jo, E.K. (2007) Protein kinase C zeta plays an essential role for *Mycobacterium tuberculosis*-induced extracellular signal-regulated kinase 1/2 activation in monocytes/macrophages via Toll-like receptor 2. *Cellular Microbiology*. **9**, 382–396.
- 229- Yang, Y., Yin, C., Pandey, A., Abbott, D., Sasseti, C., Kelliher, MA. (2007) NOD2 pathway activation by MDP or Mycobacterium tuberculosis infection involves the stable polyubiquitination of Rip2. *Journal of Biological Chemistry*. **282**, 36223–36229.

230- Yong Gao, L ., Guo, S., McLaughlin, B., Morisaki, H., Engel, J., and Brown, J. (2004) A mycobacterial virulence gene cluster extending RD1 is required for cytolysis, bacterial spreading and ESAT-6 secretion. *Molecular Microbiology*. **53**, 1677-1693.

231- Zhao, B., Bowden, RA., Stavchansky, SA., Bowman, PD.,(2001) Human endothelial cell response to gram-negative lipopolysaccharide assessed with cDNA microarrays. *Am J Physiol Cell Physiol*. **5**, C1587-95.